REGULATION OF MESENCHYMAL PROGENITOR PROLIFERATION AND DIFFERENTIATION BY THROMBOSPONDIN-2 AND NOTCH SIGNALING

by

Hailu Shitaye

A dissertation submitted in partial fulfillment
of the requirements for the degree of
Doctor of Philosophy
(Cellular and Molecular Biology)
in The University of Michigan
2010

Doctoral Committee:

Professor Renny T. Franceschi, Co-chair
Assistant Professor Kurt D. Hankenson, Co-chair, University of Pennsylvania
Professor Paul H. Krebsbach
Professor Ormond A. MacDougald
Assistant Professor Joshua D. Miller

To my parents and brothers

TABLE OF CONTENTS

LIST OF FIGURES

Figure

LIST OF TABLES

ABSTRACT

REGULATION OF MESENCHYMAL PROGENITOR PROLIFERATION AND DIFFERENTIATION BY THROMBOSPONDIN-2 AND NOTCH SIGNALING

by

Hailu Shitaye

Co-chairs: Renny T. Franceschi and Kurt D. Hankenson

Mesenchymal Stem Cells (MSC) give rise to osteoblasts, adipocytes and chondrocytes. A decrease in MSC number and a shift in their differentiation to the adipogenic fate is observed with aging and have been proposed as possible mechanisms for the pathogenesis of age associated osteoporosis. Mice deficient in thrombospondin-2 (TSP2) have an increase in MSC number and as a result, TSP2-null mice have an increase in bone mass. In-vitro, TSP2 promotes osteogenic differentiation and inhibits MSC proliferation. There is a reciprocal relationship between osteogenic and adipogenic differentiation such that factors which promote osteogenic differentiation inhibit adipogenic differentiation, therefore we hypothesized that TSP2 inhibits adipogenesis. MSC isolated from bone marrow as well as adipose tissue of TSP2-null mice display an increase in lipid accumulation relative to those isolated from wild type mice. In addition TSP2-null mice are heavier due to increased adiposity.

Recent studies have demonstrated that TSP2 modulates activation of notch signaling in various cell types. Activation of Notch signaling by plating MSC onto Jagged-1 increases primary MSC proliferation, and decreases osteogenic differentiation. Jagged-1 also increases lipid accumulation in part by increasing their proliferation. Expressing a dominant negative form of mastermind-like-1 (dnMAML) to selectively inactivate canonical notch signaling in vivo in osteoblasts results in vertebral malformations similar to Alagille Syndrome patients. dnMAML expression in early mesenchymal tissue results in decreased trabecular bone volume fraction at 8 weeks of age but has no apparent effect on trabecular bone at 6 or 14.5 months of age. Post-natal induction of global dnMAML expression results in decreased trabecular bone at 6 months of age without significantly altering CFU-F numbers suggesting the decrease in bone mass could be secondary to increased bone resorption.

We evaluated the effect of TSP2 on Jagged-1 mediated notch activation and found that notch target gene expression is increased in TSP2-null MSC. Over-expressing TSP2 in C3H10T1/2 cells decreases Hey-1 expression and notch reporter activity. We propose a model in which TSP2 decreases notch activation resulting in a decrease in MSC proliferation and an increase in osteogenic differentiation which in turn leads to a decrease in the osteoprogenitor pool.

CHAPTER I

INTRODUCTION

Bone is a dynamic organ that is remodeled throughout life. Bone remodeling, the process of removing old bone (bone resorption) and replacing it with new (bone formation), is maintained in homeostasis (1, 2). Conditions that disrupt this equilibrium and cause a net increase in bone resorption lead to decreased bone mass (osteopenia). If osteopenia is severe enough, it leads to the clinical condition osteoporosis which is characterized by increased risk of bone fracture (3).

In the U.S., more than 10 million individuals have clinical osteoporosis and greater than 34 million more have low bone mass. Osteoporosis is responsible for more than 1.5 million fractures annually. It is estimated that one out of every two women and one in eight men over age 50 will have an osteoporosis-related fracture in their lifetime. The number of patients with osteoporosis is likely to increase in the future due to changes in demographics and increases in life expectancy (4, 5).

Although the causes of osteoporosis are multi-factorial and likely involve many risk factors, the most common causes of osteoporosis are associated with aging and are classified as type I (estrogen associated) and type II (senile

or age associated). In type I osteoporosis, the loss of estrogen leads to an increase in bone resorption, and although there is a concomitant increase in bone formation, it is unable to balance the increased bone resorption. In type II osteoporosis, both bone formation and bone resorption decrease with age but the decrease in bone formation is greater than the decrease in bone resorption (6-11).

Bone remodeling is accomplished by osteoclasts which resorb bone and osteoblasts which lay down new bone. Osteoclasts are derived from hematopoetic stem cells (HSC) while osteoblasts are derived from mesenchymal stem cells (MSC). Although most clinically available treatments for osteoporosis target bone resorption, a significant limitation of this approach is that it is ineffective at increasing bone mass in patients who are already osteopenic. Novel treatment approaches will target osteoblasts and aim at increasing their number by driving their differentiation from MSC or increasing their proliferation, survival or activity.

Mesenchymal Stem Cells (MSC) -"Osteogenic Stem Cells"

Seminal work by Friedenstein and colleagues in the 1960's and 70's showed that when whole bone marrow is plated onto tissue culture plastic, fibroblastic, adherent colonies are formed which they termed colony-forming-unit-fibroblastic (CFU-F). Using in vitro and in vivo implantation experiments, they showed that all of the "osteogenic activity" resided in these adherent cells and proposed the existence of an "osteogenic stem cell", distinct from HSC, that

gives rise to the osteoblast lineage (12-15). Subsequent experiments showed that plating whole bone marrow at very low density gives rise to single cell derived CFU-F that had significant proliferative capacity and the ability to differentiate into osteoblasts, adipocytes and chondrocytes (16). Cells derived from these clones were also able to form bone when implanted into host animals which firmly established the existence of cells with stem cell like properties (17). With later demonstration that this adherent population of bone marrow cells can be induced to differentiate into other mesenchymal derived tissues such as muscle, the term 'Mesenchymal Stem Cell' was proposed and has gained wide use to describe not only those fibroblastic cells derived from bone marrow but also similar cells derived from other connective tissues that show similar differentiation potential (18, 19).

MSC differentiation potential

In their native endocortical bone environment, MSC give rise to osteoblasts, adipocytes, and stromal support cells. During embryonic development and bone regeneration processes such as during fracture healing, MSC also differentiate into chondrocytes. Various studies show that bulk cultures of marrow stromal cells can also be induced to differentiate into various cell types including neurons, muscle cells and tendon-like tissue (20-22). However, single cell derived MSC have been demonstrated to only differentiate into osteoblasts, adipocytes and chondrocytes. Additionally, the ability of MSC to differentiate into other lineages has not been demonstrated in vivo, therefore,

whether MSC give rise to any other committed, fully-differentiated lineages remains controversial (19).

In vivo, bone formation involves commitment of MSC into pre-osteoblasts. As pre-osteoblasts mature into active osteoblasts, they change in morphology to polarized, cuboidal cells that line the bone surface and secrete osteoid, an un-mineralized bone matrix that is rich in type I collagen, and other non-structural extracellular matrix proteins (ECM) proteins. Some osteoblasts surround themselves with bone matrix and these cells are referred to as osteocytes present in lacunae (23).

Several key transcription factors involved in osteoblastogenesis have been identified through a combination of genetic and molecular studies. Runx-2, a runt homology domain transcription factor, was initially identified in a screen of proteins that bind to the promoter of the osteoblast specific osteocalcin gene (24, 25). In humans, haploinsufficiency in Runx-2 causes an autosomal dominant disease called cleidocranial dysplasia (CCD) that is characterized by partial or complete absence of the clavicles, unclosed fontanelles, short stature, underdeveloped bones, and supernumerary teeth (26, 27). Transgenic mice in which both copies of Runx-2 have been disrupted by homologous targeting (Runx-$2^{-/-}$) develop no osteoblasts while Runx-$2^{+/-}$ mice display a phenotype similar to CCD (28, 29). In vitro, forced expression of Runx-2 in non-osteogenic cells results in expression of many osteoblast specific ECM proteins establishing Runx-2 as “master regulator” of osteogenesis (30).

Another transcription factors required for osteogenesis is the zinc finger containing protein osterix (Sp7). Osterix null mice completely lack osteoblasts. The fact that Runx-2 null mice do not express osterix while Runx-2 expression is normal in osterix null mice, along with in vitro experiments showing that Runx-2 over-expression induces osterix suggests that osterix is a down stream target of Runx-2 (31) . A recent study that examined the phenotype of mice in which osterix expression was specifically deleted in osteoblasts using 2.3kb type I collagen promoter, demonstrated an osteopenic phenotype accompanied by an increase in immature osteoblasts indicating that osterix plays an important role in terminal differentiation of osteoblasts (32).

Another transcription factor that regulates osteogenic differentiation is ATF4. Mice deficient in ATF4 are osteopenic due to defect in terminal differentiation of osteoblasts and defect in type I collagen synthesis (33). ATF4 regulates osteocalcin gene transcription and its transcriptional activity is in turn regulated by FIAT (33-39). Over-expression and deletion studies have also identified other transcription factors including ΔFosB, Fra-1, Dlx5 and Dlx6 that play a role in regulating osteoblast differentiation (40-50)

Adipogenic differentiation

Adipogenic differentiation, including its transcriptional regulation, has been extensively characterized in pre-adipocyte cell lines such as 3T3-L1 cells. Upon adipogenic induction, pre-adipocytes undergo 2-3 cycles of cell division in a process referred to as mitotic clonal expansion, and begin to express high levels

of transcription factors of the C/EBP family which in turn activate PPAR-γ expression. PPAR-γ is a member of the nuclear receptor family of transcription factors and is referred to as master-regulator of adipogenesis because its expression is both necessary and sufficient for adipogenesis. PPAR-γ activates transcription of many genes that are required for adipocyte function (51-53). As cells differentiate and mature into adipocytes, they undergo changes in their morphology from fibroblastic (spindle-shape and stellate) to rounded and they eventually accumulate lipid droplets. Although there is some argument as to whether primary MSC undergo mitotic clonal expansion, they clearly exhibit similar changes in expression of key adipocyte specific transcription factors, undergo similar morphological changes and accumulate lipid droplets (54).

Reciprocal relationship between osteogenesis and adipogenesis

An increase in bone marrow adipocytes is observed in several bone loss conditions including those caused by aging (11, 55-57). There is also an inverse correlation between increased adipocyte number and reduced bone formation rate in humans (58). Additionally, many growth factors such as Wnts which promote osteogenesis, also decrease adipogenesis (59-61).

In vitro and in vivo studies demonstrate interactions between transcription factors that regulate differentiation into the two fates. In animal models, decreasing PPAR-γ activity results in increased osteoblast differentiation and bone mass. Similarly, a decrease in bone mass is observed when PPAR-γ agonists are administered to either mice or humans (62-65). A study by Hong et

identified TAZ (transcriptional co-activator with PDZ-binding motif) as a BMP2 induced protein that acts as a transcriptional co-activator for Runx-2 and promotes osteogenic differentiation of MSC. Interestingly, TAZ also acts as a co-repressor for PPAR-γ mediated transcription and acts to inhibit adipogenesis suggesting that it may play an important role in a switch from an adipogenic to osteogenic fate (66).

Systemic and local control of MSC differentiation and bone formation

Several systemic hormones have been shown to regulate bone mass. Parathyroid hormone (PTH) has both anabolic and catabolic effects on bone. Intermittent PTH administration results in increased osteoblast number and bone formation and is used clinically for the treatment of osteoporosis, while chronic administration results in an increase in osteoclast number and bone resorption (67). PTH has been shown to affect osteoblast proliferation and survival in vitro and in vivo (68, 69). In addition, PTH has a positive effect on osteoclast function by inducing osteoblasts to produce RANKL and M-CSF, two factors that promote osteoclast function.

Adipocyte produced leptin is another hormone that has been shown to have complex effects on bone. Leptin deficient (ob/ob) mice have a decrease in most bone parameters including total body bone mineral density, long bone cortical thickness and mineralizing surface but have an increase in trabecular bone. A similar bone phenotype is observed in leptin receptor deficient (db/db) mice. Leptin appears to exert its negative effect on bone though its effect on

catecholamine release from the central nervous system. Other systemic hormones that regulate bone mass include steroid hormones estrogen and progesterone, vitamin-D3, and glucocorticoids (70-73).

Several, locally produced growth factors, including BMPs and Wnts also play crucial roles in regulating MSC differentiation and bone formation. BMPs are members of the TGF-β super family and play important roles in skeletal development. MSC and osteoblasts secrete several BMPs including BMP-2, -4,-6 and -7 which have been shown to promote bone formation in various cell types (74). Additionally, activation of BMP signaling in vivo has been shown to cause heterotopic ossification (75-77). BMPs signal through receptor tyrosine kinases. Receptor binding results in phosphorylation of the receptor activated smads (R-Smads). R-Smads then bind to common mediator smad (Smad 4), translocate to the nucleus and initiate transcription of target genes (78).

Wnts are another group of growth factors produced by MSC lineage cells. Although it is now clear that Wnts can signal through different mechanisms, the best characterized signaling process, the canonical pathway, acts through the stabilization of β-catenin. In the absence of Wnt, β-catenin is phosphorylated by GSK-3β and is directed for proteosomal degradation. Binding of Wnts to frizzed receptors and LRP5 and LRP6 initiates a signaling cascade that blocks GSK-3β activity and causes β-catenin to accumulate in the cytoplasm. β-catenin then translocates to the nucleus, binds to TCF/LEF family of transcription factors and initiates transcription of Wnt target genes. In humans, loss off function mutations in LRP5 result in decreased bone mass while gain of function mutations result in

increased bone mass. Transgenic mice with similar gain of function mutation in LRP5 show increase in bone mass while LRP5 and LRP6 null mice show defect in bone mass accrual (79). Transgenic mice that over-express Wnt-10b specifically in adipocytes from AP2 promoter have an increase in bone mass and a decrease in fat tissue (60). In-vitro, Wnt10b promotes osteogenic differentiation and blocks adipogenic differentiation by inhibiting expression of CEBP and PPAR-γ expression (80).

MSC differentiation is also influenced by extracellular matrix (ECM) proteins. Cells interact with the ECM thorough a variety of receptors including integrins. Integrin binding to the ECM activates signaling through the MAP kinase pathway which in turn has been shown to post-translationally modify Runx-2 and increase it transcriptional activity (81-83). Cell adhesion and shape also have been shown to influence cell differentiation. For instance, heparin promotes adipogenic differentiation and inhibits osteogenic differentiation by decreasing focal adhesion formation (84). Plating MSC on substrates that allow cell spreading promotes their differentiation into the osteogenic lineage while substrates that cause them to have a rounded shape promote adipogenic differentiation (85).

MSC secrete a variety of ECM proteins. While some of these ECM proteins are vital for the structural integrity of bone, others referred to as matricellular proteins, play a minimal structural role but rather are important in mediating interactions between cells and the extracellur environment (86-88). Several mouse knock out models have revealed that matricellular proteins play

important roles in MSC physiology. As examples, osteonectin-null mice develop age-associated osteopenia due to a decrease in MSC number, while the phenotype of osteopontin-null mice is more subtle and best revealed through physiological challenges such as ovariectomy and fracture (88).

Thrombospondin-2

Thromospondin-2 (TSP2) is a matricellular protein that is highly expressed in MSC. It belongs to a family of five structurally related proteins (TSP1-TSP5). TSP1 was the first member to be identified as a factor secreted from thrombin-stimulated platelets hence the name for the group. TSPs are large, multi-modular, glycoproteins that form either homotrimers (TSP1 and TSP2) or homopentamers (TSP3-TSP5). In addition to being trimeric, TSP1 and TSP2 have the same modular structure with an N-terminal heparin binding domain, a linker region, a procollagen-homology domain, three type I repeats, three EGF-like type II repeats, seven calcium binding type III repeats and a globular C-terminal domain. TSP3-5 are structurally different from TSP1 and TSP2 and form pentamers, lack procollagen and type I repeats, and have four instead of three type II repeats (89-91).

TSP2 expression in vivo has been evaluated most extensively in mouse embryos. TSP2, as measured by in-situ hybridization and immuno-histochemistry, is highest in organs with high connective tissue content such as dermis, blood vessels, meninges, ligaments, pericardium, periosteum, and pleura. TSP2 expression is also high in the developing skeleton and muscle. In the

developing skeleton, TSP2 expression localizes to the proliferative zone of growth plates and to bony spicules in the endosteal space (92-94). TSP2 expression is highest in undifferentiated mesenchymal cells five days post fracture in a tibial fracture model and its expression decreases in more mature fracture calluses (95).

Analysis of the phenotype of TSP2-null mice has revealed that TSP2 has important function in several tissues. TSP2 null mice have tendon and ligament laxity due to abnormal collage fibrillogenesis. The skin of TSP2-null mice is fragile, which may be due to decreased adhesion and spreading of dermal fibroblasts. Similar to TSP1, TSP2 also has anti-angiogenic properties as demonstrated by the increase vascular density in multiple tissues in TSP2-null mice (96-101).

TSP2-null mice have also revealed an important role for TSP2 in bone homeostasis. TSP2-null mice have an increase in cortical bone thickness due to an increase in endocortical bone formation. Increases in bone formation can be accomplished either by increasing the number of osteoblasts or increasing the activity of osteoblasts that are present (102). In vitro, MSC from TSP2 null mice display a delay in mineralization suggesting that TSP2 actually promotes osteogenic differentiation. TSP2 also inhibits MSC proliferation in vitro and CFU-F numbers are increased in TSP2 null mice suggesting the increase in bone formation observed in TSP2-null mice may be due to increased osteoblast progenitor number (102, 103).

The ability of TSP2 to influence such diverse cellular processes is due to its' modular structure which allows it to interact with various cell surface receptors, secreted growth factors and cytokines, enzymes and other ECM proteins. The N-terminal domain (NTD) of TSP1 and TSP2 contains high affinity heparin binding domains that bind to heparin-sulfate-proteoglycans. The NTD is also responsible for interaction with the scavenger receptor, low density lipoprotein-related receptor protein (LRP) which is responsible for endocytosis and degradation of TSPs. In addition, the NTD contains a binding domain for α3β1 integrin. TSP1 and TSP2 can bind to latent TGF-β through their type-I repeats. The type I repeats also interact with CD36 and this interaction has been shown to be important for the anti-angiogenic effects of TSP1. In addition to binding calcium, the type III repeats contain an RGD domain that mediates interaction with αvβ3 and αIIbβ3 integrins. Finally, the C-terminal domain interacts with another adhesion receptor, CD47/Integrin associated protein (IAP). TSP2 also binds to matrix-metalloproteinase 2 (MMP2) and decreases it activity indirectly by promoting clearance by LRP mediated endocytosis (99, 104). Most recently TSP2 was shown to physically interact with Notch receptors and ligands and regulate activation of this developmentally important signaling pathway (105).

Notch Signaling

Notch receptors are evolutionarily conserved single pass transmembrane proteins. In mammals there are 4 known notch receptors (Notch1-4). Structurally, the extracellular domain of notch receptors is composed of a DSL

domain and from 28 to 36 EGF like repeats that are responsible for interaction with ligands, three LN repeats, and a heterodimerization domain. The intracellular domain contains seven ankyrin repeats flanked by two nuclear localization signals (NLS), a transactivating domain, and a proline, glutamine, serine, threonine rich (PEST) domain. The receptor is initially synthesized as a single precursor protein containing both the extracellular and intracellular domains but is cleaved during transport (S1 cleavage) in the trans-golgi by a furin-like convertase. Following cleavage, the hydrophobic heterodimerization domain forms a stable, non-covalent complex with the extracellular portion of the membrane bound intracellular notch (106).

The ligands for Notch receptors are also single pass transmembrane proteins expressed by neighboring cells. In mammals there are five ligands (delta-like (Dll) 1, 3 and 4 and Jagged (Jag) 1 and 2). Dll and Jag ligands are structurally similar in that they contain an N-terminus DSL domain and EGF like repeats responsible for receptor interaction. However Jag-1 and Jag-2 contain more EGF repeats than Dll1, 3 and 4 and also contain a cystine rich domain (107, 108).

Ligand binding to notch receptors results in a series of enzymatic cleavages that ultimately results in release of the intracellular domain (NICD) into the cytoplasm. The first of these cleavages, the S2 cleavage, is accomplished by the ADAM/TACE (a disintegrin and metallopeptidase/ tumor necrosis factor α converting enzyme) family of membrane bound proteases and results in shedding of the receptor's ectodomain. The remaining, membrane bound notch

receptor then undergoes two transmembrane cleavages (S3/S4) mediated by a γ-secretase enzyme complex composed of presenilins 1 and 2 (PSN), nicastrin (NCT), anterior pharynx defective-1 (Aph-1) and presenilin enhancer-2 (Pen-2). This cleavage releases NICD into the cytoplasm which then translocates into the nucleus and initiates transcription of notch target genes by interacting with the DNA binding CSL (for C-promoter binding factor1 (CBF-1), RBP-Jκ/Su(H) in mammals/Drosophila/ C.elegans) protein. In the absence of NICD, CSL normally binds to promoters of target genes in association with co-repressors including silencing mediator of retinoid and thyroid receptor (SMRT)/nuclear receptor co-receptor (N-coR) and SHARP (SMRT/HDAC-1 associated proteins). NICD interaction with CSL is mediated through its ankryrin repeats and results in displacement of co-repressors from CSL. NICD then recruits the transcriptional co-activator mastermind-like-1 (MAML). Formation of this ternary complex between NICD, CSL and MAML, is required for recruitment of basic transcription machinery to initiate transcription of notch target genes (106-112).

The best characterized primary notch target genes are the beta helix-loop-helix transcription factors of the HES/HERP family. In mammals seven HES (HES1-7) and three Hey (Hey1, 2, L) genes have been identified. Hes and Hey family members often act as transcriptional repressors by either binding to their target genes and recruiting histone modifying enzymes to silence gene transcription or by associating with and rendering other bHLH transcription factors ineffective at binding to their respective promoter elements (113).

Notch signaling function in stem cells

Notch signaling is believed to have two conserved functions in stem cells. First, notch signaling is involved in alternate fate determination whereby activation of the pathway promotes differentiation towards a certain cell fate from a common progenitor at the expense of the alternate fate (114). This function is best exemplified in the development of sensory organ precursor cells in *Drosophila*. A group of ectodermal cells with potential to become neurons arises as pre-neuronal clusters. Some of these cells will express slightly higher levels of Delta and activate notch signaling in the neighboring cells. Loss of function mutations in notch component genes result in the accumulation of neurons (so called neurogenic phenotype) indicating notch signaling inhibits neuronal differentiation (115-117). Similar role for notch in the development of the vertebrate CNS has been shown in neural crest stem cells that have the potential to become either neurons or glia. In these cells, notch signaling directs differentiation towards glia at the expense of neurons (118). Notch signaling plays a similar role in other tissues including directing differentiation towards T-cells at the expense of B-cells from a common lymphoid progenitor in the hematopoetic system and directing differentiation towards enterocytes at the expense of secretory goblet cells in the intestine (119-122).

A second conserved function of notch signaling is in progenitor pool maintenance, as a so called ‘gate keeper’ (119, 123). In many instances, activating notch signaling increases the number of stem/progenitor cells. For example, in the intestine, both enterocytes and goblet cells arise from a common

crypt progenitor cell. Gut specific expression of NICD results in expansion of the crypt progenitor pool. Similarly, notch inhibition using gamma secretase inhibitors or using tissue specific inactivation of CSL/RBP-J results in almost complete absence of crypt progenitors (124-126). In the central nervous system, both gain of function and loss of function studies have shown that Notch signaling maintains undifferentiated progenitor cells. Although recent studies show that functional Notch signaling may be disposable for maintaining HSC pool in adult mice in vivo (127), several gain and loss of function studies show that notch signaling can increase the self renewal capability of HSC in vitro (128-130). For instance, inhibiting notch signaling using dominant negative CSL/RBPJ or MAML or by γ-secretase inhibitor (GSI) treatment, results in accelerated HSC differentiation in vitro and loss of long-term repopulating capability in recipient animals in vivo (130).

Notch signaling function in MSC lineage cells and bone

Genetic mutations or deletion of Jagged-1 results in the autosomal dominant disorder Alagille Syndrome (131). This disorder is characterized by paucity of bile ducts in the liver and abnormal development of multiple organs including the heart, eye, kidney, face and vertebrae (132, 133). The vertebral malformations are due to the role of Notch signaling in the somitogenesis from which vertebral bodies are derived. Somites are derived from presomitic mesoderm by periodic activation of differentiation. The notch target gene Hes-7 is cyclically expressed in the presomitic mesoderm and activates lunatic fringe

which inhibits notch activation. In the absence of this cyclic activation and inhibition of notch signaling, normal patterning of somites is lost and results in abnormal vertebrae patterning (134). Patients with Alagille syndrome also have a decrease in bone mass and are at increased risk for fractures at young age (135). It is not clear, however, whether the decrease in bone mass in Alagille syndrome is secondary to abnormalities in the liver and/or kidney or whether it arises primarily from defects in bone remodeling associated with altered notch signaling (136).

Recent studies using various mouse models have firmly established that notch signaling plays an important role in skeletal development. Engin *et al* (2008) generated a Notch gain of function mouse by over-expressing NICD in osteoblast lineage cells using a 2.3 kb type I collagen promoter (Col2.3). Long bones from these mice appear thickened and on histological examination have increased trabecular bone and increased osteoblast surface. However, both trabecular and cortical bones were composed of immature woven bone, indicating that activating notch in committed osteoblasts either inhibits their terminal differentiation or affects their function. Consistent with this hypothesis, calvarial cells from these mice were found to express higher levels of early osteogenic markers osterix, alkaline phosphatase and Col1A1, but expressed very low levels of the late differentiation marker osteocalcin (137). In another study, Zanotti *et al* used a 3.6kb fragment of the rat type I collagen promoter (Col3.6) to drive expression of NICD in osteoblasts and reported high levels of embryonic lethality, but the few mice that survived were small and had an

osteopenic phenotype with decrease trabecular bone that is due to decrease in osteoblast numbers (138). The difference in phenotype of these two notch gain of function models is likely due to the difference in the pattern of expression of the two promoters used (Col2.3 and Col3.6) to drive NICD expression and suggests that the temporal activation of Notch signaling is important for its effect on osteogenic lineage cells. Engin et al also generated a Notch loss of function mouse using Cre-loxP system to delete presenilins 1 and 2 by crossing presenillin1 $^{fl/fl}$ /presnillin2$^{-/-}$ mice with Col2.3-Cre mice. Although no defect in osteoblast number or bone formation was observed, these mice develop osteopenia at 6 months of age due to an increase in osteoclast activity. The increase in osteoclast activity was due to decreased production of osteoprotegerin by osteoblasts (137). Osteoprotegerin is a decoy receptor that decreases osteoclast activity by antagonizing RANKL.

In a separate study, Hilton *et al* generated transgenic mice in which notch signaling is inhibited in earlier progenitors using Prx-1 promoter (139). Prx-1 is expressed in mesenchymal condensations of developing bones starting at E10.5 (140). The investigators crossed presenillin1 $^{fl/fl}$ /presnillin2$^{-/-}$ mice with Prx-1Cre (PNN) mice to inactivate notch signaling in these early mesenchymal progenitors. Analysis of long bones of the resulting mice which lack both presenilins (PNN) at 8 weeks of age revealed short bones and massive accumulation of trabecular bone. Histomorphometric analysis revealed that the increase in bone mass was due to an increase in osteoblast number and not due to either an increase in osteoblast activity or decreases in osteoclast number or activity indicating the

notch signaling normally inhibits osteogenic differentiation of early progenitors. Investigation of CFU-F numbers as an indicator of progenitor numbers revealed that 8 week old PNN mice had markedly decreased CFU-F numbers indicating that notch signaling normally maintains mesenchymal progenitor numbers in vivo presumably by inhibiting their premature differentiation. Interestingly, even though young PNN mice have markedly increased bone, they progressively lose bone mass as they age such that by 24 months they have ~10% of the bone mass when compared to controls. The authors concluded that notch signaling maintains the osteoprogenitor pool by preventing their premature differentiation.

In addition to the increased osteoblast numbers and trabecular bone at 8 weeks of age, PNN mice have a 'wedge' of cartilage, made up of hypertrophic chondrocytes that extends into the marrow space suggesting that notch signaling also affects chondrogenesis in the growth plate. Indeed, analysis of the long bones from E18.5 embryos revealed that in addition to increase in the numbers of osteoblasts, PNN mice had significant expansion of hypertrophic chondrocytes in the bone marrow space. The increase hypertrophic chondrocytes was due to an increase in proliferation and a delay in their terminal differentiation (139). This embryonic phenotype in growth plate development complicates the interpretation of the increase in trabecular bone.

Both of these groups investigated the molecular mechanisms through which notch signaling affects MSC differentiation and found that Notch signaling inhibited transcriptional activity of Runx-2. Engin *et al* reported physical interaction between NICD and Runx-2 while Hilton et al found that Hey-1 and

Hey-2 were responsible for the decrease in Runx-2 activity. It is therefore possible that Notch signaling could act both in a CSL dependent mechanism through Hey-1 and Hey-2, and a CSL independent mechanism through NICD-Runx-2 interaction to inhibit osteogenic differentiation. Another proposed mechanism for the effects of notch signaling on osteogenic differentiation is through inhibition of Wnt signaling. Over-expressing NICD inhibits Wnt-3a and BMP2 induced alkaline phosphate activity (a measure of osteogenic differentiation) in ST2 marrow stromal cell lines. Although NICD had no effect on BMP2 induced SMAD or MAPK signaling, it was able to inhibit Wnt3a mediated β-catenin stabilization and reporter activity. Restoring β-catenin levels did not rescue NICD mediated decrease in alkaline phosphate activity suggesting that the interaction between Wnt and Notch signaling occurs downstream of GSK-3β. siRNA mediated knock down of Hes-1 was able to partially rescue NICD mediated decreases in wnt signaling activation and decreased alkaline phosphatase activity indicating that Hes-1 is an important mediator of NICD in ST2 cells (141-143).

In addition to the studies mentioned above, several in vitro studies have investigated the effects of notch signaling on the proliferation and differentiation of osteogenic cell lines. Similar to its effect on ST2 cells, stable over-expression of a NICD in Kusa cells (murine MSC cell line) inhibits their osteogenic differentiation while transient over-expression of NICD in ST2 cells or ligand mediated activation in MC3T3E1 pre-osteoblast cell lines promotes their osteogenic differentiation (143-146). These apparently conflicting results again

suggest that temporal expression and/or magnitude of activation may be important for the specific effect of notch signaling on MSC differentiation. Indeed, notch signaling has been shown to have different effects on proliferation and differentiation of other cells types depending on the level of activation (147, 148). Notch signaling has also been shown to influence differentiation towards the chondrogenic and adipogenic cell fates. Activating notch signaling in chick limb bud micro-mass cultures, in ATDC5 cells or in human MSC inhibits their chondrogenic differentiation (149, 150). Similarly, activating notch signaling has been reported to inhibit adipogenic differentiation in 3T3-L1 preadipocytes (151).

TSP2 Notch interaction

Activation of notch signaling can be regulated at multiple levels including transcription, post-translational modifications and stability and transport of either receptors or ligands (152). In addition, recent studies have shown that components of the extracellular matrix, including CCN/NOV, SPARC, and thrombospondins can modulate notch activation in various cell types (153-156).

A study by Meng *et al* recently showed that either over-expressing TSP2 cDNA or treatment with recombinant TSP2 but not TSP1 increases Jag-1 or Dll-4 mediated activation of Hes-1 reporter activity in H460 lung cancer cell lines which selectively expresses Notch 3, but not Notch 1, 2 and 4. Additionally, expression of notch target genes Hes-1, Hes-5 and Hey-1 in arterial smooth muscle cells, which also selectively express Notch-3, was found to be significantly increased in TSP2-null mice relative to wild type controls suggesting that TSP2 regulates

Notch-3 mediated signaling in-vivo. In-vitro binding as well as co-immunoprecipitation assays revealed that TSP2 can directly bind to Notch-3 and Jagged-1. Furthermore, ligand treatment of H460 cells resulted in decreased cell proliferation and over-expressing TSP2 in these cells was able to potentiate ligand mediated inhibition of cell proliferation, indicating that TSP2 modulation of notch signaling likely plays a physiologically relevant function (157).

Rationale/Hypothesis:

In conjunction with decreases in bone mineral density and changes in bone architecture, decreases in MSC number (as measured by CFU-F) and an increase in adipogenic differentiation is observed with aging. These changes in MSC are believed to contribute to the pathogenesis of age associated osteoporosis. However, our understanding of the mechanisms of how progenitor pools are maintained or alternate fate decisions between the osteogenic and adipogenic fates are made is limited.

TSP2 null mice have an increase in CFU-F at a young age and MSC from TSP2 null mice display a delay in mineralization therefore TSP2 is involved in both progenitor pool maintenance and osteogenic differentiation. Whether TSP2 plays a role in adipogenesis is however not known. Furthermore, the molecular mechanisms through which TSP2 affects MSC are also unknown.

Recent studies demonstrate that TSP2 can interact with Notch signaling and modulate it's activation in various cell types. Notch signaling has been shown to maintain MSC pool and inhibit osteogenic differentiation. Because of

the demonstrated interactions between TSP2 and Notch activation, and the similar role TSP2 and Notch signaling appear to play in MSC pool maintenance and differentiation, we hypothesize that TSP2 effects on MSC are mediated through modulation of Notch signaling. **Our overall hypothesis is therefore, as a positive regulator of osteogenesis, TSP2 will inhibit adipogenic differentiation and that TSP2 effects on MSC proliferation and differentiation are mediated through modulation of notch activation.**

Dissertation Overview

In chapter 2, we will investigate whether TSP2 plays a role in adipogenic differentiation in vitro and in vivo. In chapter 3, we will investigate whether notch signaling regulates proliferation and osteogenic and adipogenic differentiation of primary MSC in vitro and whether canonical notch signaling is required for MSC pool maintenance and bone formation in vivo. Finally, in the chapter 4, we will investigate whether TSP2 modulates Notch signaling in MSC (figure 1.1).

Figure 1.1

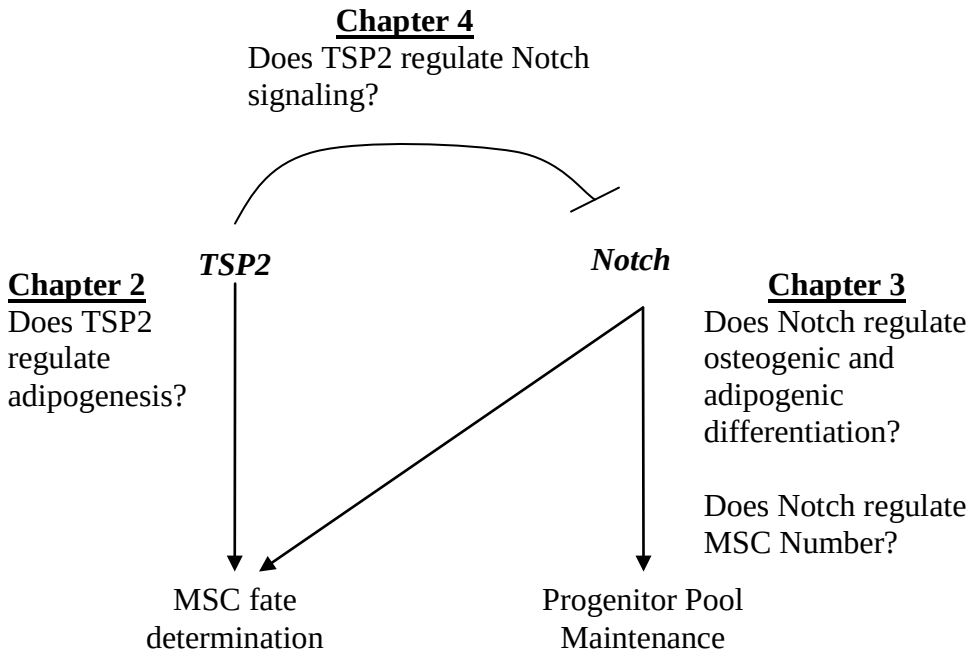

Figure 1.1 Dissertation Overview

CHAPTER II

THROMBOSPONDIN-2 REGULATION OF ADIPOGENIC DIFFERENTIATION

Introduction

Osteoporosis is a disease characterized by osteopenia and increased risk of bone fracture. Along with a decrease in bone mass, an increase in bone marrow adiposity is observed in osteoporosis patients and is believed to contribute to the pathogenesis of the disease (11, 55-57). Although the mechanism for increased adipocytes is currently unknown, one hypothesis is that there is a shift in differentiation of mesenchymal stem cells (MSC) to adipocytes. MSC are precursor cells that give rise to osteoblasts, adipocytes and chondrocytes. Many growth factors and cytokines as well as systemic hormones that regulate MSC differentiation have been identified, and interestingly, in most instances factors that promote osteogenic differentiation also appear to inhibit adipogenic differentiation lending support to the 'differentiation shift' hypothesis (59-61).

The process of adipogenic differentiation is highly-coordinated and is characterized by distinct changes in transcription factor expression and alterations in genes associated with fatty acid metabolism and growth factor

activity. Adipogenic induction results in up regulation of transcription factors in the C/EBP family including C/EBPα and C/EBPβ. These transcription factors in turn activate transcription of PPAR-γ, often referred to as a master regulator of adipogenesis as its activity is both necessary and sufficient for adipogenic differentiation. PPAR-γ then orchestrates expression of genes required for fatty acid metabolism and adipocyte maturation (51-53).

In addition to changes in transcription factors, there are distinct changes in the expression of extracellular matrix (ECM) proteins that occur with the development of mature adipocytes (85, 158). The function of the ECM in regulating adipogenic differentiation is however not well-understood. Recent studies have demonstrated that adhesive substrates promote osteogenesis and inhibit adipogenesis. We have recently reported that heparin promotes adipogenic differentiation by inhibiting focal adhesion formation (84). ECM proteins function not only for adhesion and structural integrity, but also bind to growth factors and interact with cell surface receptors not required for adhesion. For example, mice deficient in the ECM protein, secreted protein acidic and rich in cystine (SPARC), exhibit an increase in subcutaneous and visceral fat due to both an increase in adipocyte numbers and adipocyte size (159). In vitro, adipogenic differentiation is enhanced in stromal cells isolated from bone marrow as well as white adipose tissue (WAT) of SPARC null mice. The molecular mechanism through which SPARC affects adipogenesis appears to be through stabilization of focal adhesions and promotion of integrin linked kinase activity which in turn results in stabilization of β-catenin. β-catenin is a component of the

Wnt signaling pathway that is known to inhibit adipogenic differentiation (160). Intriguing studies recently showed that osteocalcin, an ECM protein exclusively produced by osteoblasts, can regulate energy metabolism by acting on distally located pancreatic islet cells (161, 162). These findings demonstrate that ECM can influence adipogenesis through diverse mechanisms.

Thrombospondin-2 (TSP2) is a large multi-modular protein that belongs to a group of ECM proteins referred to as matricellular proteins— a group of proteins, including SPARC, that interact with cells and other structural ECM proteins but by themselves play minimal structural role (99). TSP2 has been shown to interact with multiple cell receptors, growth factors and ECM proteins and regulates apoptosis, cell proliferation and adhesion. TSP2 is highly expressed in MSC and other mesenchymal derived tissues including adipose tissue (51-53). Previous work has shown that, in mouse adipose tissue, TSP2 mRNA is decreased in the mature adipocyte fraction when compared to the stromal-vascular fraction which contains undifferentiated stem and progenitor cells suggesting that TSP2 expression decreases with adipogenic differentiation (163).

Previous studies have also shown that TSP2 inhibits bone marrow derived MSC proliferation. In addition, TSP2-null MSC display a delay in matrix mineralization indicating that TSP2 promotes osteogenic differentiation in vitro (100, 101). However, whether TSP2 plays a role in adipogenic differentiation is unknown. Because of the reciprocal relationship between osteogenic and

adipogenic fates, we hypothesized that as a protein that promotes osteogenic differentiation, TSP2 will inhibit adipogenic differentiation.

Herein we report that MSC isolated from TSP2 null bone marrow and WAT display an increase in lipid accumulation. TSP2 null mice are heavier than wild type controls due to an increase in adipose tissue. Finally, consistent with its role in promoting osteogenesis and decreasing adipogenesis, TSP2 expression increases during osteogenic differentiation and is inhibited during adipogenesis.

Materials and Methods

Mice: All procedures were approved by the institutional animal care and use committee. TSP2-null mice have been described previously and were generated by targeted disruption of the Thbs2 gene which results in a functional TSP2-null phenotype (101). Coisogenic wild-type 129/SvJ mice were used as controls for comparison. For high fat diet studies, one month old TSP2-null and wild-type control mice were fed control or high fat chow (D12450B or D12451, respectively, Research Diets Inc., New Brunswick, NJ) for 5 months. Mice were weighed weekly and at the end of the 5 month study period, they were anesthetized with pentobarbital sodium (50 mg/kg BW i.p.), and body composition was measured using dual-emission x-ray absorptiometry (DEXA) (PIXImus DEXA, General Electric, Madison, WI). Mice were then euthanized and subcutaneous and visceral fat pads as well as skin and brown fat was isolated and weighed.

Bone marrow MSC isolation: Whole bone marrow was harvested from femora and tibiae of three to four month old TSP2-null and wild type control mice as previously reported (101). Single cell suspensions from three mice were pooled, and then plated onto four 100mm tissue culture plates in MSC media (alpha-minimum Eagle's medium supplemented with 10% fetal bovine serum, 2 mM L-glutamine, 25µg/mL sodium ascorbate, and 100U/mL penicillin and 100µg/mL streptomycin). Cells were cultured for 8 to 10 days with half the media being replaced four days post plating, and every three days until harvest. When cultures reached 80% confluence, cells were trypsinized, and then plated onto 12-well tissue culture plates for differentiation experiments.

Stromal vascular fraction (SVF) cell isolation: Perilumbar fat pads from 3 to 5 mice were minced then digested for 30-60 minutes at 37°C with 2.5mg/ml collagenase II (Sigma-Aldrich). The digest was filtered through a 70µm filter and centrifuged at 500g for 6 min to pellet the SVF cells. The stromal vascular cells were then plated onto 10cm tissue culture plates in SVF media (Dulbecco's modified eagle medium (DMEM) + 10% fetal bovine serum + 100U/mL penicillin and 100µg/mL streptomycin) and passaged when they reached 80% confluence. Third passage cells were used for all experiments.

Cell Culture and treatments:

For adipogenic differentiation, $1X10^5$ primary bone marrow derived MSC or $5X10^4$ ST2 and SVF cells were plated into each well of 12-well tissue culture

plates. Three days post plating, bone marrow derived MSC and ST2 cells were treated with induction media (MSC media containing MDI; 57µM isobutyl-methylxanthine, 1µM dexamethasone, and 1µg/mL insulin or MDI/T; MDI and 5µg/ml troglitazone) for three days then maintained in MSC media containing 1µg/mL insulin for the remaining duration of the experiments. SVF cells were induced two days post plating with the same induction cocktail in SVF media then were switch and maintained in SVF media with 1µg/mL insulin two days post induction. Cells were stained with Oil Red-O and DAPI and five representative images at 40X magnification were captured. Cells staining positive for DAPI and Oil Red-O were counted and compared to total DAPI positive cells. Oil Red-O was then extracted and quantified by measuring absorbance at 540nm in a Varioscan spectrophotometer (Thermo Fisher Scientific, Waltham, MA USA). For osteogenic differentiation, ST2 cells were treated and maintained in MSC media containing 10nM BMP2, 25µg/mL sodium ascorbate and 10mM β-glycerol phosphate.

For pharmacomimetic and inhibitor studies, 3T3-L1 cells were plated at a density of $1X10^5$ cells per well into each well of a 6 well tissue culture plate in L1 media (DMEM, 10% fetal bovine serum, 100U/mL penicillin, 100ug/mL streptomycin) and cultured for 3 days. Cells were then treated with the indicated combinations and concentrations of drugs for 24 hours.

Quantitative RT-PCR: RNA was extracted using RNeasy RNA extraction kit (QIAGEN) according to the manufacturer's instruction and 1µg of total RNA was

reverse transcribed in a 30μL reaction. 2μL of the cDNA generated was used for quantitative real-time PCR reaction using SybrGreen for detection on either a MJR Opticon or an ABI 7500 Fast. Relative change in expression of genes of interest was determined using the $2^{\Delta\Delta C(T)}$ method using β-actin expression as an endogenous control.

Western Blot Analysis: Equal volumes of media collected at the indicated time points were resolved on 8% SDS-PAGE gels, transferred onto nitrocellulose membranes and probed with a mouse TSP2 polyclonal antibody. After incubating with HRP-conjugated secondary antibody, membranes were developed with ECL Chemiluminescent reagent.

Statistical Analysis: Student's t-tests were used to compare means between TSP2-null and wild type and between treated groups and untreated controls.

Results

TSP2-null bone marrow MSC exhibit increased lipid accumulation.

TSP2-null MSC display a delay in osteogenic differentiation. To determine whether TSP2 also plays a role in adipogenic differentiation, first passage bone marrow-derived MSC from TSP2-null and wild-type control mice were induced to undergo adipogenic differentiation using MDI or MDI/T and extent of adipogenic differentiation was evaluated at 10 days post induction by staining intracellular lipid droplets with Oil Red-O and then measuring total extracted Oil Red-O using

spectrophotometry. TSP2-null MSC showed 24% and 25% more Oil Red-O incorporation than wild-type controls at 4 and 10 days post-adipogenic induction, respectively (Figure 2.1 A-C). Evaluation of adipogenic marker gene expression showed expected increases in C/EBP-α, PPAR-γ or FABP-4 expression following adipogenic induction at day 4 and 10 post-induction. However, there were no differences between TSP2-null and wild type MSC in any of the treatment groups at 4 days post adipogenic induction. At 10 days post induction, a 37% increase in C/EBP-α expression in MDI/T induced and a 15% increase in FABP-4 expression was detected in un-induced TSP2-null MSC when compared to wild type MSC that received the same treatments. There was no significant difference in PPAR-γ expression between TSP2-null and wild-type MSC at 10 days post adipogenic induction (Figure 2.2). The increase in lipid accumulation in TSP2-null MSC without significant increases in C/EBP-α, PPAR-γ or FABP-4 expression suggests that TSP2 does not directly affect adipogenic commitment but may act through other mechanisms, such as inhibition of cell proliferation and/or fatty acid uptake, to influence lipid accumulation.

TSP2-null mice exhibit an increase in adipose tissue.

Since TSP2-null marrow MSC showed increased lipid accumulation in vitro, we asked whether TSP2 regulates adipose tissue development in vivo. Age and gender matched six-week old TSP2-null and wild type control mice were placed on either control or high fat diet and were weighed weekly for 22 weeks (Figure 2.3). TSP2-null female mice gained significantly more weight than wild-

type control female mice under control diet. The difference in weight became statistically significant at 17 weeks and was greatest at 22 weeks with TSP2-null mice weighing 30% more than wild-type controls. Interestingly, there was no significant difference in weight between TSP2-null and wild type control male mice fed the control diet or in either male or female TSP2-null and wild type control mice fed a high fat diet (Figure 2.3 A,B).

To determine whether the increase in weight in TSP2-null mice was due to an increase in adipose tissue, we measured body composition of TSP2-null and wild-type mice at the end of the 22 week study period using dual energy X-ray absorptiometry (DEXA) (Figure 2.4). The percentage of total body fat was significantly higher in TSP2-null female mice on control diet when compared to gender matched wild-type controls. No appreciable difference was detected in percent body fat in male mice fed control diet or male or female mice fed high fat diet (Figure 2.4 A,B). There was no appreciable difference in either lean body mass or bone mass between male or female TSP2-null or wild type control mice fed control or high fat diet (data not shown). These results are consistent with results that show significant differences in weight between TSP2-null and control mice for female mice and suggest that the explanation for increased body mass in TSP2-null mice is increased adipose tissue.

To determine whether the increase in adipose tissue in TSP2-null mice occurs at specific sites, subcutaneous fat pads from interscapular and perilumbar regions, visceral fat pads from perirenal and reproductive (ovarian or testicular) regions, as well as brown fat and skin were isolated and weighed (Figure 2.5).

There was a 2.7 fold increase in both perilumbar and interscapular (subcutaneous) fat pads and 1.5 fold increase in skin weight in female TSP2-null mice on control diet when compared to wild type controls. There was no statistically significant difference in visceral (perirenal and reproductive) or brown fat pad weights in either female or male TSP2-null and wild type control mice (Figure 2.5 A). With the exception of a decrease in ovarian fat pad weight in TSP2-null mice, there was no difference in fat pad or skin weights between TSP2-null and wild type control mice fed a high fat diet (Figure 2.5 B). Taken together, these results indicate that TSP2-null female mice weigh more than wild type controls due to an increase in weight of skin and subcutaneous fat.

Adipose tissue derived MSC from TSP2-null mice show increased proliferation and lipid accumulation.

The stromal vascular (S/V) fraction of white adipose tissue contains cells with similar differentiation potential as bone marrow derived MSC. To determine whether the increase in adiposity in TSP2-null mice is due to TSP2 having an effect on proliferation and/or adipogenic differentiation of these adipose tissue derived MSC (AdMSC), cell proliferation and differentiation were examine in S/V cells isolated from perilumbar fat pads of TSP2-null and wild type control mice. To determine whether TSP2 plays a role in AdMSC proliferation, TSP2-null and wild type AdMSC were plated at equal density then were trypsinized and counted every 24 hours for 5 days. The total number of TSP2-null cells was 1.3, 3.3, 4.2 and 4.5 fold higher than wild type controls at 48, 72, 96 and 120 hours,

respectively. This is consistent with published data on marrow-derived TSP2-null MSC which show increased proliferation relative to wild type.

To evaluate whether TSP2 plays a role in adipogenic differentiation of AdMSC, TSP2-null and wild type AdMSC were induced to undergo adipogenic differentiation using MDI or MDI/T and extent of lipid accumulation at 4, 7, and 14 days post induction was measured using Oil Red-O incorporation (Figure 2.7). A statistically significant increase in Oil Red-O staining was observed in TSP2-null AdMSC induced with MDI/T at days 4 and 7 and in MDI induced cells at day 7. There was also significantly more Oil Red-O incorporation in un-induced TSP2 null AdMSC at days 4 and 14 (Figure 2.7 A). To determine whether the increase in Oil Red-O staining in TSP2-null cells was due to an increase in cell number, the number of Oil Red-O staining cells was counted and normalized to the total number of cells as determined by counting the number of DAPI stained nuclei. Similar to Oil Red-O absorbance findings, the number of Oil Red-O positive cells normalized to the total number of cells was significantly increased in MDI/T induced TSP2 null AdMSC at days 4 ,7 and 10, in MDI treated cells at day 7 and in un-induced controls at day 4 and day 7 (Figure 2.7 B). Taken together, these results show that in the absence of TSP2 there is increased lipid accumulation in AdMSC and its effect on lipid accumulation in these cells is independent of its effect on cell proliferation.

TSP2 expression is differentially regulated during osteogenic and adipogenic differentiation

TSP2 is expressed at lower levels in mature adipocyte fractions when compared to the stromal and vascular fractions of adipose tissue suggesting that TSP2 expression may be down-regulated during adipogenic differentiation (163). To better understand the regulation of TSP2 expression during MSC differentiation, bone marrow stromal cell derived ST2 cell lines were induced to undergo osteogenic and adipogenic differentiation and TSP2 mRNA as well as protein secreted into the media was examined at 1, 3, 6, 9, and 12 days post induction (Figure 2.8). TSP2 mRNA levels initially decreased at day 1 post osteogenic induction but gradually increased such that at days 6, 9 and 12 there were 1.7, 3.8, and 6.9 fold increases in TSP2 mRNA expression in osteogenic induced cells relative to un-induced controls, respectively (Figure 2.8 A). TSP2 mRNA decreased to 30% of un-induced controls by day 1 following adipogenic induction and remained at that low level at days 3, 6, 9 and 12 post induction (Figure 2.8 B). To determine whether the differences in TSP2 mRNA expression translated to the protein level, media was collected at the time of RNA harvest and TSP2 protein present in the media was analyzed by western blot. A similar pattern of gradual increase with osteogenic induction and rapid and sustained decrease with adipogenic induction relative to un-induced control cells was observed in TSP2 protein secreted into the media (Figure 2.8 C). Therefore, TSP2 expression at both the mRNA and protein levels, increases with osteogenic differentiation and decreases with adipogenic differentiation.

Components of adipogenic induction cocktail have additive effects in down-regulating TSP2 expression.

To begin to understand the molecular mechanism of TSP2 down-regulation during adipogenesis, we evaluated the influence of the components of the adipogenic cocktail in the down-regulation of TSP2 in 3T3-L1 cells—a pre-adipocyte cell line in which the adipogenic differentiation program has been more thoroughly characterized (Figure 2.9) (164). Similar to ST2 cells, the combination, isobutyl-methylxanthine (IBMX), dexamethasone, and insulin (MDI) had profound effects in down-regulating TSP2 expression in 3T3-L1 cells reducing it to 12.6% of un-induced controls at 24 hours post treatment. When used alone, IBMX, dexamethasone and insulin reduced TSP2 expression to 46%, 51% and 64% of un-induced controls, respectively. Using two of these agents in combination resulted in greater decrease in TSP2 expression than using each one alone indicating that IBMX, dexamethasone and insulin have additive effects in down regulating TSP2 expression (Figure 2.9 A).

IBMX is a phosphodiesterase inhibitor that acts to increase levels of cAMP therefore we examined the relative importance of the cAMP/PKA pathway in regulating TSP2 expression. To determine whether PKA activity is required for down-regulating TSP2 expression, we treated cells with H89, which blocks PKA activity in the presence or absence of the IBMX, Forskolin (a PKA activator), and 8-Br cAMP (a cAMP analog). Treatment with IBMX or Forskolin individually reduced TSP2 expression to 51% and 61% of untreated controls, respectively,

and when used in combination, they reduced TSP2 levels to 12.4% of untreated controls suggesting that these two agents have a synergistic effect on down-regulating TSP2 expression. Although 8-Br cAMP, used at 0.5mM dose did not significantly reduce TSP2 expression, it acted synergistically with IBMX to reduce TSP2 mRNA to 14.7% of untreated controls. H89 by itself did not affect TSP2 expression but it completely abrogated the effect of IBMX and Forskolin on down-regulating TSP2 expression (Figure 2.8 B). To determine whether increasing cAMP levels is sufficient to inhibit TSP2 expression, cells were treated with increasing doses of 8-Br cAMP for 24 hours and TSP2 mRNA levels were analyzed. Although treating cells with 0.5mM of 8-Br cAMP did not result in a statistically significant decrease in TSP2 expression, 2.5mM and 12.5mM of 8-Br cAMP reduced TSP2 mRNA to 22.4% and 11.5% of untreated controls, respectively, indicating that increasing cAMP levels is sufficient to down regulate TSP2 expression in 3T3-L1 cells.

Discussion

We have previously shown that TSP2 promotes osteogenic differentiation of bone marrow derived MSC. Because of the reciprocal relationship between osteogenic and adipogenic cell fates, in this study, we examined the role of TSP2 in adipogenesis in vitro and in vivo.

Our results show that bone marrow derived TSP2-null MSC show an increase in lipid accumulation when compared to wild type controls. Surprisingly, there was no significant increase in expression of PPAR-γ, a key transcription

factor believed to be a master regulator of adipogenesis, at either day 4 or day 10 post adipogenic induction. C/EBP-α, an early adipogenic transcription factor that acts to up-regulate PPAR-γ, only showed a slight increase in expression at day 10 after peak expression in all three marker genes examined has occurred. The lack of major differences in gene expression of these two transcription factors between TSP2-null and wild type MSC suggests that TSP2 decreases lipid accumulation in bone marrow MSC not by directly regulating adipogenic differentiation but rather though an independent mechanism. Similar to bone marrow MSC, TSP2-null adipose tissue derived MSC showed an increase in proliferation and lipid accumulation. By normalizing the number of lipid droplet containing adipocytes to the total number of cells, we found that TSP2 decreases lipid accumulation in AdMSC independent of its effect on cell proliferation.

The cellular and molecular mechanisms through which TSP2 influences adipogenesis were not investigated in this study, but there are several possible considerations. First, because TSP2 binds to CD36, Fatty Acid Transporter, which is a Class B Scavenger Receptor, TSP2 could interfere with CD36 uptake of long-chain fatty acids and disrupt adipogenesis (165). Alternatively, it has been proposed that pre-adipocytes need to progress through clonal expansion early in adipocyte differentiation and TSP2, as a potent inhibitor of cell proliferation, may play an inhibitory role in this processes (166). Intriguing recent work has shown that TSP2 directly interacts with Notch, and depending on the cell-type examined may either promote or inhibit Notch signaling (156). Notch

signaling has been shown to regulate adipogenesis and TSP2 could also act through notch to decrease adipogenesis (167).

We also examined whether TSP2 plays a role in adipose tissue development in vivo and found that TSP2-null female mice weigh more than age and gender matched wild type control mice. The increase in weight appeared to be due to an increase in adipose tissue and skin. One primary function of adipose tissue is to store excess energy in the form of neutral triglycerides. Excess energy can occur in a closed system either secondary to a decrease in energy expenditure or an increase in food intake. Future studies should examine whether an increase in food intake or a decrease in energy expenditure enables an increase in adipose tissue in TSP2-null female mice.

The effects of TSP2 on body weight and adipose tissue development were only observed in female mice suggesting that TSP2 may alter adipose tissue regulation by female sex hormones. Interestingly, the absence of TSP2 has been shown to protect against ovariecomy-induced bone loss (168). It is well known that estrogen, produced by the ovaries, is a major regulator of adipose tissue development (169). It will be interesting to determine whether TSP2 can modulate the actions of estrogen or other female sex hormones on adipose tissue development.

We also examined TSP2 expression during MSC differentiation and found that consistent with a role in promoting osteogenic differentiation and decreasing adipogenesis, TSP2 expression is up-regulated during osteogenic differentiation and is inhibited during adipogenic differentiation. The observation that TSP2

down-regulation occurs within 24 hours of adipogenic induction suggests that down regulation of TSP2 expression may be important for early adipocyte development and maturation. We also found that activation of cAMP dependent PKA pathway during adipogenic differentiation plays a major role in down-regulating TSP2-expression. Although their mechanisms were not examined further in this study, dexamethasone and insulin used in the adipogenic induction cocktail were also found to play a role in down-regulating TSP2 expression.

Here we have described an inhibitory role for TSP2 on adipogenesis in-vitro and in vivo and have characterized the changes that occur in TSP2 expression levels with MSC differentiation. Future studies will address the mechanisms through which TSP2 affects adipose tissue development at the molecular, cellular and whole animal level.

Figure 2.1

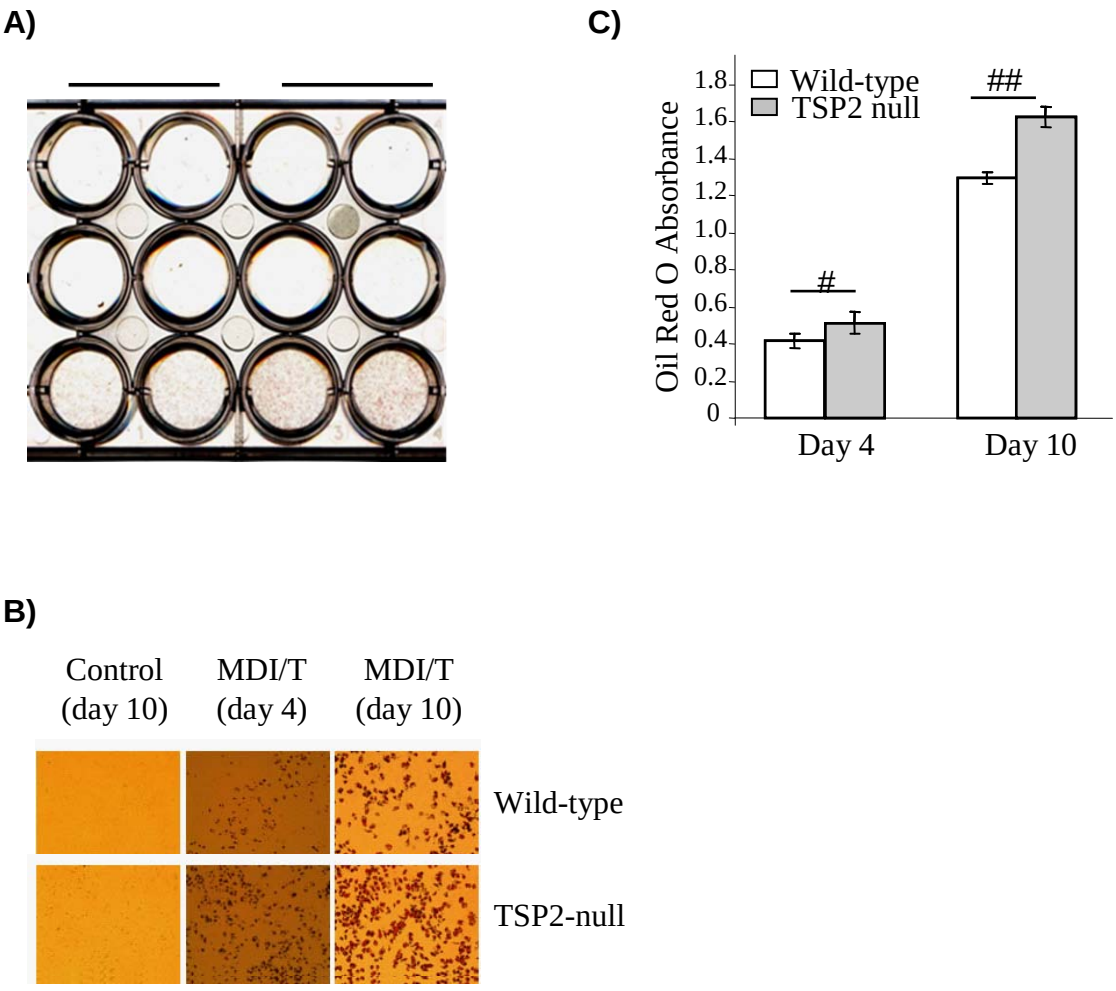

Figure 2.1 TSP2 Inhibits lipid accumulation in bone marrow MSC. MSC isolated from bone marrow of wild-type and TSP2-null mice were induced to undergo adipogenic differentiation using MDI or MDI/T then stained with Oil Red-O at 4 and 10 days post induction. Image of representative Oil Red-O stained plate at 10 days post adipogenic induction **(A)** and representative 10X magnification images of cells induced with the indicated treatments **(B)** are shown. To quantify lipid accumulation, Oil-Red O was extracted from MDI/T induced cells at 4 and10 days post adipogenic induction and absorbance was measured at 540 nm **(C)**. The results shown are representative of two independent experiments each performed in duplicate. For each experiment MSC were obtained from 3 wild type and 3 TSP2-null mice and whole marrow pooled to yield MSC. (Error bars represent standard deviation. # = TSP2-null significantly different from wild type; #, *p < 0.05; ##, p<0.005).*

Figure 2.2

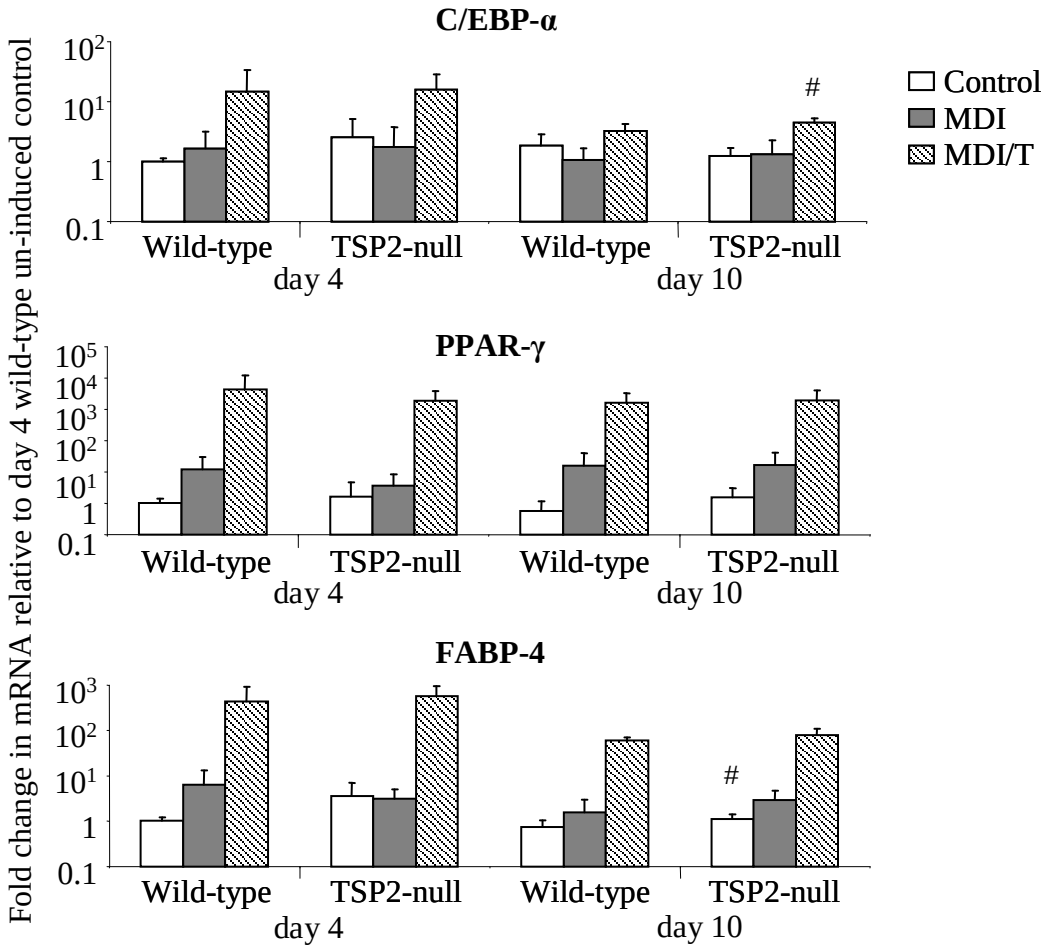

Figure 2.2 Minor differences in expression of adipogenic marker genes exist between TSP2-null and wild-type MSC. Bone marrow derived MSC from TSP2-null and wild-type control mice were induced to undergo adipogenic differentiation with either MDI or MDI/T. Cells were harvested at 4 and 10 days post adipogenic induction and expression of adipogenic differentiation marker genes C/EBP-α, PPAR-γ, and FABP-4 was analyzed by qPCR. The results shown are averages of two independent experiments each performed in duplicate. Error bars represent standard deviation. # =TSP2-null significantly different from wild type; $p < 0.05$

Figure 2.3

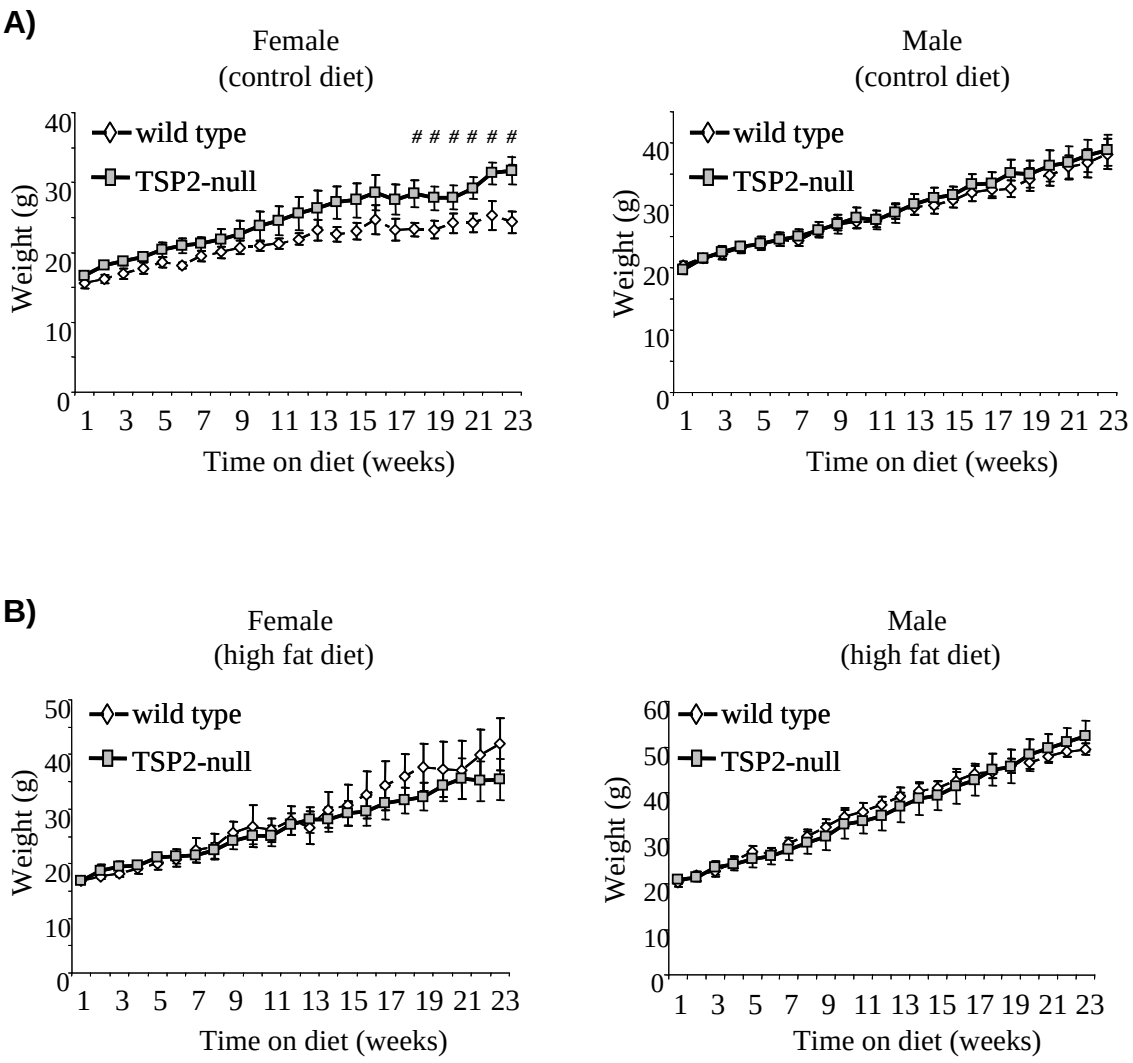

Figure 2.3 TSP2-null mice are heavier than wild-type control mice but do not gain appreciably more weight on high fat diet. 6 week old TSP2-null and wild-type mice from at least four litters were randomly placed on either a control or a high fat diet for 22 weeks. Mice were weighed weekly and the average body weight for each group (± SEM) at each time point is depicted in the graphs. **(A)** Control diet: Female (wild-type n=5, TSP2-null n=5); Male (wild-type n=8; TSP2-null n=6) **(B)** High calorie diet: Female (wild-type n=5, TSP2-null n=5); Male (wild-type n=9; TSP2-null n=6). A statistically significant increase in body weight was observed at weeks 17 through 22 for female TSP2 null mice fed the control diet relative to wild type control mice on the same diet. (# = TSP2-null significantly different from wild type; $p < 0.05$).

Figure 2.4

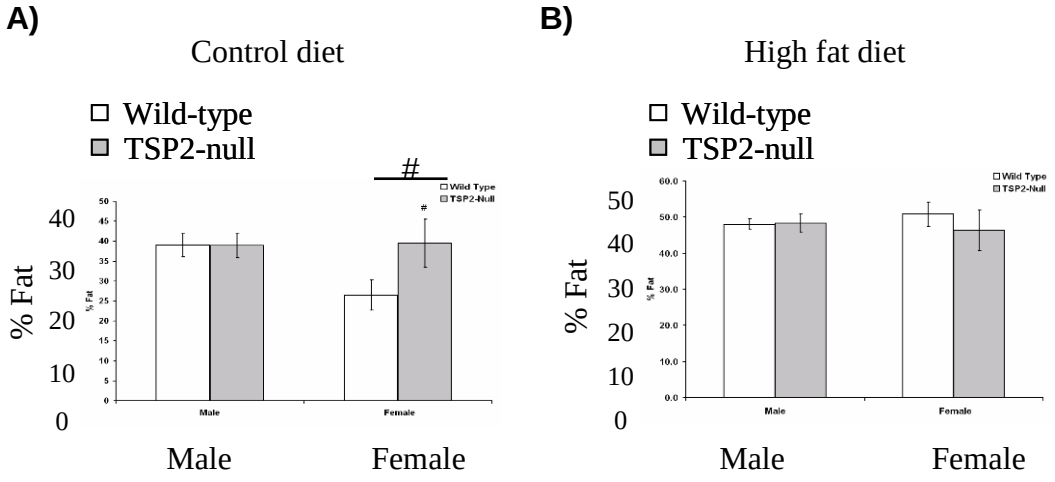

Figure 2.4 TSP2-null female mice on control diet have an increase in adipose tissue. Total body composition of TSP2-null and wild-type control mice fed either a control diet **(A)** or a high fat diet **(B)** for 22 weeks starting at 6 weeks of age was measured using dual-emission x-ray absorptiometry (DEXA). The percentage of fat tissue is depicted as mean ± SEM . Wild-type (control diet, male n=7, female n= 5) and high calorie diet (male n=9, female n= 5)) and TSP2-Null (control diet male n=6, female n= 5 and high fat diet male n=6, female n= 5); # = significantly different from wild type; $p < 0.05$. There was no significant difference in lean mass or bone mass percentages between TSP2-null and wild-type control mice (data not shown).

Figure 2.5

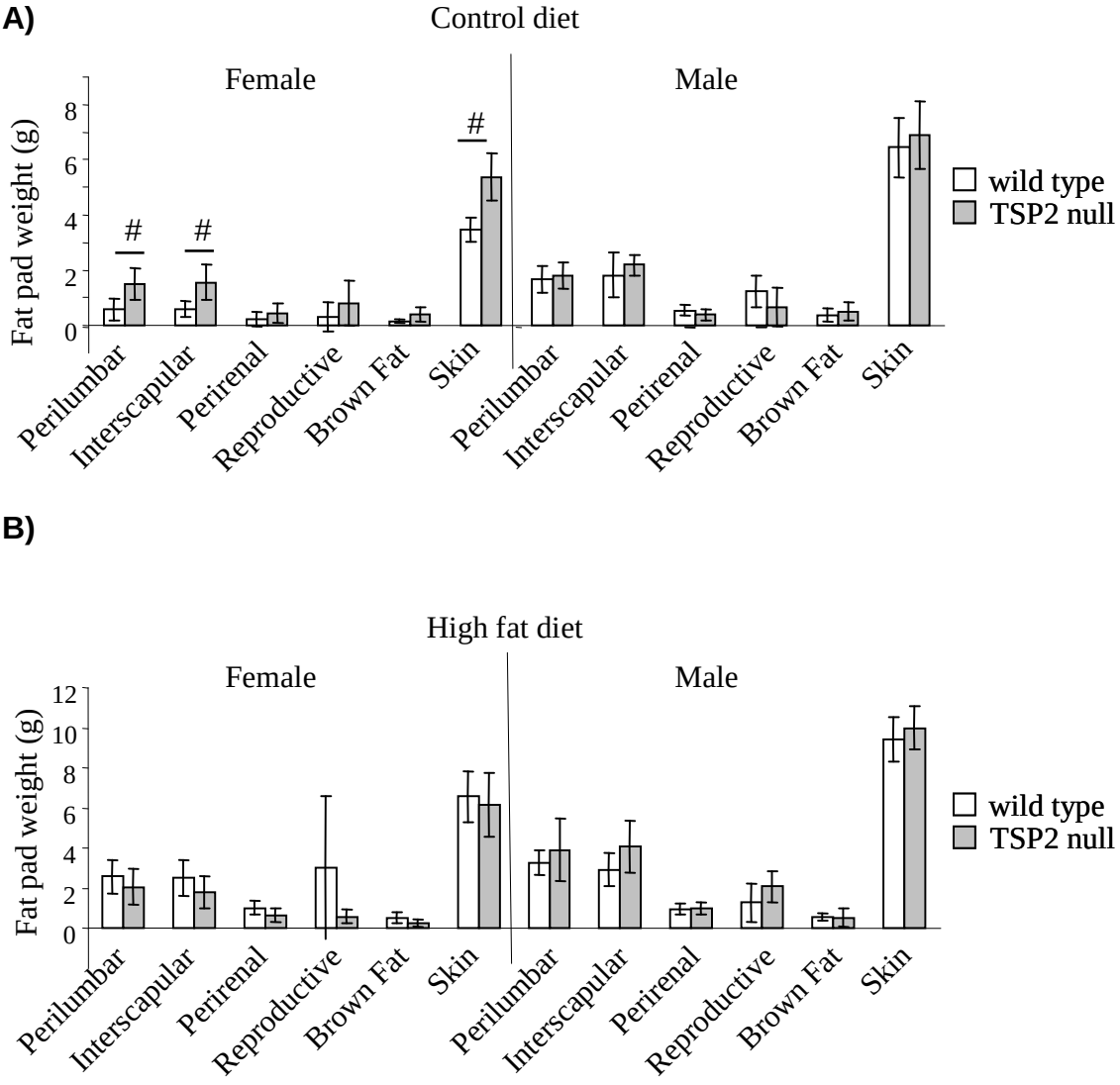

Figure 2.5 Subcutaneous fat pads and skin from TSP2-null mice weigh more that wild-type controls. Fat pads and skin from TSP2-null and wild type mice fed either control **(A)** or high fat diet **(B)** were harvested and weighed. A statistically significant increase in perilumbar and interscapular (subcutaneous) fat pad as well as skin weight was observed in female TSP2-null mice on control diet. Values are mean ± SEM. Wild type (control diet male n=7, female n= 5 and high calorie diet male n=9, female n= 5) and TSP2-null (control diet male n=6, female n= 5) and high calorie diet male n=6, female n= 5); # = TSP2-null significantly different from wild type; $p < 0.05$.

Figure 2.6

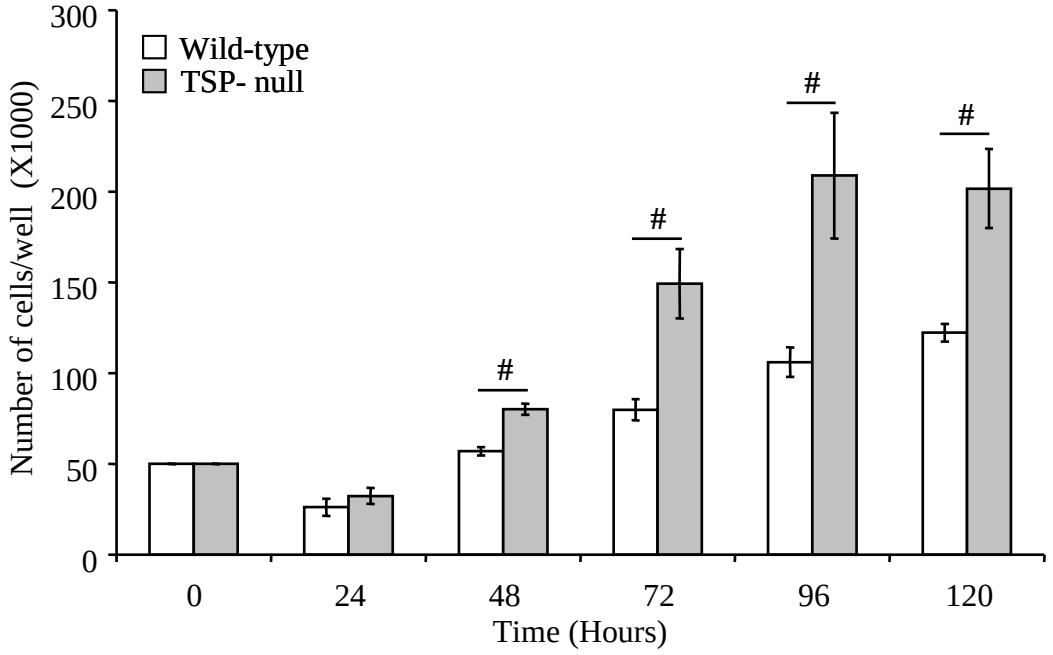

Figure 2.6 Adipose tissue derived MSC from TSP2-null mice show increased proliferation. Adipose tissue derived MSC were plated at 50,000 cells/well in 12 well tissue culture plates then were trypsinized and counted at the indicated time points. Statistically significant increase in TSP2-null cell numbers relative to wild type controls was observed at 48, 72, 96, and 120 hours post plating. Values shown are mean $\pm$ SEM of five independent experiments conducted on five independent age-matched cell harvests. # = TSP2-null significantly different from wild type; $p < 0.05$

Figure 2.7

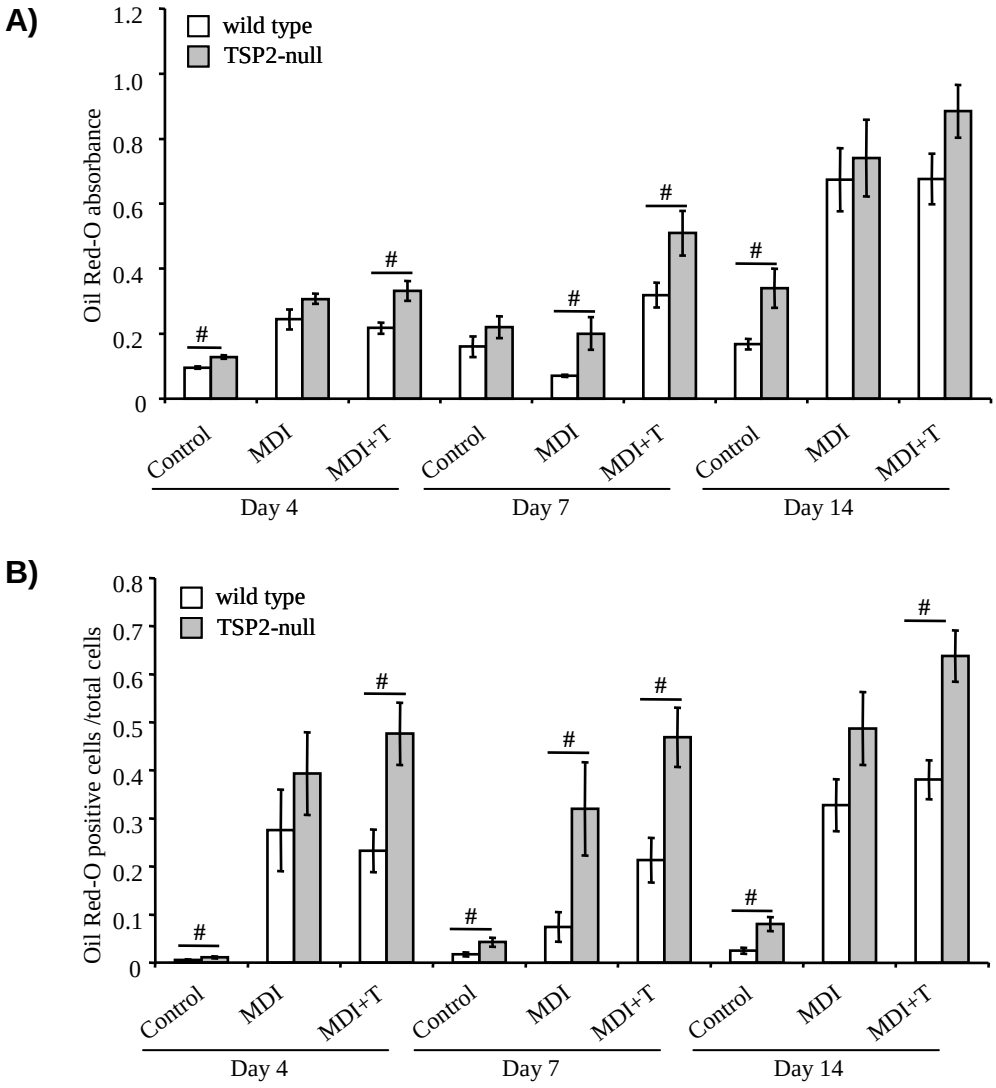

Figure 2.7 TSP2-null adipose tissue derived MSC show increased lipid accumulation. Adipose tissue derived MSC were induced to undergo adipogenesis with either MDI or MDI/T then were fixed and stained with DAPI and Oil Red-O at days 4, 7 and 14 post induction. Five representative images were captured at 40X magnification from each well then Oil Red-O was extracted and quantified by measuring absorbance at 540 nm (A). The number of Oil Red-O stained cells in captured image were counted and normalized to the total number of cells (DAPI staining nuclei) to account for differences in cell proliferation between TSP2 null and wild type MSC (B). Values are mean $\pm$ SEM of 3 independent experiments from 3 independent harvests. # = TSP2-null significantly different from wild type; $p < 0.05$.

Figure 2.8

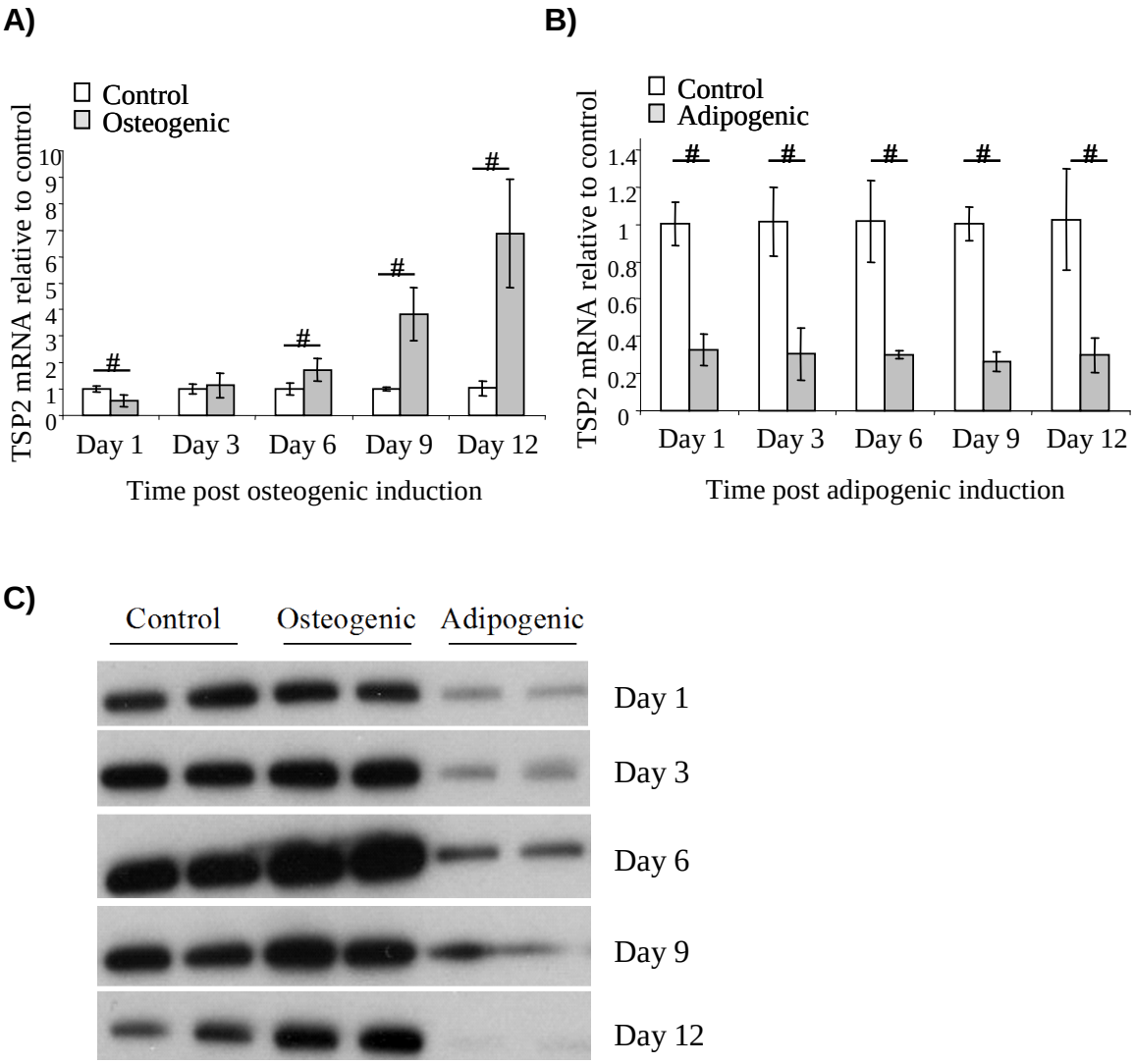

Figure 2.8 TSP2 expression is reciprocally regulated during adipogenic and osteogenic differentiation. ST2 cells were induced to undergo osteogenic and adipogenic differentiation for 12 days. Cells were harvested at the indicated time points following induction and TSP2 mRNA expression relative to un-induced control cells harvested at the same time was measured by quantitative real-time PCR (A,B). Media was also collected at the indicated time points and the amount of TSP2 protein secreted into the media was estimated by resolving equal volumes of media on SDS-PAGE gels and western-blot analysis (C). Results shown are mean ± S.D. of two independent experiments each done in duplicate. # = TSP2-null significantly different from control treated cells; $p < 0.05$.

Figure 2.9

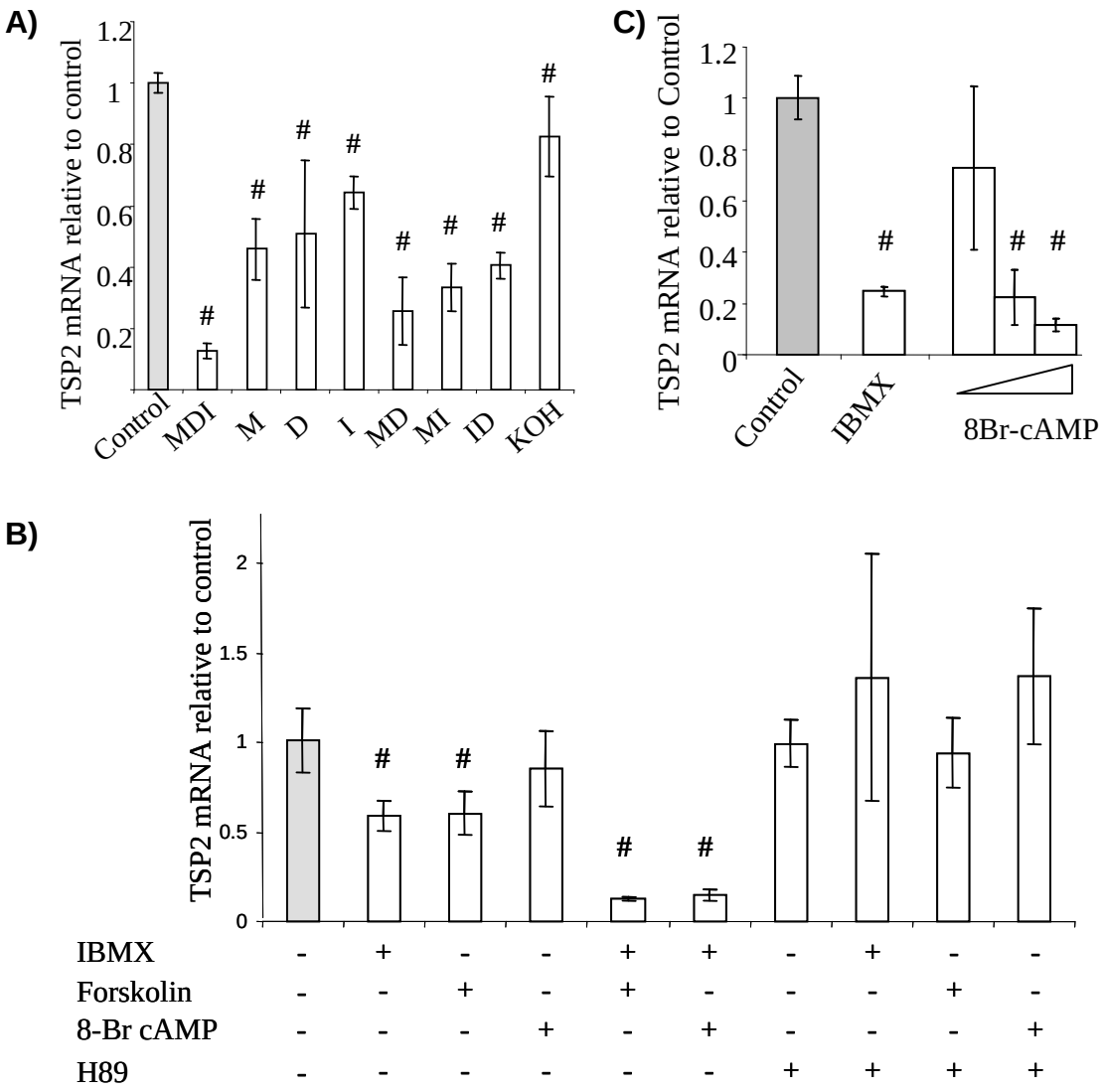

Figure 2.9 Components of adipogenic induction cocktail additively down-regulate TSP2 expression. Confluent 3T3-L1 cells were treated with the indicated combinations of adipogenic induction cocktail for 24 hours then TSP2 mRNA was measured using qPCR. (M, IBMX: D, Dexamethasone: I, Insulin) **(A)** 3T3-L1 cells were treated with the indicated combination of IBMX (100µM), forskolin (10µM), 8-Br cAMP (0.5mM) or H89 (20µM) for 24 hours and TSP2 mRNA levels were analyzed by qPCR **(B)**. 3T3-L1 cells were treated with either 100mM IBMX or increasing doses of 8Br-cAMP (0.5mM, 2.5mM and 12.5mM) for 24 hours and TSP2 expression was analyzed by qPCR **(C)**. Data shown are mean ± S.D. of two independent experiments each done in duplicate. (# = TSP2-null significantly different from control treated cells; $p < 0.05$).

CHAPTER III

MSC FATE DETERMINATION BY NOTCH SIGNALING

Introduction

Bone remodeling is a complex process by which old bone is resorbed and new bone is formed through the actions of osteoclasts and osteoblasts. Under normal physiological conditions, bone resorption and bone formation are maintained in homeostasis (1, 2). Imbalances from either a net decrease in bone formation or a net increase in bone resorption result in decreased bone mass (osteopenia). If osteopenia is severe enough, it results in the clinical condition osteoporosis which is characterized by increased risk of bone fracture. Although the causes of osteoporosis are multi-factorial and include genetic and environmental causes, increased age is one of the most significant risk factors. In age associated (senile) osteoporosis, there is a decrease in both bone formation and bone resorption but the decrease in bone formation is greater than the decrease in bone resorption, therefore age associated osteoporosis is primarily a disease of decreased bone formation (6-11).

Bone is formed by osteoblasts derived from mesenchymal stem cells (MSC). MSC are a mixed population of cells that are isolated from bone marrow by their ability to strongly adhere to tissue culture plastic. When whole bone

marrow is plated at low density, MSC form single cell derived fibroblastic colonies (CFU-F). The number of CFU-F correlates with the number of osteoprogenitor cells in vivo and is commonly used to estimate the number of progenitor cells that are present in vivo. CFU-F numbers decline with ageing which suggests that a decline in osteoprogenitor numbers may contribute to age associated decrease in bone formation (170, 171).

In addition to a decrease in bone mass, an increase in bone marrow adiposity is also observed in osteoporosis patients and in other bone loss conditions (55, 57). Since bone marrow adipocytes are also derived from MSC, a shift in differentiation from osteoblast to adipocyte lineage has also been proposed as another possible mechanism for age associated decrease in bone formation. However, mechanisms responsible for maintaining MSC number in vivo and determining osteogenic vs. adipogenic fate are not well understood.

Notch is a highly conserved cell-to-cell signaling mechanism that appears to have two conserved functions in stem cells. First, notch signaling directs differentiation of stem cells towards one cell fate at the expense of an alternative fate. For instance, activation of notch signaling in neural stem cells results in their differentiation to glia at the expense of neurons (112). Similarly, in the hematopoetic system, notch directs differentiation of common lymphoid progenitors towards T-cells at the expense of B-cells (172). Second, Notch signaling maintains the stem/progenitor cell pool in many organs often by inhibiting differentiation. For example, in skeletal muscle, activation of notch signaling inhibits differentiation of muscle progenitors and interfering with the

pathway results in excessive myogenic differentiation and depletion of the progenitor cell pool. Stem cell depletion in notch loss of function models and/or stem cell expansion in notch gain of function studies have been reported in stem cells in the intestine, central nervous and hematopoetic systems (117-120).

Notch receptors are single pass transmembrane proteins that interact with ligands of the delta/serrate (delta-like and Jagged) family. Ligand binding to receptor results in a series of enzymatic cleavages that ultimately result in the release of the notch intracellular domain (NICD) into the cytoplasm. The first cleavage is mediated through ADAMS/TACE family of membrane bound metaloproteinases and results in the removal of the notch receptor ectodomain. The second cleavage, mediated by a multi-protein γ-secretase enzyme complex which includes presenilins (PSN1 and 2) as its catalytic unit, results in the release of NICD from the cell membrane into the cytoplasm. NICD then translocates to the nucleus and binds to the DNA binding transcription factor CSL (for CBF1, Suppressor of Hairless, or Lag-1). In the absence of NICD, CSL binds to promoter elements in association with co-repressors and acts to inhibit target gene expression. NICD binding to CSL displaces co-repressors and recruits the transcriptional co-activator Mastermind Like-1 (MAML). Formation of NICD/CSL/MAML complex is required for recruitment of the basic transcriptional machinery to initiate transcription of notch target genes (104-110). The best characterized notch targets are the beta-helix-loop-helix transcription factors of the Hes and HERP/Hey family (111). In mammals 4 members of the Hes family

(Hes-1, 3, 5 and 7) and 3 members of the Hey family (Hey-1, 2 and L) have been shown to be direct targets of CSL mediated “canonical” notch signaling (111).

Several lines of evidence indicate that notch signaling plays an important role in development and maintenance of bone. A loss of function mutation in the notch ligand Jagged-1 in humans results in Alagille Syndrome; an autosomal dominant disorder characterized by abnormalities of the bile duct, heart and vertebrae (173). Mutations in Dll-3 in mice has also been reported to cause vertebral malformation indicating that notch signaling plays a role in vertebral segmentation during embryonic development (174).

Several studies that have investigated the role of notch signaling on MSC proliferation and differentiation in vitro have reported conflicting results. For instance, while stable over-expression of a constitutively active notch intracellular domain (NICD) in ST2 or Kusa cells (both are murine MSC cell lines) inhibits their osteogenic differentiation, transient over-expression of NICD in ST2 cells or ligand mediated activation in MC3T3E1 pre-osteoblast cell lines promotes their osteogenic differentiation (143-146). Similarly, over-expressing NICD has been reported to inhibit adipogenic differentiation, while siRNA medicated knock down of Hes-1 also decreased adipogenesis in 3T3-L1 pre-adipocytes (151). These apparently conflicting results suggest that effects of Notch signaling on MSC differentiation in vitro are either cell type dependent or the temporal expression and magnitude of activation is important for the specific effect of notch on MSC differentiation.

More recent studies have established the importance of Notch signaling in regulating MSC lineage cells in vivo. Over-expressing NICD in osteoblasts using a 2.3kb type I collagen promoter was shown to increase immature, woven trabecular and cortical bone. The increase in bone mass was due to an increase in osteoblast number caused by an increase in proliferation. The osteoblasts present were less mature than wild-type controls as demonstrated by decreased expression of late differentiation markers (137). This gain of function model demonstrates that notch signaling is sufficient to promote osteoblast proliferation but it inhibits terminal differentiation or proper function of osteoblasts. In another study, over-expressing NICD from a different type I collagen promoter (Col3.6) resulted in high levels of embryonic lethality. In contrast to the Col2.3-NICD mice, the few mice that survived displayed an osteopenic phenotype with decreased trabecular bone mass (136). Taken together, these two studies again suggest that temporal activation of Notch signaling may be important for its effect on osteogenic differentiation.

Hilton et al crossed Prx-1Cre mice with Notch1$^{-/f}$ /Notch2$^{fl/fl}$ or Psen1$^{fl/fl}$/ Psen2 $^{-/-}$ mice to inactivate notch signaling in early mesenchymal progenitors by deleting Notch 1 and 2 or presenilins 1 and 2 (175). Mice in which notch signaling was inactivated in these early mesenchymal progenitors displayed a decrease in CFU-F numbers and massive accumulation of trabecular bone at 8 weeks of age. Interestingly, as these mice aged, there was significant decrease in bone mass such that at 24 weeks of age, they had ~10% of the bone mass as

wild type controls. The authors of that study concluded that notch signaling maintains osteoprogenitor numbers by preventing osteogenic differentiation.

Molecular mechanisms through which notch signaling influences osteogenic differentiation have also been examined. Engin et al demonstrated direct interaction between NICD and the osteoblast transcription factor Runx-2, while Hilton et al showed that both Hey-1 and Hey-2 physically interact with Runx-2 (137, 175). Both studies further showed these physical interactions with Runx-2 resulted in a decrease in Runx-2 transcriptional activity at a well-characterized osteocalcin promoter. Another proposed mechanism for notch mediated inhibition of osteogenesis is that Notch signaling, acting through Hes-1, blocks osteogenic differentiation by blocking wnt signal activation (139-141). Considered together, these results suggest that Notch may act through both canonical (through CSL and Hes and Hey transcription) and non canonical (direct interaction between NICD and Runx-2) mechanisms to regulate MSC differentiation.

Although these previous studies firmly establish a role for notch signaling in regulating MSC fate, several questions remain. First, although the role of notch signaling on osteogenic and adipogenic differentiation was investigated in various cell lines, no study to our knowledge has examine the effects of activating notch on differentiation and proliferation of primary MSC. Second, whether any or all of the effects of notch signaling in vivo are mediated through CSL-mediated signaling has not been shown. Finally, it is not clear whether the increase in bone mass seen at a young age in Prx-1 mediated Notch inactivation

models is due to embryonic developmental defects that persist post-natal or whether it is something that truly arises from an increase in osteogenic differentiation.

Herein, we address these issues by examining the role of notch signaling on primary murine MSC proliferation and differentiation. Additionally, we examine the impact of specifically inactivating canonical notch signaling using a Cre-loxP regulated dominant negative form of MAML (dnMAML).

Materials and Methods:

Mice: Prx-1Cre, Mx-1Cre, Col2.3Cre and dnMAML$^{fl/fl}$ mice have been described (121, 176-178). All procedures were approved by the institutional animal care and use committee. Cre transgenic mice were crossed with dnMAML$^{fl/fl}$ and either F1 or F2 generation mice were euthanized at indicated ages and hind-limbs harvested for either microCT analysis or cell harvest. To induce cre recombinase expression in Mx1Cre/dnMAML mice, 500µg Polyinosinic:Polycytidylic acid (P(I):(C))(Sigma, St. Louis, MO) was administered i.p. every 2 days for 20 days starting at eight week of age as previously described (127).

Cell culture and treatment: Whole bone marrow from femora and tibiae of C57/BL6 mice was cultured in MSC media (alpha-Minimum Eagle's medium supplemented with 10% fetal bovine serum, 2 mM L-glutamine, 25µg/mL sodium ascorbate, and 100U/mL penicillin and 100µg/mL streptomycin) for 8 to 10 days.

When cultures reached 80% confluence, cells were trypsinized, then plated onto 12-well or 24-well tissue culture plates at a density of $1X10^5$ or $0.5X10^5$ cells per well, respectively. To activate Notch signaling using immobilized Jagged-1 tissue culture plates were pre-coated with 10µg/mL anti-Fc IgG antibody (Jackson Immunoresearch) for 1 hour then treated with the indicated concentration of recombinant rat Jagged-1/human Fc-IgG chimeric protein for 2 hours (R&D Systems). Wells that were coated with the anti-Fc antibody but not treated with the Jagged-1 protein served as negative controls.

CFU-F assay: Single cell suspensions of whole bone marrow were counted and $3X10^6$ cells were plated onto 60cm tissue culture plates in MSC media. Half the media was replaced four days post plating then every 3 days for 13 days. CFU-F plates were then fixed and stained for alkaline phosphatase activity as previously described (103) and total, as well as alkaline phosphatase positive colonies were counted under a dissecting microscope.

Induction of osteogenic and adipogenic differentiation: For osteogenic differentiation, cells were treated and maintained in osteogenic media containing 5mM β-glycerol phosphate and 100µM ascorbate. For adipogenic induction, cells were grown until they reached confluence and induced with MDIT (57µM isobutyl-methylxanthine, 1µM dexamethasone, and 1µg/mL insulin, and 5µg/mL troglitazone) for three days then maintained in 1µg/mL insulin for the remainder of the differentiation experiments. Extent of osteogenic and adipogenic

differentiation was evaluated by Alizarin Red-S or Oil Red-O staining, respectively. In some experiments 1μM of gamma secretase inhibitor (GSI), L-685,458 (Sigma) was added daily to cells to bock notch signaling.

RNA extraction and quantitative RT- PCR: RNA was extracted using RNeasy RNA extraction kit (Qiagen) according to the manufacturer's instruction and 1μg of total RNA was reverse transcribed in a 20μL reaction. 1μL of the cDNA generated was used for quantitative real-time PCR reaction using SybrGreen for detection on ABI 7500 Fast real-time PCR machine. Relative changes in gene expression were determined by the $2^{\Delta\Delta C(T)}$ method using β-actin as an endogenous control.

Statistical Analysis: Student's t-tests were used to compare means between control treated and Jagged-1 treated groups. Two-way ANOVA analysis was used to determine whether micro-CT parameters were significantly different between Cre^{+} mice and Cre^{-} controls.

Results

Jagged-1 decreases matrix mineralization and osteocalcin expression.

Several investigators have examined the role of notch signaling on osteogenic and adipogenic differentiation in vitro and have reported conflicting results (141-144). Significant limitations of these previous studies include the use of

immortalized cell-lines which may not accurately reflect the behavior of primary cells and the reliance on over-expressed NICD to activate notch signaling which may result in super-physiological levels of notch activation. To overcome these limitations, we evaluated the effects of ligand mediated activation of notch signaling on MSC differentiation.

Primary MSC from wild type C57/BL6 mice were plated onto wells coated with either Fc-control or Jagged-1 and were induced to undergo osteogenesis 4 days later in the presence or absence of a γ-secretase inhibitor (GSI) (Figure 3.1 A). Alizarin Red-S staining at 4 and 8 days post induction revealed decreased mineralized matrix formation in cells plated on Jagged-1 relative to cells plated on Fc-control. Although GSI treatment by itself did not have an apparent effect on mineralized matrix formation, it was able to rescue the decrease in mineralization caused by Jagged-1 treatment. To determine whether Jagged-1 affects osteogenic differentiation, expression of the late osteogenic differentiation marker osteocalcin was evaluated in MSC plated on either Fc control or Jagged-1 and induced to undergo osteogenesis for 8 days. Jagged-1 treatment reduced osteocalcin expression to 26% of cells treated with the Fc-control (Figure 3.1 B). To determine whether Jagged-1 causes decreased mineralization by decreasing cell numbers, equal numbers of MSC were plated onto wells coated with either Jagged-1 or Fc-control then were trypsinized and counted using a hemocytometer. Plating cells on Jagged-1 resulted in a 59% increase in cell number relative to Fc-control (Figure 3.1 C). Taken together, these results

suggest that Jagged-1 reduces osteogenic differentiation and increases cell number.

Osteogenic induction decreases Hey-1 and Hey-L expression.

Members of the Hes and Hey family of transcription factors are believed to be major effectors of notch signaling. To determine if Jagged-1 treatment or osteogenic induction alter expression of these notch target genes, MSC were plated onto wells coated with either Jagged-1 or Fc-control and were induced to undergo osteogenic differentiation 4 days later. RNA was harvested at 4 and 8 days post osteogenic induction and expression of the six Hes and Hey family members believed to be notch responsive (Hes-1, Hes-5, Hes-7, Hey-1, Hey-2 and Hey-L) was measured by qPCR. No appreciable change in expression of Hes-1, Hes-5 or Hes-7 was detected with either Jagged-1 treatment or osteogenic induction. Hey-1, Hey-2 and Hey-L expression increased greater than 10 fold in cells plated on Jagged-1 relative to Fc controls in both osteogenic induced and control treated cells at day 4 and remained at that increased level at day 8 (Figure 3.2, data not shown). Interestingly, osteogenic induction reduced Hey-1 expression to 56% and 27% of un-induced controls at 4 and 8 days post osteogenic induction, respectively. Similarly, osteogenic induction decreased Hey-L levels to 72% and 28% of un-induced controls 4 and 8 post induction, respectively (Figure 3.2). There was no appreciable change in Hey-2 expression with osteogenic induction (data not shown). Taken together, these results suggest that Hey-1, Hey-2 and Hey-L are responsive to notch signaling

activation by Jagged-1 in MSC and Hey-1 and Hey-L may be important mediators of notch signaling in MSC during osteoblast differentiation.

Jagged-1 increases lipid accumulation by increasing cell number.

To examine the role of activating notch signaling on adipogenic differentiation, primary MSC were grown on either Jagged-1 or Fc-control coated wells for four days. Cells were then induced to undergo adipogenic differentiation for 10 days in the presence or absence of GSI and were stained with Oil Red-O and DAPI (Figure 3.3). Absorbance measurements on Oil Red-O extracted from cells induced to undergo adipogenesis showed a 2.5 fold increase in Oil Red-O incorporation in cells plated on Jagged-1 relative to cells plated on Fc-control. Interestingly, treating cells with GSI starting at the time of adipogenic induction also resulted in a significant increase in Oil-Red-O incorporation relative to non-GSI treated cells plated on either Fc-control (2.1 fold increase) or Jagged-1 (1.9 fold increase). The greatest increase in Oil Red-O incorporation was observed in cells grown on Jagged-1 and treated with GSI at the time of adipogenic induction (Figure 3.3 A). Next we asked whether the increase in adipogenic differentiation observed with either Jag-1 or GSI treatment is related to cell number. Counting the number of DAPI staining nuclei in each well revealed a 2 fold increase in the number of DAPI staining nuclei in Jagged-1 treated cells relive to Fc treated cells under control, adipogenic and adipogenic + GSI induction conditions. Normalizing Oil Red-O absorbance measurements to cell number resulted in no significant difference in Oil Red-O incorporation

between Jagged-1 and Fc-control treated cells induced with either adipogenic media or adipogenic media containing GSI. Oil Red-O incorporation remained significantly higher in GSI treated cells plated on either Fc-control (2.6 fold increase) or Jagged-1 (1.9 fold increase) after normalizing to cell number. Therefore, Jagged-1 increases lipid accumulation in MSC cultures by increasing cell number and GSI increases lipid accumulation independent of cell number.

Canonical Notch regulates bone mass in vivo.

Previous studies have shown that both NICD and the down-stream target of canonical notch signaling, Hey-1, can physically interact with Runx-2 and block its' transcriptional activity (137, 175)**.** Studies that examined the role of notch signaling in vivo have relied on either over-expressing NICD or deleting notch receptors or presenilins. All of these approaches could potentially influence both canonical (CSL-mediated) and non-canonical notch signaling pathways such as NICD interaction with Runx-2. To determine the effects of specifically blocking canonical notch signaling in bone formation in vivo, we used mice that carry a transgene for a dominant negative form of Mastermind-like-1 fused with GFP ($dnMAML^{fl/fl}$). The dnMAML transgene is only expressed under Cre-mediated deletion of an upstream stop codon (178). We crossed $dnMAML^{fl/fl}$ mice with Col2.3Cre and Prx-1Cre mice to drive dnMAML expression in osteoblasts and early mesenchymal progenitor cells, respectively, and with Mx-1Cre mice to temporally regulate global expression of dnMAML by administering P(I):P(C) (Figure 3.5) (119, 172-174).

To activate dnMAML expression in osteoblast lineage cells, Col2.3Cre mice were first crossed with dnMAML$^{fl/fl}$ mice and the resulting F1 generation offspring Col2.3Cre^{+}/dnMAML$^{fl/+}$ mice were crossed again with dnMAML$^{fl/fl}$ mice. Out of greater than 10 breeding pairs set up between Col2.3Cre^{+}/dnMAML$^{fl/+}$ X dnMAML$^{fl/fl}$ mice, there were no Col2.3^{+}/ dnMAML$^{fl/fl}$ pups that survived until weaning but both F1 and F2 generation Col2.3Cre^{+}/dnMAML$^{fl/-}$ were viable and survived to at least 6 months of age. Tails of less than 5% of F1 generation Col2.3Cre^{+}/dnMAML$^{fl/-}$ mice appeared crooked at the time of weaning (6 weeks of age) but otherwise the mice appeared normal. In contrast, all F2 generation Col2.3Cre^{+}/dnMAML$^{fl/-}$ mice developed a “crooked-tail” phenotype and in addition appeared to be smaller than their Col2.3Cre^{-}/dnMAML$^{fl/-}$ littermates and had patchy grey hair on the dorsal surface of their body (Figure 3.4 A). Radiographic examination revealed that affected F2 generation Col2.3Cre^{+}/dnMAML$^{fl/-}$ mice had vertebral malformations similar to what is described in Alagille Syndrome patients, including hemi-vertebrae (butterfly-spine) (Figure 3.4 B). The severity of vertebral malformation as well as the vertebral segment affected (thoracic vs. lumbar vertebrae) varied from mouse to mouse. The hind-limbs of more severely affected mice were paralyzed and they could only ambulate using their fore-limbs. Because the severe vertebral malformations and paralysis of hind-limbs of F2 generation Col2.3Cre^{+}/dnMAML$^{fl/-}$ mice would make interpretation of the effects of dnMAML on bone formation difficult, only F1 generation mice, which rarely displayed any vertebral malformation, were analyzed further. Micro-CT analysis of femora from eight

week old mice revealed no significant difference in bone volume fraction (bone volume/total volume (BV/TV)), trabecular connective density, trabecular number or trabecular thickness between F1 generation Col2.3Cre^{+}/dnMAML $^{fl/-}$ mice and age matched Col2.3Cre^{-}/dnMAML $^{fl/-}$ littermate controls (Table 3.1).

To determine the effects of dnMAML expression on osteogenic differentiation, MSC from eight week old Col2.3Cre^{-}/dnMAML $^{fl/-}$ and Col2.3Cre^{+}/dnMAML $^{fl/-}$ controls were induced to undergo osteogenic differentiation in the presence or absence of GSI. Alizarin Red-S staining of plates at 10 days post osteogenic induction revealed increased mineralized matrix formation in MSC harvested from Col2.3Cre^{+}/dnMAML$^{fl/-}$ mice relative to MSC harvested from Col2.3Cre^{-}/dnMAML$^{fl/-}$ controls. GSI treatment started at the time of osteogenic induction had no apparent effect on mineralized matrix formation in either Col2.3Cre^{-}/dnMAML$^{fl/-}$ or Col2.3Cre^{+}/dnMAML $^{fl/-}$ MSC.

dnMAML$^{fl/fl}$ mice were also crossed with Prx-1Cre mice to activate expression of the dnMAML in early mesenchymal progenitors. Gross observation and radiographic examination of 8 week and 6 month old F1 and F2 generation Prx-1Cre^{+}/dnMAML$^{fl/-}$ and Prx-1Cre^{-}/dnMAML$^{fl/-}$ mice did not reveal any apparent skeletal malformations, differences in whole body size or abnormalities of the skin. Micro-CT analysis of trabecular parameters of bone mass in femurs from 8 week old mice showed an 18% decrease in bone volume fraction (BV/TV) in Prx-1 Cre^{+}/dnMAML $^{fl/-}$ when compared to Prx-1Cre^{-} /dnMAML$^{fl/-}$ littermate controls. However, trabecular connectivity density, trabecular number, trabecular thickness or trabecular spacing were not

significantly different between 8 week old Prx-1 Cre^{+}/dnMAML $^{fl/-}$ mice and Prx-1Cre^{-}/dnMAML$^{fl/-}$ littermate controls (Table 3.2 A). Trabecular bone mass parameters of femora from 6 month and 14.5 month old mice were also analyzed but revealed no significant differences in BV/TV, trabecular connective density, trabecular number, trabecular thickness or trabecular spacing between Prx-1 Cre^{+}/dnMAML $^{fl/-}$ mice and Prx-1 Cre^{-}/dnMAML$^{fl/-}$ littermate controls (Table 3.2 B,C).

In order to study the effects of inducing dnMAML expression globally on bone formation, dnMAML$^{fl/fl}$ mice were crossed with Mx1Cre mice in which Cre expression can be induced globally by administering P(I:C) to mice. First, the efficacy of a P(I:C) treatment regimen (shown to be effective in inducing recombination and dnMAML expression in >95% of HSC lineage cells) in inducing dnMAML expression in mesenchymal lineage cells was examined. 8 week old Mx1Cre^{-}/dnMAML$^{fl//fl}$ and Mx1Cre^{+}/dnMAML$^{fl//fl}$ mice were treated with P(I:C) then euthanized at 6 months of age and adherent population of cells were expanded in vitro and GFP expression was analyzed using fluorescence microscopy and FACS analysis (Figure 3.7). Using microscopy, GFP expression was detected in the majority of the adherent cells with fibroblastic morphology (Figure 3.7 A). Similarly, on average greater than 85% of the adherent cells were found to express GFP using FACS analysis (Figure 3.7 B,C). Trabecular bone mass parameters in femurs of 6 month old Mx1Cre^{+}/dnMAML$^{fl//fl}$ mice and Mx1Cre^{-}/dnMAML$^{fl//}$ littermate controls treated with P(I:C) starting at 8 weeks of age were then analyzed using micro-CT. Bone volume fraction (BV/TV),

trabecular number and thickness were reduced by 39.8%, 49.0%, 8.3%, respectively, and trabecular spacing was increased by 11.3% in $Mx1Cre^{+}/dnMAML^{fl//fl}$ mice relative to $Mx1Cre^{-}/dnMAML^{fl//}$ littermate controls (Table 3.3). To determine whether the decrease in trabecular bone mass in $Mx1Cre^{+}/dnMAM^{fl/fl}$ mice was due to a decrease in osteoprogenitors, CFU-F assays were performed on bone marrow cells harvested from $Mx1Cre^{+}/dnMAML^{fl//fl}$ mice and $Mx1Cre^{-}/dnMAML^{fl//}$ littermate controls mice. No significant difference in either the total number or the percentage of alkaline phosphatase positive colonies was detected between P(I:C) treated 6 month old $Mx1Cre^{+}/dnMAML^{fl//fl}$ mice and $Mx1Cre^{-}/dnMAML^{fl//}$ littermate control (Figure 3.8).

Discussion

In this study, we investigated the role of activating notch signaling using immobilized Jagged-1 on primary MSC differentiation and found that Jagged-1 decreases mineralized matrix formation and gene expression of the late osteogenic differentiation marker, osteocalcin. Previous studies that investigated the role of activating notch signaling on osteogenic differentiation have reported conflicting results. Possible reasons for these conflicting results are differences in cells types used and the extent and duration of notch activation. Considered together, results from these previous studies indicate that stable activation of notch signaling in cells with multi-lineage differentiation potential inhibits osteogenic differentiation while transient activation in committed pre-osteoblasts promotes osteogenic differentiation (138, 142-144, 146).

Our experimental approach of using immobilized Jagged-1 to activate notch signaling in primary MSC most resembles the stable NICD over-expression models because expression of notch target genes remain elevated for the duration of our differentiation experiments and resulted in a similar outcome. Consistent with previous reports that showed GSI treatment decreases human MSC proliferation, we found that plating cells on Jagged-1 results in an increase in cell number (179). It is therefore possible that the increase in matrix mineralization that is seen with transient notch activation models is due to an increase in cell number. In future experiments it would be interesting to determine the length of time that immobilized Jagged-1 can continue to activate notch signaling and whether an increase in matrix mineralization can be observed once Jagged-1 is no longer active.

We also examined changes in expression of Hes-1, Hes-5, Hes-7, Hey-1, Hey-2 and Hey-L in primary MSC and found that only Hey-1, Hey-2 and Hey-L were responsive to Jagged-1 treatment and Hey-1 and Hey-L levels decrease with osteogenic differentiation. Our results are consistent with a previous report that showed of the six notch targets examined, expression of only Hey-1, Hey-2 and Hey-L mRNA was detectable in mRNA harvested from mouse tibiae. Interestingly, Hey-1 and Hey-L but not Hey-2 mRNA was shown to be decreased in tibias from mice in which γ-secretase activity was deleted using the Prx1 promoter, further suggesting that Hey-1 and Hey-L may be key mediators of notch signaling effects on MSC (175). Our results which show decreased Hey-1 and Hey-L expression during osteogenic differentiation further suggest that notch

signaling is inhibited during osteogenic differentiation and provides a possible explanation for why GSI treatment starting at the time of osteoblast induction has a minimal effect on differentiation, but is able to rescue Jagged-1 mediated decrease in matrix mineralization.

We also examined the role of Jagged-1 mediated notch activation on adipogenic differentiation of primary MSC and found that it increases lipid accumulation as determined by Oil-Red-O and cell number and that the effect on lipid accumulation appears to be primarily due to an increased cell number. GSI treatment starting at the time of adipogenic induction also increases lipid accumulation but its' mechanism appears to be independent of any effect on cell number. Previous studies on the role of notch signaling in adipogenesis have reported conflicting results. For instance, over-expression of Hes-1 inhibits adipogenesis and siRNA mediated knock down of Hes-1 also decreases adipogenesis in 3T3L1 cells suggesting that while some Hes-1 expression is required, too much expression may be inhibitory for adipogenesis (151, 180). Our results that show GSI treatment increases lipid accumulation contradict a previous report by Hilton et al that showed a decrease in lipid accumulation in MSC isolated from mice in which notch signaling was inactivated using Prx1 promoter (175). The same study also showed that MSC from these same mice undergo accelerated osteogenic differentiation, therefore it is possible that the decrease in lipid accumulation is due to increased osteogenic commitment in vivo and not a direct effect of notch inactivation on adipogenic differentiation in vitro.

We also examined the effects of over-expressing dnMAML in MSC lineage cells on trabecular bone mass. Unexpectedly, we found that driving dnMAML expression using Col2.3Cre mice results in vertebral malformations similar to that is seen in Alagille Syndrome. Alagille syndrome is caused by mutations in Jagged-1 and the vertebral malformations seen in these patients are thought to arise from disruption of cyclic activation of notch signaling during somitogenesis. Our findings, therefore, suggest that the Col2.3 promoter drives Cre expression in somites but more studies are required to determine whether dnMAML expression is induced during somitogenesis in Col2.3Cre^{+}/dnMAMLfl/$^{-}$ mice.

Our finding that Prx1Cre driven expression of dnMAML results in no significant change in trabecular bone mass at either 8 weeks, 6 months or 14.5 months of age contradict Hilton et al's study that showed massive increase in trabecular bone at 8 weeks of age and severe osteopenia seen at 6 months of age when notch receptors were inactivated using the Prx1Cre mice. There are a number of possible explanations for the disparity in phenotype between this previous report and our results. First, there could be differences in the extent of notch inhibition between the previous report in which Notch-1 and Notch-2 or presenillin-1 and presenillin-2 were deleted and our dnMAML expression model. Second, it is possible that inactivating canonical notch signaling alone, as our dnMAML approach presumably does, is not sufficient to influence MSC function and that decreasing NICD levels are also required for the effects of notch on MSC function to become apparent. This explanation is supported by a report by Engin et al that showed physical and functional interactions between NICD and

Runx-2. Future studies should examine the extent of notch inhibition achieved using the dnMAML approach relative to what is achieved by receptor deletion models. Whether specifically inhibiting canonical notch signaling in mesenchymal progenitors is dispensable for MSC function, as our results suggest, should also be confirmed using other mouse models in which CSL mediated notch signaling can be selectively inactivated.

Our results that show P(I:C) induced dnMAML expression decreases trabecular bone mass while Prx1Cre induced expression has little effect suggests that dnMAML, when driven from Mx1Cre promoter, may have a more dominant effect on osteoclast lineage cells than in osteoblast lineage cells. This notion is supported by the our observation that CFU-F numbers were not significantly decreased in P(I:C) induced Mx1Cre^{+}/dnMAML $^{fl/fl}$ mice and previous reports that have shown that inactivating notch signaling increases bone resorption directly by promoting osteoclast differentiation from osteoclast progenitors and indirectly by increasing RANK-L expression in osteoblasts (137, 181). Future studies should address whether the decrease in trabecular bone mass in Mx1Cre^{+}/dnMAML $^{fl/fl}$ mice is due to a decrease in bone formation and/or an increase in bone resorption.

Figure 3.1

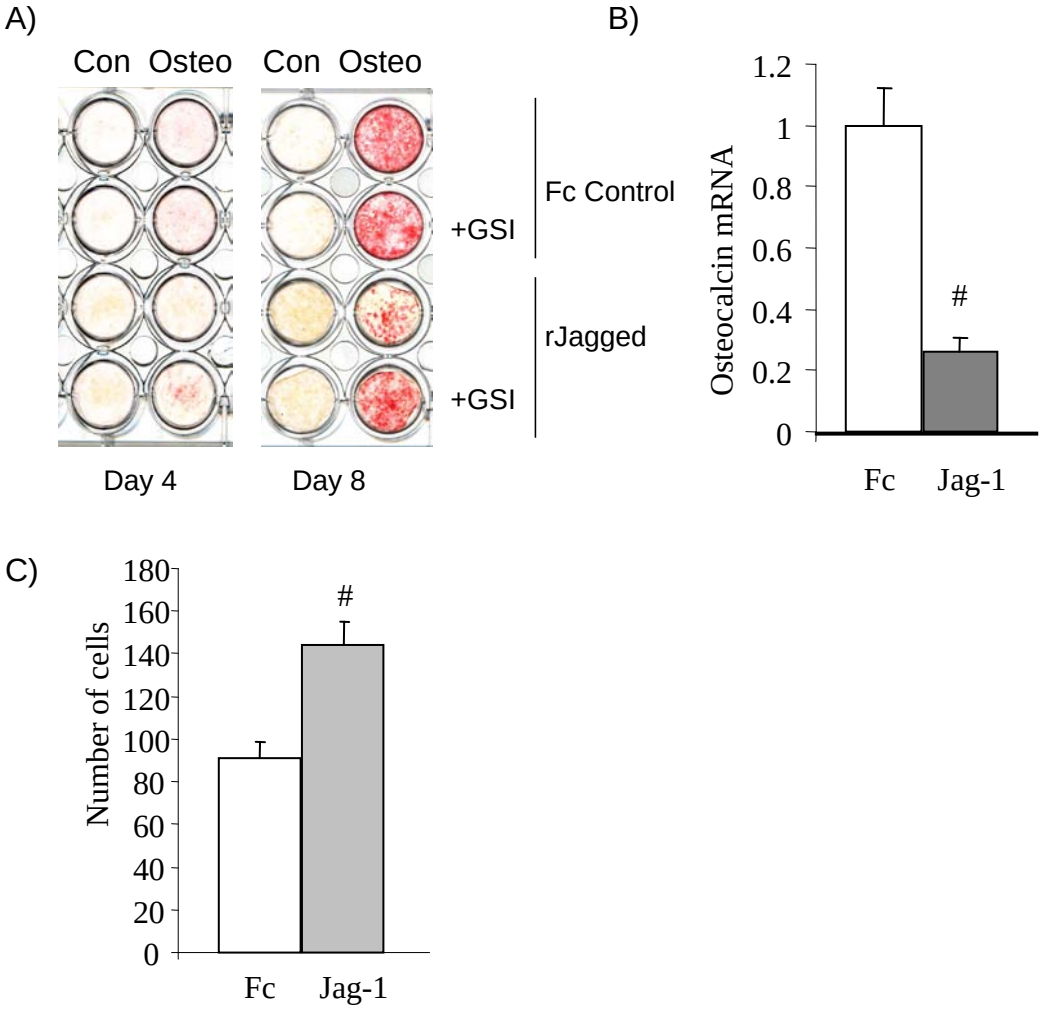

Figure 3.1 Immobilized Jagged-1 decreases matrix mineralization and osteocalcin expression and increases cell number. MSC were cultured on plates coated with either Fc-control (Fc) or 5μg/mL of Jagged-1 (Jag-1) for 4 days and were induced to undergo osteogenic differentiation in the presence or absence of a γ-secretase inhibitor (+GSI). **A)** Plates were stained with Alizarin Red-S at 4 and 8 days post induction and representative images from two independent experiments done with two independent MSC harvests is shown. **B)** MSC were induced to undergo osteogenic differentiation on either Fc-control or 5μg/mL of Jagged-1 for 8 days and RNA was harvested and change in osteocalcin expression on Jag-1 relative to Fc-controls was determined by qPCR. Graphs represent mean + S.D of two independent experiments done on two independent MSC harvests each done in duplicate. **C)** MSC were plated on either Fc-control or 5μg/mL of Jagged-1 in triplicates then were trypsinized and counted 4 days later. Data shown are representative of two independent experiments and graphs are mean + S.D. of triplicate samples. (#= Jag-1 significantly different from Fc controls; *p<.05)*

Figure 3.2

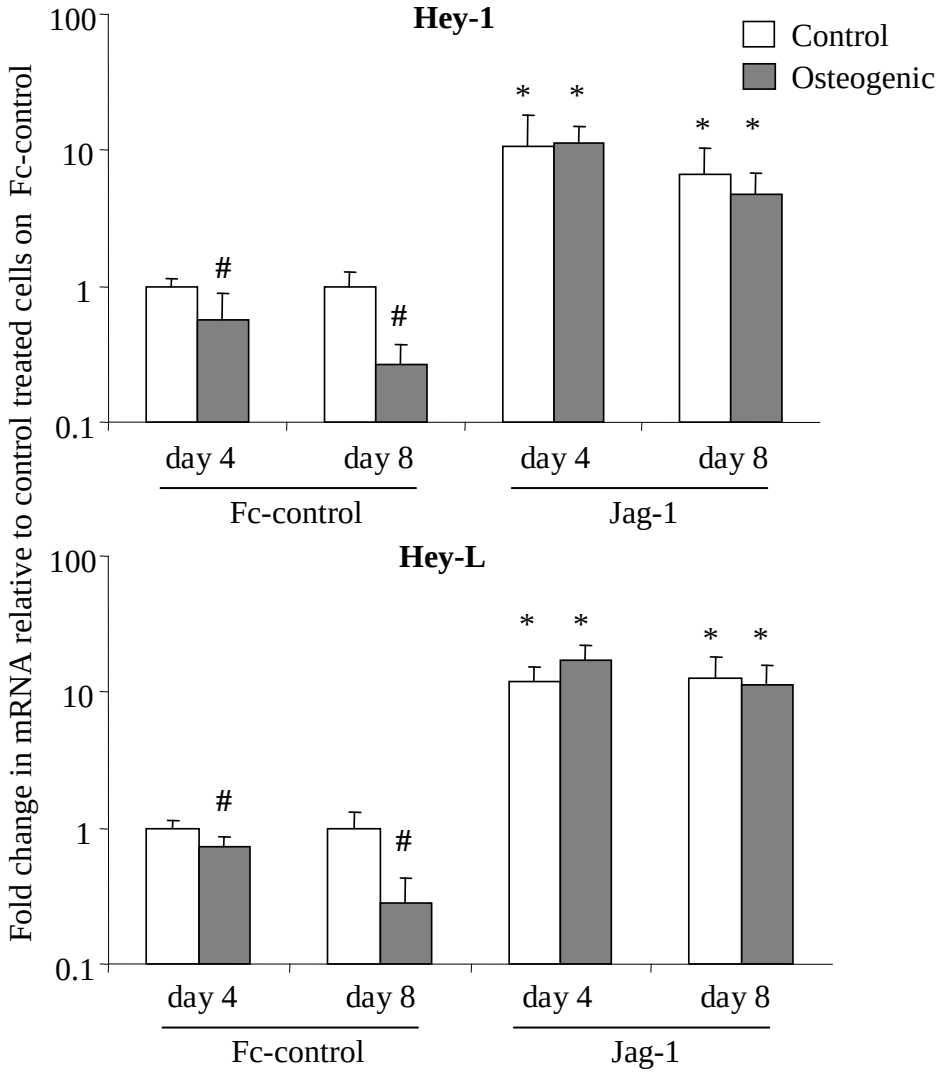

Figure 3.2 Osteogenic induction decreases Hey-1 and Hey-L expression and Jagged-1 treatment increases and maintains it at elevated levels. MSC were plated onto either Fc-control or 5μg/mL Jagged-1 (Jag 1) coated wells and were induced to undergo osteogenic differentiation. RNA was harvested at 4 and 8 days post osteogenic induction and expression of Hey-1 and Hey-L was analyzed by quantitative-RT PCR. Graphs represent fold change in expression of Hey-1 and Hey-L relative to un-induced control cells plated on Fc-control (value of 1). Graphs are mean + S.D. of two independent experiments from two independent cell harvests each done in duplicate. For each experiment, whole bone marrow from 3 mice was pooled to yield MSC. (#=osteogenic induced significantly different from un-induced controls, *=Jag-1 significantly different from Fc-control; *p< .05).*

Figure 3.3

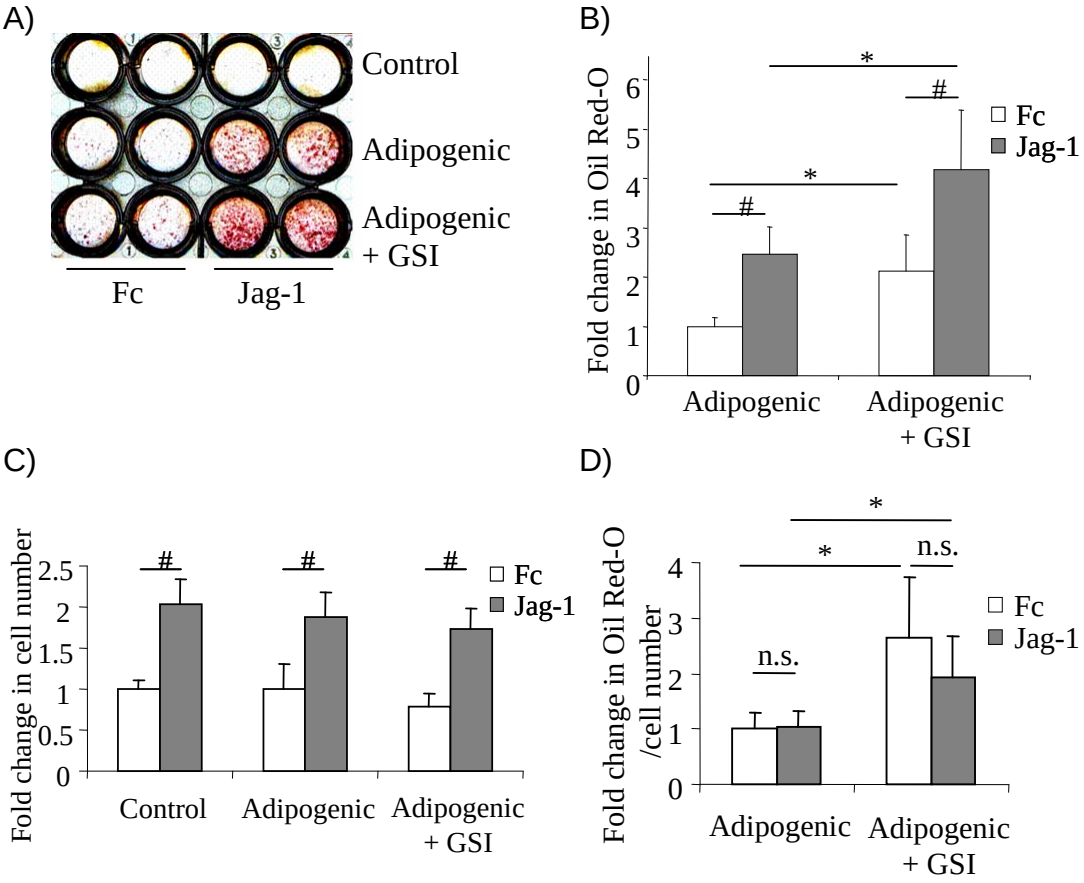

Figure 3.3 Jagged-1 increases lipid accumulation by increasing cell number. MSC were plated onto either Fc-control (Fc) or 5µg/mL Jagged-1 (Jag-1) coated wells and induced to undergo adipogenic differentiation 4 days later (Adipogenic) in the presence or absence of γ-secretase inhibitor (GSI) (Adipogenic + GSI). Ten days post induction, cells were stained with Oil Red-O and DAPI and 5 representative 10X DAPI fluorescence images were obtained. **A)** Scanned image of a representative Oil Red-O stained plate is shown **B)** Oil Red-O was extracted and quantified by measuring absorbance at 540nm and graphed as fold change over cells induced to undergo adipogenesis on Fc-control. **C)** the total number of DAPI staining nuclei in 5 images obtained from each well was averaged and used as an estimate of the total number of cells in each well and graphed as fold change over un-induced control cells plated on Fc control. **D)** Oil Red-O absorbance readings were normalized to cell number (number of DAPI staining nuclei) and graphed as fold change over cells induced to undergo adipogenesis on Fc-control. Data shown are mean + S.D. of two independent experiments each done in duplicate on two independent MSC harvests. (#=Jag-1 significantly different from Fc control, *=GSI treated significantly different from non-GSI treated. *p<.05,* n.s.=not significant).

Figure 3.4

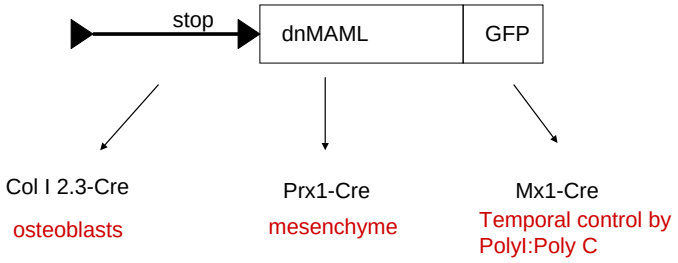

Figure 3.4 dnMAML construct and experimental approach. The dnMAML mice carry a PGK-Neo-tpA cassette with a stop codon flanked by loxP sites (floxed) upstream of dnMAML-GFP fusion protein knocked into the *ROSA* locus. Crossing them with mice that express cre recombinase from a Col2.3, Prx1, and Mx1 promoter excises out the PGK-Neo-tpA cassette and allows transcription of dnMAML-GFP from the *ROSA* promoter in osteoblasts, mesenchymal progenitors, or in a PolyI:PolyC inducible manner, respectively.

Figure 3.5

A)

Col2.3Cre^{+}/dnMAML$^{fl/-}$ Col2.3Cre^{-}/dnMAML$^{fl/-}$

B)

Col2.3Cre^{+}/dnMAML$^{fl/-}$ Col2.3Cre^{-}/dnMAML$^{fl/-}$

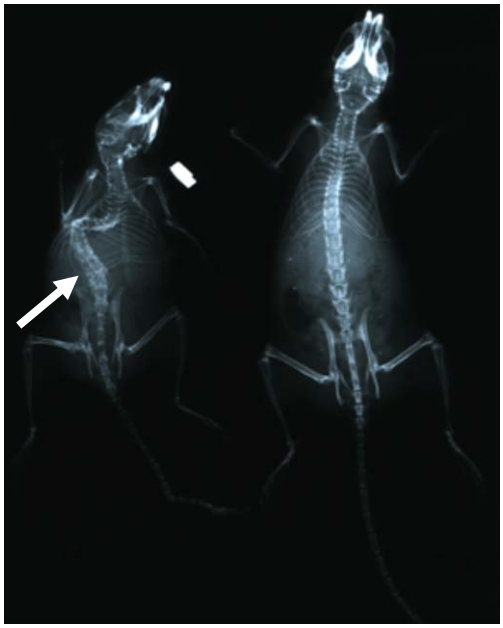

Figure 3.5 Col2.3dnMAML mice develop vertebral malformations similar to Alagille Syndrome patients. A) Picture of 6 month old F2 generation mice illustrates the characteristic appearance of Col2.3^{+}/dnMAML$^{fl/-}$ and Col2.3^{-}/dnMAML$^{fl/-}$ mice. Col2.3^{+}/dnMAML$^{fl/-}$ mice are smaller and have a characteristic "crooked tail". The hind-limbs of more severely affected mice are paralyzed but they can move around their cage using their fore-limbs. B) Radiographic image of a Col2.3^{-}/dnMAML$^{fl/-}$ and Col2.3^{+}/dnMAML$^{fl/-}$ mice demonstrates vertebral malformation in Col2.3^{+}/dnMAML$^{fl/-}$ mice similar to what is seen in Alagille Syndrome patients including characteristic hemi-vertebrae (butterfly-spine) (arrow).

Figure 3.6

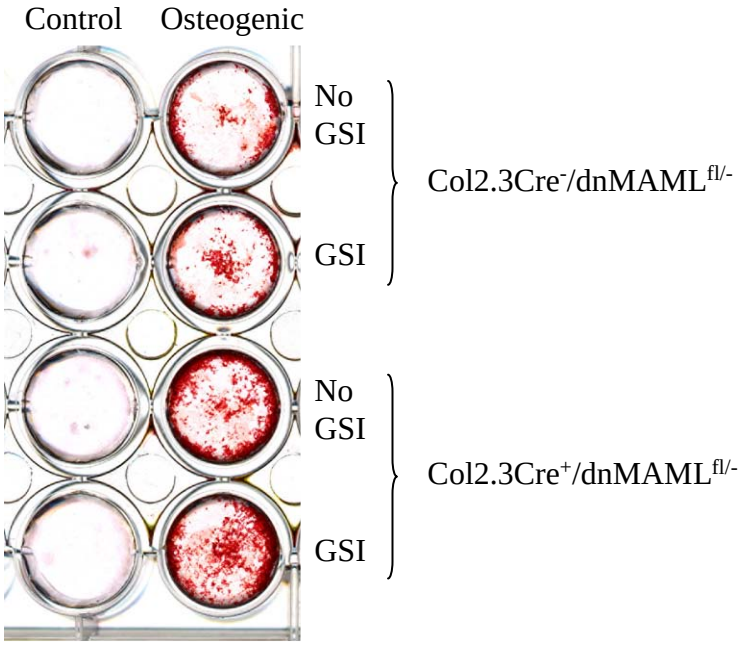

Figure 3.6 MSC from Co2.3Cre^{+}/dnMAML$^{fl/-}$ mice show increased mineralized matrix formation. MSC isolated from hind-limbs of eight week old F1 generation Co2.3Cre^{+}/dnMAML$^{fl/-}$ mice and Co2.3Cre^{+}/dnMAML$^{fl/-}$ littermate controls were induced to undergo osteogenesis in the presence or absence of GSI for 8 days and were stained with Alizarin-Red-S. Representative wells from two independent experiments performed on two independent MSC harvests are depicted. For each harvest, bone marrow from three Co2.3Cre^{+}/dnMAML$^{fl/-}$ and three Co2.3Cre^{-}/dnMAML$^{fl/-}$ mice was pooled together to yield MSC.

Table 3.1

Trabecular microCT parameter	**Col2.3Cre^{-}/dnMAML$^{fl/-}$**		**Col2.3Cre^{+}/dnMAML$^{fl/-}$**	
BV/TV	0.0968	(0.0141)	0.0977	(0.0178)
Connectivity density	85.058	(8.903)	74.728	(11.262)
Trabecular number	3.112	(0.166)	2.973	(0.210)
Trabecular thickness (mm)	0.0548	(0.00337)	0.0590	(0.00426)
Trabecular spacing (mm)	0.321	(0.0174)	0.334	0.0221

(Cre negative, n=5; Cre positive, n=4), Mean (SEM)

Table 3.1 Femora from 8 week old F1 generation Co2.3Cre^{+}/dnMAML$^{fl/-}$ mice have normal trabecular bone mass and geometry. Femora from gender matched 8 week old Col2.3Cre^{+}/dnMAML$^{fl/-}$ mice and Col2.3Cre^{-}/dnMAML$^{fl/-}$ littermate controls were harvested and trabecular bone mass parameters were determined using micro-CT. Only F1 generation mice were analyzed because F2 generation Col2.3^{+}Cre/dnMAML$^{fl/-}$ mice develop vertebral malformations that affected use of their hind-limbs for locomotion. There were no significant differences in any of the trabecular bone mass parameters between Col2.3^{+}Cre/dnMAML$^{fl/-}$ mice and Col2.3^{-}Cre/dnMAML$^{fl/-}$ littermate controls.

Table 3.2

A)

8 weeks old

Trabecular microCT parameter	**Prx1Cre^{-}/dnMAML$^{fl/-}$**		**Prx1Cre^{+}/dnMAML$^{fl/-}$**	
BV/TV	0.242	(0.0157)	0.199	(0.00864)*
Connectivity density	503.076	(27.913)	460.482	(15.329)
Trabecular number	6.064	(0.330)	5.437	(0.181)
Trabecular thickness (mm)	0.0511	(0.00210)	0.0481	(0.00115)
Trabecular spacing (mm)	0.175	(0.00509)	0.185	(0.00280)

(Cre negative, n=7; Cre positive, n=19), Mean (SEM), *, *p<0.05*

B)

6 months old

Trabecular microCT parameter	**Prx1Cre^{-}/dnMAML$^{fl/-}$**		**Prx1Cre^{+}/dnMAML$^{fl/-}$**	
BV/TV	0.121	(0.0167)	0.127	(0.0125)
Connectivity density	86.759	(15.743)	110.185	(10.765)
Trabecular number	3.199	(0.192)	3.279	(0.144)
Trabecular thickness (mm)	0.0554	(0.00210)	0.0529	(0.00157)
Trabecular spacing (mm)	0.359	(0.0330)	0.357	(0.0247)

(Cre negative, n=6; Cre positive, n=13), Mean (SEM)

C)

14.5 months old

Trabecular microCT parameter	**Prx1Cre^{-}/dnMAML$^{fl/-}$**		**Prx1Cre^{+}/dnMAML$^{fl/-}$**	
BV/TV	0.0967	(0.0294)	0.0915	(0.0285)
Connectivity density	79.710	(38.251)	97.894	(26.608)
Trabecular number	2.402	(0.195)	2.588	(0.189)
Trabecular thickness (mm)	0.0611	(0.00406)	0.0497	(0.00393)
Trabecular spacing (mm)	0.528	(0.0516)	0.437	(0.0499)

(Cre negative, n=4; Cre positive, n=5), Mean (SEM)

Table 3.2 Femora from 8 week old Prx1Cre^{+}/dnMAML$^{fl/-}$ mice have a decrease in trabecular bone volume fraction. Femora from gender matched 8 week old **(A)**, 6 month old **(B)** and 14.5 month old **(C)** Prx1Cre^{+}/dnMAML$^{fl/-}$ mice and Prx1Cre^{-}/dnMAML$^{fl/-}$ littermate controls were harvested and trabecular bone mass parameters were determined using micro-CT. 8 week old Prx1Cre^{+}/dnMAML$^{fl/-}$mice have significantly decreased bone volume fraction (BV/TV) when compared to Prx1Cre^{-}/dnMAML$^{fl/-}$ littermate controls. There were no significant differences between Prx1Cre^{+}/dnMAML$^{fl/-}$ and Prx1Cre^{-}/dnMAML$^{fl/-}$ mice in any of the trabecular parameters analyzed at either 6 month or 14.5 month of age.

Figure 3.7

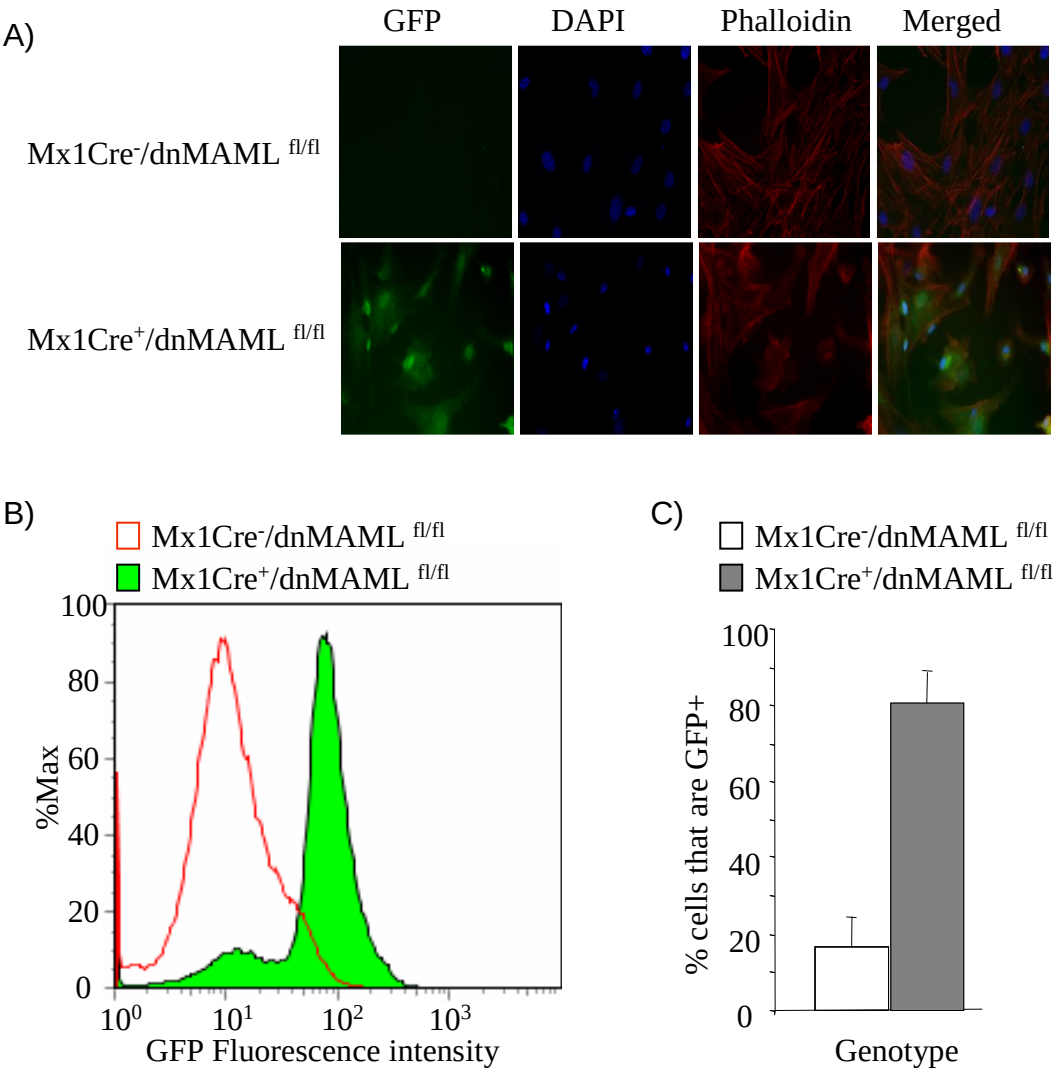

Figure 3.8 P(I:C) treatment induces dnMAML expression in MSC. 8 week old Mx1Cre^{-}/dnMAML$^{fl/fl}$ and Mx1Cre^{+}/dnMAML$^{fl/fl}$ mice were treated with a regimen of P(I:C) injections then were euthanized at 6 months of age and extent of dnMAML expression in MSC was determined by monitoring GFP expression. **A)** First passage MSC were stained with TRITC conjugated phalloidin and DAPI to stain actin cytoskeleton and nuclei, respectively. Most Mx1Cre^{+}/dnMAML$^{fl/fl}$ cells with fibroblastic morphology also express GFP indicating that dnMAML expression has been activated. **B)** A representative FACS analysis showing the shift in GFP fluorescence intensity in first passage MSC from an Mx1Cre^{-}/dnMAML$^{fl/fl}$ mouse relative to MSC from an Mx1Cre^{-}/dnMAML$^{fl/fl}$ control. **C)** The percentage of GFP positive cells in first passage MSC from Mx1Cre^{-}/dnMAML$^{fl/fl}$ (n=6) and Mx1Cre^{+}/dnMAML$^{fl/fl}$ (n=5) were quantified and graphed as mean + S.D.

Table 3.3

Trabecular microCT parameter	$Mx1Cre^{-}/dnMAML^{fl/fl}$		$Mx1Cre^{+}/dnMAML^{fl/fl}$	
BV/TV	0.0841	(0.00418)	0.0506	(0.00441)*
Connectivity density	101.715	(7.338)	52.242	(7.735)*
Trabecular number	3.612	(0.0902)	3.279	(0.0950)*
Trabecular thickness (mm)	0.0426	(0.00121)	0.0370	(0.00128)*
Trabecular spacing (mm)	0.283	(0.00878)	0.315	(0.00925)*

(Cre negative, n=6; Cre positive, n=5), Mean (SEM), *, $p<0.05$

Table 3.3 P(I:C) induced expression of dnMAML decreases trabecular bone mass. 8 week old $Mx1Cre^{-}/dnMAML^{fl/fl}$ and $Mx1Cre^{+}/dnMAML^{fl/fl}$ mice were treated with P(I:C) injections then were euthanized at 6 months of age. Femurs were collected and trabecular bone mass parameters were analyzed using micro-CT. P(I:C) treated $Mx1Cre^{+}/dnMAML^{fl/fl}$ mice had a significant decrease in BV/TV, trabecular connective density and number and an increase in trabecular spacing when compared to P(I:C) treated $Mx1Cre^{-}/dnMAML^{fl/fl}$ littermate controls.

Figure 3.9

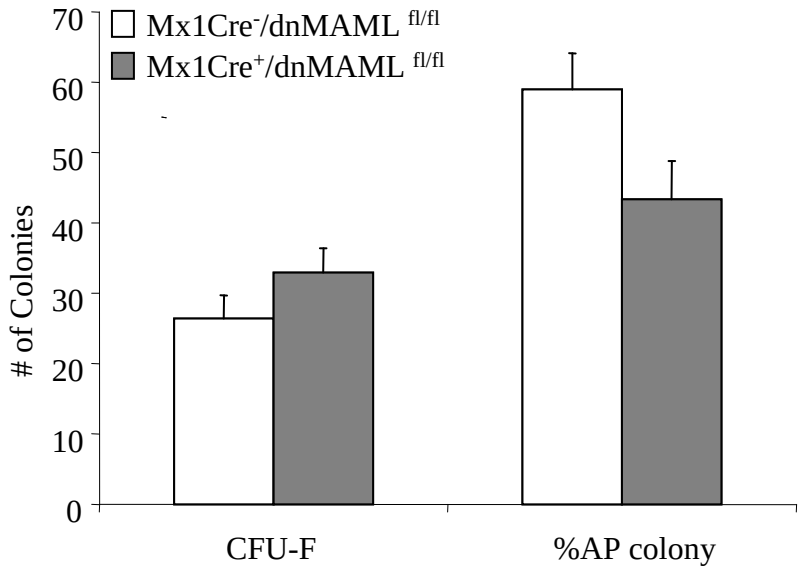

Figure 3.9 P(I:C) induced expression of dnMAML does not alter CFU-F numbers. 8 week old Mx1Cre^{-}/dnMAML$^{fl/fl}$ and Mx1Cre^{+}/dnMAML$^{fl/fl}$ mice were treated with P(I:C) then were euthanized at 6 months of age and bone marrow was harvested from hind-limbs and was plated for CFU-F assay. Cells were fixed and stained for alkaline phosphatase (AP) activity 13 days post plating and total and AP positive colonies were counted and percentage of AP positive colonies (%AP) was determined. Total number of CFU-F and percentage of AP positive colonies from five Mx1Cre^{-}/dnMAML$^{fl/fl}$ and five Mx1Cre^{+}/dnMAML$^{fl/fl}$ mice were averaged and graphed as mean + SEM. There were no statistically significant differences in either total number of CFU-F or percentage of AP positive colonies between P(I:C) treated Mx1Cre^{-}/dnMAML$^{fl/fl}$ and Mx1Cre^{+}/dnMAML$^{fl/fl}$ mice.

CHAPTER IV

THROMBOSPONDIN-2 MODULATION OF NOTCH SIGNALING

Introduction

Bone marrow derived mesenchymal stem cells (MSC) are precursors that give rise to osteoblasts, adipocytes, and chondrocytes. MSC numbers are known to decrease with age and this decrease has been proposed as a possible explanation for age-associated osteoporosis (166, 167). In addition to a decrease in MSC number, an increase in bone marrow adipocytes is observed with ageing and a switch from osteogenic to adipogenic fate is also thought to contribute to the pathogenesis of osteoporosis (55, 57). A better understanding of molecular mechanisms that maintain the MSC pool as well as those that are involved in osteogenic and adipogenic fate are therefore important for designing novel treatment strategies for age-associated osteoporosis.

Thrombospondn-2 (TSP2) is an extracellular matrix (ECM) protein that is highly expressed by MSC and belongs to a group of proteins often referred to as matricellular proteins. Matricellular proteins interact with cells as well as other ECM proteins, but have minimal structural role. Extensive study of TSP2 deficient mice has revealed that TSP2 functions in a variety of physiological and

patho-physiological processes such as angiogenesis, skin wound healing, foreign body reaction and fracture healing (87-89*)*. TSP2-null mice have an increase in cortical bone thickness due to an increase in osteoprogenitor numbers. In vitro, TSP2 inhibits MSC proliferation and promotes osteogenic differentiation (100, 101). The molecular mechanism through which TSP2 acts to regulate MSC function is however unknown.

Structurally, TSP2 is a large glycoprotein that is secreted as a homo-trimer. Each TSP2 chain in the trimeric complex is composed of N-terminal, pro-collagen, type I repeat, type II repeat, type III repeat and c-terminal domains. Each of these modules has been shown to interact with distinct cell surface receptors, ECM proteins, and growth factors to influence a variety of cellular processes such as cell adhesion and proliferation. Recent studies have shown that TSP2 can physically interact with Notch receptors and ligands and modulate activation of the Notch signaling pathway (103).

Notch family receptors (Notch 1 to 4) are highly conserved, single pass trans-membrane proteins that are activated by cell surface bound ligands of the Delta-Serrate like (DSL) family. In vertebrates there are five DSL family members (Delta-like (Dll) -1, -3, -4, and Jagged (Jag)-1,- 2). Ligand binding initiates a series of enzymatic cleavages. The first cleavage, mediated through ADAM family of metalloproteinase, results in shedding of the receptor's ectodomain. A second cleavage by a γ-secretase enzyme complex results in the release of Notch intracellular domain (NICD) into the cytoplasm. NICD then translocates to the nucleus where it binds the transcription factor

CSL (for CBF1, Suppressor of Hairless, or Lag-1). CSL bound NICD recruits the transcriptional co-activator Mastermind Like-1 (MAML) and initiates transcription of notch target genes. The best characterized Notch targets are members of the HES and HERP family of beta-helix-loop-helix family of transcription factors. Members of this family that have been shown to be notch responsive are Hey-1, Hey-2, Hey-L, Hes-1, Hes-5 and Hes-7 (104-110).

Notch signaling has recently been shown to play an important role in MSC fate determination. Over-expressing NICD in osteoblasts in vivo results in an increase in their proliferation and inhibits their terminal maturation and/or function. Similarly, inactivating notch signaling in early mesenchymal progenitors results in increased osteogenic differentiation and depletion of the osteoprogenitor pool. In chapter III, we have shown that activating notch signaling increases primary MSC proliferation and decreases osteogenic differentiation. Therefore, Notch signaling appears to maintain the MSC pool by preventing premature osteoblast differentiation and increasing proliferation (137, 175).

Notch signaling is regulated at multiple levels including ligand and receptor expression, post translational modification and transport. In addition, Notch signaling has been reported to be modulated by ECM proteins including CCN/Nov and SPARC (153-155). More recently, it was reported that TSP2 can physically interact with Notch-3 and Jagged-1. TSP2 increases Hes-1 promoter activity and Notch target gene expression in a lung cancer

cell line and in smooth muscle cells, respectively (156). The similarity in function between TSP2 and Notch signaling in regulating MSC proliferation and differentiation, as well as the demonstrated interaction between them in other cell types lead us to hypothesize that TSP2 will modulate notch signaling in MSC.

Materials and Methods:

Cell culture and treatments: Whole bone marrow from femurs and tibias of TSP2-null and wild-type control mice was collected and cultured in MSC media (alpha-Minimum Eagle's medium supplemented with 10% fetal bovine serum, 2 mM L-glutamine, 25µg/mL sodium ascorbate, and 100U/mL penicillin and 100µg/mL streptomycin) for 8 to 10 days with half the media being replaced at 4 days and every three days there after. When cultures reached 80% confluence, cells were trypsinized, then plated onto 12-well tissue culture plates at a density of $1X10^5$ cells per well. To activate Notch signaling using immobilized Jagged-1, tissue culture plates were pre-coated with 10µg/mL of antibody against the Fc portion of human IgG (Jackson ImmonoResearch) for 1 hour then were incubated with the indicated concentration of recombinant rat Jagged-1/human Fc IgG chimeric protein (R&D Systems) for 2 hours. For notch reporter activity experiments, Fc/Jagged-1 (Jag-1) or Fc/Trail (control) conditioned media (kind gifts from Dr. Tom Kadesch) was used to coat plates instead of the recombinant Fc/Jagged-1 protein.

Induction of adipogenic differentiation: First passage TSP2-null and wild type MSC were induced to undergo adipogenesis four days post plating using MDIT (57μM isobutyl-methylxanthine, 1μM dexamethasone, and 1μg/mL insulin, and 5μg/mL troglitazone) for three days then were maintained in 1μg/mL insulin for the remainder of the differentiation experiments. For γ-secretase inhibitor (GSI) treatment, 1μM of L-685,458 (Sigma) was added daily to cells starting at the time of adipogenic induction. Cells were fixed 10 days post induction and extent of adipogenic differentiation was evaluated by staining with Oil Red-O.

RNA extraction and quantitative RT- PCR: RNA was extracted using RNeasy RNA extraction kit (QIAGEN) according to the manufacturer's instruction and 1μg of total RNA was reverse transcribed in 20μL reactions. 1μL of the cDNA generated was used for quantitative real-time PCR reactions using SybrGreen I for detection on ABI 7500 Fast real-time PCR machine. Relative changes in gene expression were determined by the $2^{\Delta\Delta C(T)}$ method using β-actin as an endogenous control.

Generation of TSP2 type I repeat deletion constructions: A retroviral construct missing all three type I repeat domains (aa 379-549, TSP2 delI3) was generated by first PCR amplifying a 1169 base pair fragment encoding amino acids 1- 378 (fragment 1) and a 1925 base pair fragment encoding

amino acids 550-1172 (fragment 2) and cloning into pCRII-TOPO vector (Invitrogen). *SfoI* restriction sites that encoded a single glycine residue in-frame were added to the 3' primer of fragment 1 and 5' primer of fragment 2 to allow ligation of the two fragments. After sequence verification by direct sequencing, fragments 1 and 2 were released from pCRII-TOPO using *BamHI* and *SfoI* and *SfoI* and *XbaI*, respectively, then were ligated into Blue Script cloning vector digested *with BamHI* and *XbaI*. The full-length TSP2 (TSP2 FL) and TS2delI3 fragment was then released from BlueScripit using *EcoRI* and cloned into pRET retroviral vector digested with *EcoRI*.

Retrovirus production and transduction: Phoenix A (amphtropic) cells were plated at a density of $4x10^5$ cells/well of a 6 well plate and cultured overnight. On the following day, the culture media was aspirated and exchanged with fresh media (DMEM, high glucose, 10% FBS, pen-strep, L-glutamine). Chloroquine dihydrochloride (Sigma, S764663) was added to phoenix cells 5 minutes prior to transfection and 2µg of plasmid DNA was transfected into cells using the Promega Profection kit (E1200). The media was changed 10 hours after transfection and replaced with fresh medium. Retroviral supernatant was collected on the following day and used to transduce GP+E86 cells. GP+E86 cells were plated at $4x10^4$ cells/well of a 6 well dish, and cultured overnight. On the following day, retroviral supernatant from phoenix cells was .45 µm filtered, supplemented with protamine sulfate (5µg/mL) and 2mL was added to GP+E86 cells. GP+E86 cells were

transduced again on the following day, and media replaced 24 hours later. Viral supernatant from GP+E86 cells was collected on the following two days and used to transduce C3H10T1/2 cells.

Transient transfection and CSL-luciferase assay: $4X10^4$ C3H10T1/2 cells were plated onto 12 well plates coated with either Fc-trail or Jag-1 and 36 hours post plating, cells were co-transfected with 0.5μg of CSL-luciferase (synthetic DNA construct in which 4 tandem repeats of CSL binding elements drive expression of firefly luciferase, kind gift from Dr. Tom Kadesch) and 100ng of pRL-TK (Promega, a constitutively active TK promoter driving expression of renilla luciferase activity) using Lipofectamine and Plus reagent (Invitrogen) according to the manufacturer's instructions. Cells were harvested 48 hours post transfection and firefly and renilla luciferase activities were measured using Dual Luciferase assay kit (Promega) according to the manufacturer's instructions.

Immunofluorescence staining of fracture callus: Generation of tibial fractures in TSP2-null and wild type mice has been described (95). Cleaved (activated) notch levels were assessed in serially sectioned (7 mm) paraffin embedded fractured tibias by immunofluorescence staining with a monoclonal antibody that recognizes notch receptors only after they have undergone γ-secretase cleavage (Cleaved Notch 1 (Val1744), Cell Signaling; 1:200). After incubation with the primary antibody at $4^{\circ}C$ overnight, sections were treated

with Alexafluor 594–labeled secondary antibody (1:200; Molecular Probes) at room temperature for 1 hour, mounted with Vectashield containing DAPI (Vector Laboratories) and visualized with fluorescence microscopy.

Statistical Analysis: Student's t-tests were used to compare means between TSP2-null and wild type and between treated groups and untreated controls.

Results

TSP2 decreases Jagged-1 mediated notch activation in mesenchymal lineage cells.

Previous studies have shown that TSP2 physically interacts with notch receptors and ligands and increases notch signal activation in lung cancer and smooth muscle cells (156). To determine whether TSP2 can modulate notch signal activation in MSC, TSP2-null and wild type MSC were plated onto wells coated with either Fc-control or varying concentrations of Jagged-1 and expression of notch target genes Hey-1, Hey-2 and Hey-L, Hes-1 and Hes-5 were evaluated by quantitative RT-PCR (qPCR). Hey-1, Hey-2 and Hey-L expression were induced in a dose dependent manner in both wild-type and TSP2-null MSC (Figure 4.1) but Hes-1 and Hes-5 expression did not increase significantly by Jagged-1 treatment (data not shown). Jagged-1 induced increases in Hey-1, Hey-2 and Hey-L expression were significantly greater in TSP2-null MSC than wild type controls at all doses of Jagged-1

except for Hey-2 expression in cells plated on 0.625µg/mL of Jagged-1. Interestingly, the largest differences between TSP2-null and wild type MSC were observed in Hey-L expression (8.4, 10.7, 23.2, and 8.2 fold greater induction in TSP2-null over wild type control at 5, 2.5, 1.25 and 0.625µg/mL Jagged-1, respectively) and Hey-L was the notch target that showed the greatest responsiveness to Jagged-1 treatment (102 fold induction in Hey-L vs. 6.7 and 24.5 fold induction in Hey-1 and Hey-2, respectively, in wild type cells plated on 5µg/mL Jagged-1). The smallest differences between TSP2-null and wild type MSC were observed in Hey-1, the least Jagged-1 responsive Hey family member, which showed 1.4, 1.5, 2.5 and 2.3 fold increase in expression in TSP2-null MSC over wild type controls treated with 5, 2.5, 1.25 and 0.625µg/mL of Jagged-1, respectively. Hey-2, which showed intermediate responsiveness to Jagged-1, also showed intermediate differences between TSP2-null and wild type MSC (2.8, 2.8, 4.9 and 3.1 fold increase in TSP2 null MSC over wild type controls treated with 5, 2.5, 1.25 and 0.625µg/mL Jagged-1, respectively) (Figure 4.1).

To determine whether TSP2 decreases notch activation, C3H10T1/2 cells were stably transduced with retrovirus constructs carrying either GFP, a full length TSP2 (FL TSP2) construct or TSP2 lacking all three type I repeat domains (TSP2dl3). Western-blot analysis of TSP2 proteins secreted into the media confirmed that TSP2dl3 is stable and is over-expressed at a similar level as FL TSP2 (Figure 4.2 A). GFP, FL TSP2 or TSP2dl3 transduced cells were then plated on either Fc-control or 2.5µg/mL Jagged-1 coated plates

and Hey-1 mRNA expression was analyzed 4 days later (Figure 4.2 B). Induction of Hey-1 expression was significantly lower in FL TSP2 over-expressing cells relative to GFP over-expressing controls (1.5 fold induction in FL TSP2 vs. 3.9 fold in GFP cells) but Hey-1 expression was induced at a similar level (3.5 fold) in TSP2dl3 over-expressing cells as GFP over-expressing controls. Hey-1 expression was evaluated in these experiments because Hey-1 showed the greatest responsiveness to Jagged-1 treatment in C3H10T1/2 cells when compared to Hey-2 and Hey-L (data not shown). These results indicate that TSP2 decreases notch target gene expression through its type I repeat domain.

While Hes and Hey family members are well known targets of notch signaling, their expression can also be regulated by other transcriptional mechanisms that TSP2 could modulate. To more directly measure whether TSP2 decreases canonical notch signaling, GFP or FL TSP2 over-expressing C3H10T1/2 cells were plated onto either Fc-trail or Jag-1 coated wells then were transiently transfected with a notch reporter (CSL-luciferase) construct. Similar to Hey-1 expression, notch reporter activity was significantly lower in TSP2 over-expressing cells when compared to GFP transduced controls (1.7 fold in TSP2 over-expressing vs. 3.7 fold in GFP over-expressing cells) confirming that the decrease in Jagged-1 induced Hey-1 expression is specifically due to a decrease in notch activation (Figure 4.3).

γ-Secretase inhibition promotes adipogenesis in both wild-type and TSP2-null MSC.

We have shown in Chapter I that TSP2 decreases lipid accumulation in MSC. Since notch activation is increased in the absence of TSP2 (Figure 4.1) we asked whether the increase in adipogenic differentiation in TSP2-null MSC was due to an increase in notch signaling. To address this question, TSP2-null and wild type MSC were induced to undergo adipogenesis in the presence or absence of a γ-secretase inhibitor (GSI) for 10 days and extent of lipid accumulation was measured by analyzing Oil Red-O incorporation (Figure 4.4). Blocking notch signaling with GSI increased Oil Red-O staining 1.9 and 1.5 fold over untreated controls in wild type and TSP2-null MSC, respectively. There was no significant difference in GSI mediated increase in Oil Red-O staining between wild-type and TSP2-null MSC (Figure 4.4 B) suggesting that either the effects of TSP2 on notch signal activation are upstream of γ-secretase or TSP2's effect on adipogenic differentiation is not mediated through its effect on notch signal activation.

Notch activation is increased in fracture calluses of TSP2-null mice.

Our results indicate that TSP2 decreases Jagged-1 mediated notch activation in vitro. Previous studies have shown that TSP2 expression increases early during fracture healing and is highest at 5 days in a tibia fracture model when the healing fracture is composed of undifferentiated mesenchymal progenitors (95). In order to evaluate whether TSP2 can

modulate notch signaling in vivo, we measured notch activation in day 5 fracture calluses of wild type and TSP2-null tibia by immunofluorescence staining with antibody that specifically binds to notch receptors only after they have undergone γ-secretase cleavage (intracellular Notch – NICD). An increase in cleaved notch was detected in TSP2-null fracture calluses relative to wild type controls (Figure 4.5). These results suggest that TSP2 may inhibit notch signal activation in vivo.

Discussion

Previous studies have shown that TSP2 inhibits MSC proliferation and promotes osteogenic differentiation and in Chapter 2 we demonstrate that TSP2 inhibits adipogenesis. The molecular mechanisms through which TSP2 influences MSC are however unknown. Here we provide one possible mechanism by demonstrating that TSP2 decreases notch signaling in MSC.

Our results contradict a previous report that showed TSP2 increases notch signaling in lung cancer cell lines and primary smooth muscle cells (156). One possible explanation for this contradictory observation is that whether TSP2 promotes or inhibits notch activation could depend on the repertoire of notch ligands and receptors expressed by the signaling and receiving cells. The cells used in the previous report were selected because they express high levels of Notch-3 but Notch-3 is expressed at relatively low levels in MSC. In addition, receptor deletion experiments have demonstrated that simultaneous inactivation of Notch-1 and Notch-2 is mesenchymal

progenitors is sufficient to generate the same skeletal phenotype as complete elimination of γ-secretase activity, further supporting the notion that Notch-3 likely plays a minimal role in notch signaling in MSC (175). Another possible explanation is the difference in the methodology of notch activation used in our study relative to that in the published report. We used ligands immobilized to the tissue culture plates to activate notch signaling while the previous study used co-culturing with L-cells that express notch ligands. It is therefore possible that whether TSP2 promotes or inhibits notch activation depends on the context in which the notch ligands are presented.

Our finding that blocking notch signaling using GSI increases adipogenic differentiation in both TSP2-null and wild type MSC suggests that TSP2's effect on adipogenic differentiation may be independent of inhibiting notch signaling. Alternatively, it is possible that TSP2 effect on notch signaling may be upstream of γ-secretase cleavage step. This later explanation is supported by a previous report that showed GSI treatment completely abrogates notch activation regardless of the presence or absence of TSP2 (156). The same study also showed that TSP2 effect on notch signaling requires Notch-3 ectodomain which further supports the notion that TSP2 acts upstream of γ-secretase to modulate notch signaling.

Our results show increased cleaved Notch levels in TSP2-null fracture calluses suggest that TSP2 may inhibit Notch activation in vivo. Previous reports have shown that fracture healing is altered in TSP2 null mice (95). It is therefore possible that the increase in cleaved Notch levels is due to

differences in the cell types present in fracture callus of TSP2-null and wild type tibias and may not reflect a direct role for TSP2 in inhibiting notch activation in vivo. Interestingly, notch signaling has been shown to regulate multiple components of the fracture healing process including MSC proliferation and chondrogenic and osteogenic differentiation as well as osteoclast maturation, and blood vessel formation (181-183). It will be interesting to investigate whether the alteration in fracture healing in TSP2-null mice is due to an increase in notch signal activation.

TSP2 null MSC have an increase in MSC numbers at young age. Transgenic mice in which notch signaling is selectively inactivated in early mesenchymal progenitors have a decrease in MSC numbers at 8 weeks of age (175). The results presented here indicate that TSP2 decreases Notch signaling therefore, it is possible that the increase in MSC number in young TSP2 null mice is due to an increase in notch signaling. Similarly, TSP2-null MSC display a delay in osteogenic differentiation in vitro and our results (chapter III) show that Jagged-1 mediate notch activation decreases osteogenic differentiation. The delay in mineralization in TSP2-null MSC could therefore also be due to an increase in notch activation in TSP2-null MSC relative to wild type controls. We propose a model in which TSP2 acts to negatively modulate notch activation in MSC which in turn increases osteogenic differentiation and decreases MSC proliferation resulting in a decreased MSC pool.

Figure 4.1

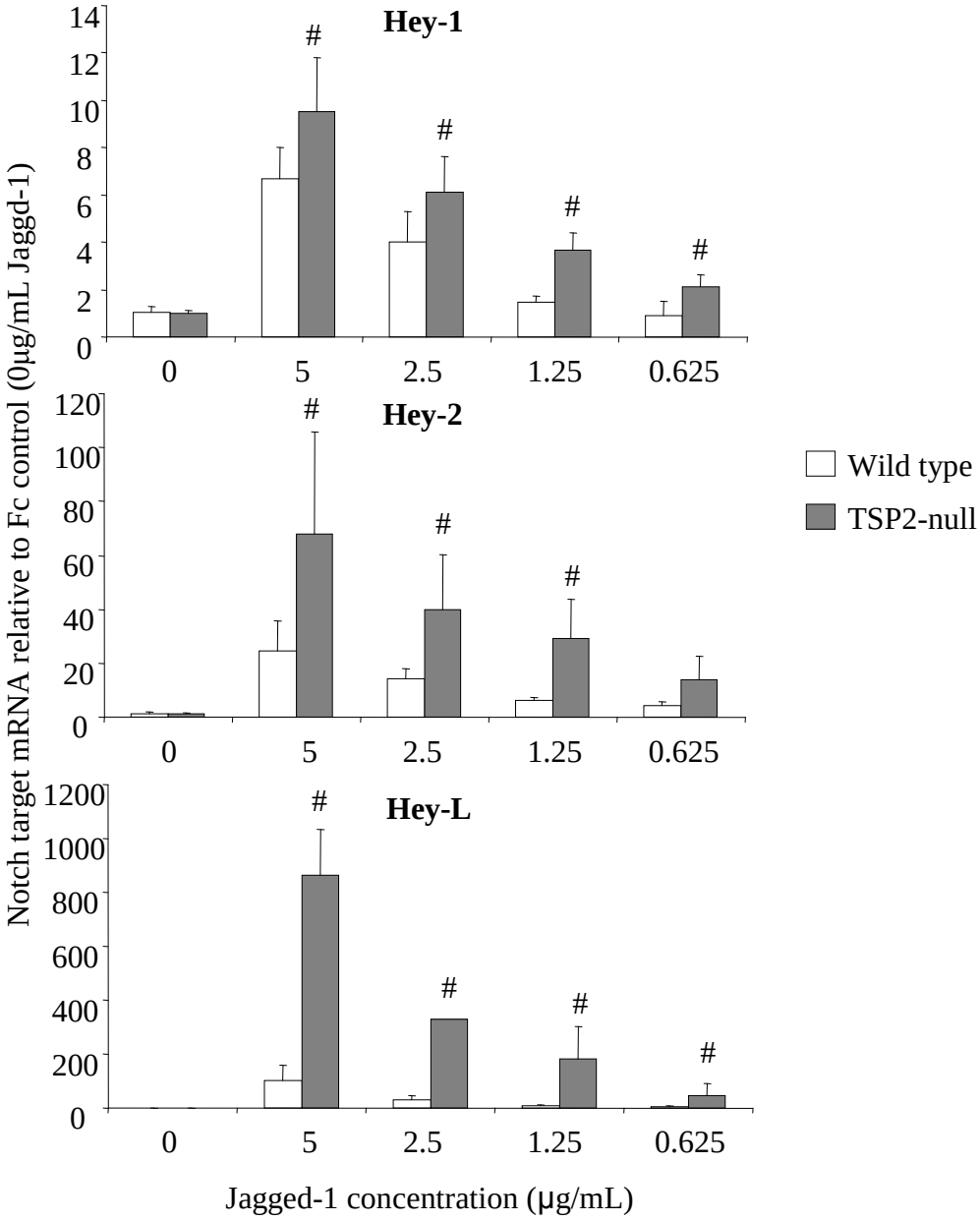

Figure 4.1 Jagged-1 mediated activation of Notch target gene expression is increased in TSP2-null MSC. TSP2-null and wild type MSC were plated onto wells coated with either 0 (Fc-control), 5, 2.5, 1.25, or 0.625 µg/mL Jagged-1. mRNA was harvested 4 days later and expression of notch targets Hey-1, Hey-2 and Hey-L were measured by qPCR. Graphs are mean + S.D. of two independent experiments from two independent cell harvests each done in duplicate. For each experiment, whole bone marrow from 3 wild type and 3 TSP2-null mice was pooled to yield MSC. #=TSP2-null significantly different from wild type; *p< .05.*

Figure 4.2

A)

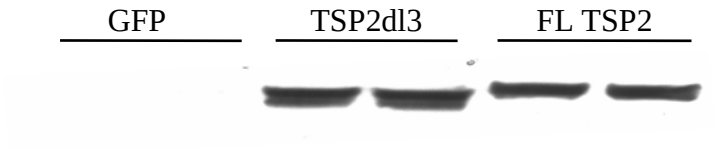

B)

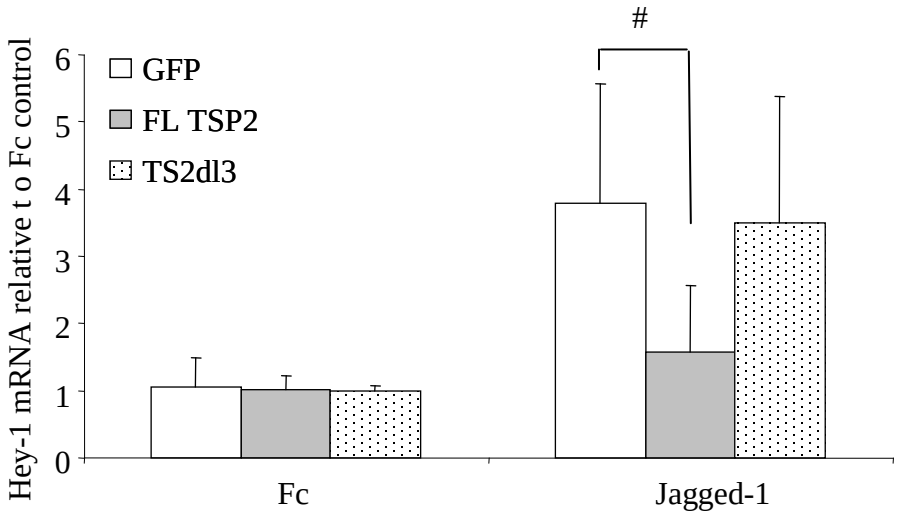

Figure 4.2 TSP2 inhibits Jagged-1 induced Hey-1 expression through its Type I repeat domain. C3H10T1/2 cells were stably transduced with retrovirus carrying GFP, full length TSP2 (FL TSP2) or TSP2 in which all three type I repeat domains have been deleted (TSP2dl3). Media was collected and stable expression of TSP2dl3 was confirmed by western-blotting with a TSP2 monoclonal antibody. **(A)**. Cells were plated onto wells coated with either Fc control (Fc) or 2.5µg/mL Jagged-1 and were harvested 4 days later and Hey-1 mRNA expression was measured using qPCR **(B)**. Graphs represent Mean + S.D of two independent experiments each done in duplicate. #= FL TSP2 transduced cells significantly different from GFP transduced controls; *p<.05.*

Figure 4.3

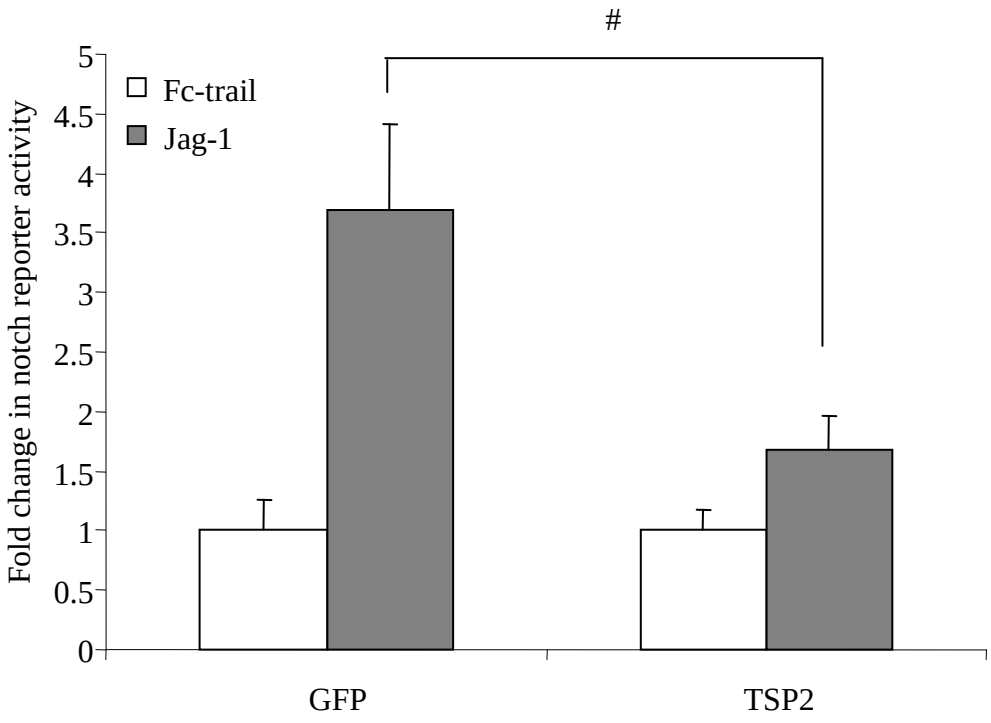

Figure 4.3 TSP2 over-expression decreases Jagged-1 induced notch reporter activity. GFP or full-length TSP2 over-expressing C3H10T1/2 cells were plated on Fc-trail (control protein), or Fc-Jagged-1 (Jag-1) coated wells then were co-transfected with notch reporter (CSL-Luciferase) and pRL-TK constructs as described in the materials and methods section. CSL-luciferase activity was measured 48 hours later and was normalized to pRL-TK activity to control for differences in transduction efficiency. Fold changes in normalized notch reporter activity in cells plated on Jag-1 relative to cells plated on Fc-trail are depicted in the graphs. Data shown are mean + S.D. of two independent experiments each done in duplicate. #=TSP2 over-expressing cells significantly different from GFP over-expressing controls. *p<.05.*

Figure 4.4

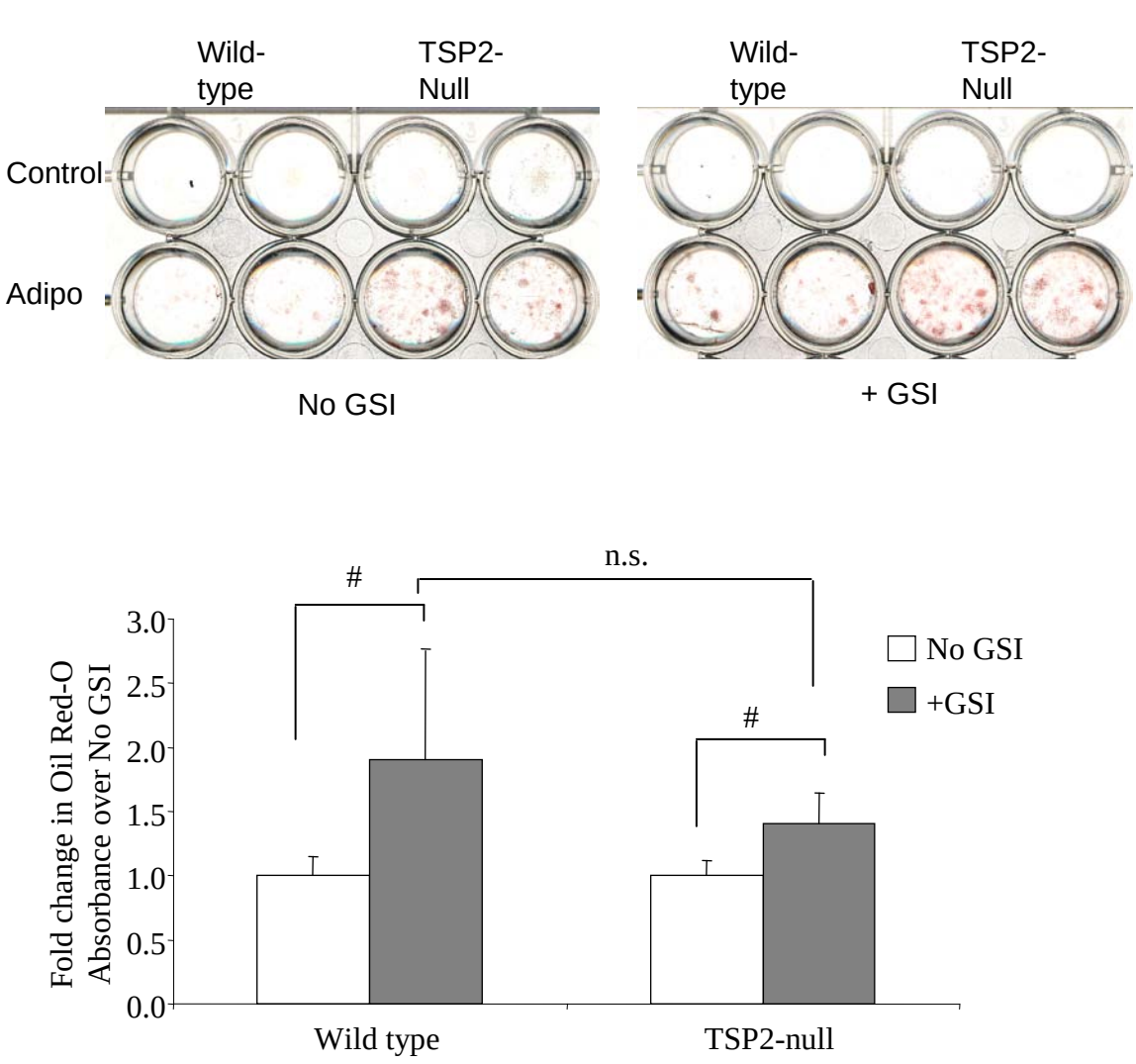

Figure 4.4 γ-secretase inhibitor treatment promotes adipogenesis in both wild-type and TSP2-null MSC. TSP2-null and wild type MSC were induced to undergo adipogenic differentiation in the presence or absence of L-685,458 (GSI) for 10 days then were stained with Oil Red-O. **(A)** plates were scanned and a representative set is shown. **(B)** Oil Red-O was extracted and quantified by measuring absorbance at 540nm. The relative increase in Oil Red-O absorbance in GSI treated cells (+GSI) over un-treated controls (No GSI) from two independent experiments each done in duplicate was averaged and is depicted in the graphs. Error bars + S.D. #=Significantly different from No GSI controls. *p< .05*. The fold change in Oil Red-O absorbance between GSI treated TSP2-null and wild type MSC was not statistically significant (n.s.).

Figure 4.5

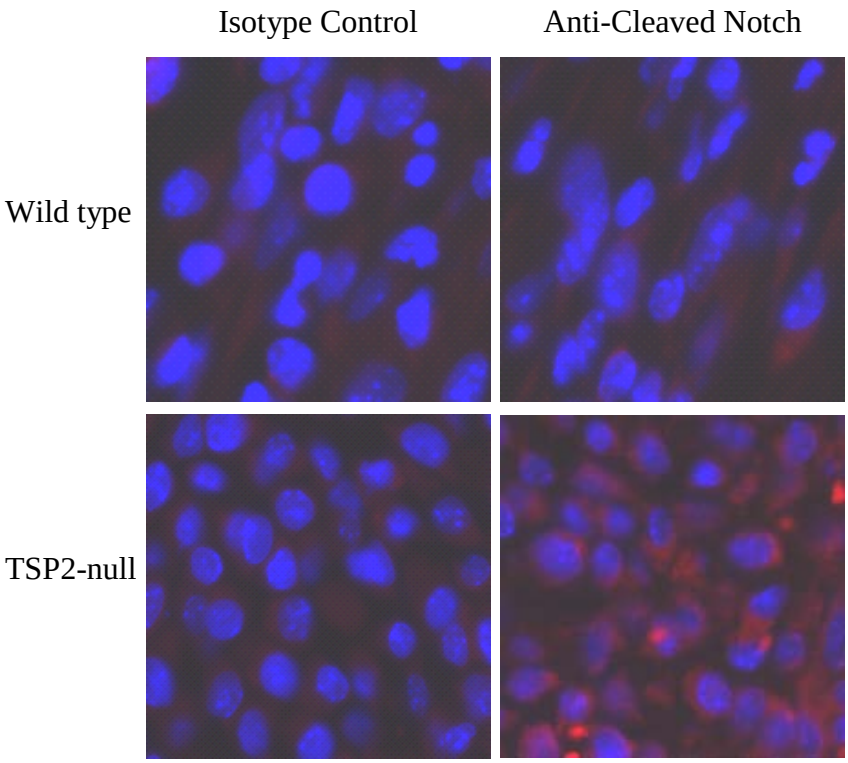

Figure 4.5 Cleaved Notch (activated notch) levels are increased in fracture calluses of TSP2 null mice. 7 micron sections of Day 5 fracture calluses from TSP2-null and wild-type control mice were stained with primary antibody that only recognized notch receptors after they have been cleaved with γ-secretase (Anti-Cleaved Notch). Staining with isotype control antibody served as control for specificity of cleaved notch antibody. Nuclei are stained blue (DAPI), and cleaved notch is located intracellularly and is stained red. Pictures shown are representative of fractured tibias from three wild type and three TSP2-null mice.

CHAPTER V

CONCLUSIONS AND FUTURE DIRECTIONS

Like other stem cells, we presume that mesenchymal stem cells reside within a niche where they receive multiple signals from local and systemic factors. These signals are then processed, integrated and ultimately cell fate is determined. ECM, in addition to serving as a substrate for cell adhesion, plays a role in how cells receive and respond to these signals. Previous reports have shown that TSP2 produced by MSC, inhibits their proliferation and promotes their osteogenic differentiation (1, 2). In this dissertation, we examined the role of TSP2 on influencing adipogenic differentiation and found that TSP2-null MSC accumulate more lipid than wild type MSC. TSP2-null female mice are also heavier than wild type mice because of an increase in adipose tissue. Stromal vascular cells isolated from TSP2-null mice show both increased proliferation and adipogenic differentiation.

Although it is clear that TSP2 plays an important modulatory role in MSC function, the molecular mechanisms through which it exerts an effect on MSC are unknown. Previous reports have shown that TSP2 can physically interact and promote Notch signal activation in other cell types (3). We examined the effect of activating notch signaling in vitro using immobilized Jagged-1 and found that it

increases MSC proliferation and inhibits osteogenic differentiation. Jagged-1 also increases lipid accumulation when cells were induced to undergo adipogenesis primarily by increasing cell number. The effects of activating notch signaling in vitro therefore are similar to the effects of an absence of TSP2; in both instances, there is a decrease in osteogenic differentiation and an increase in lipid accumulation and proliferation.

We examined whether TSP2 can modulate notch signaling in MSC and found that Jagged-1 mediated notch target gene expression was enhanced in TSP2-null MSC, and that over-expressing TSP2 in an MSC line decreased notch target gene expression and notch reporter activity. We propose a model whereby TSP2 negatively regulates notch signaling which in turn decreases MSC proliferation and increases osteogenic differentiation. In the absence of TSP2, notch signaling increases and results in a decrease in osteogenic differentiation and an expansion of the osteoprogenitor pool (Figure 5.1).

Our results which show TSP2 decreases notch activation are in contrast to Meng et al's study that showed TSP2 increases notch activation in lung cancer cell lines and in primary smooth muscle cells (3). One possible explanation for these contradictory results is that the effects of TSP2 on promoting or inhibiting notch signaling are dependent on the repertoire of notch receptors and ligands expressed by affected cells. A recent study by Benedito et al showed that expression of notch targets Hes-1 and Hey-1 was increased when Jagged-1 was inactivated in endothelial cells. Using various in vitro experiments, the authors demonstrated that Jagged-1 antagonizes delta-like-4 mediated notch activation

and its ability to do so was dependent on whether the glucosaminyltransferase manic-fringe was over-expressed in either the signaling or receiving cell (4). TSP2 has been shown to interact with Jagged-1 but whether it also interacts with delta-like-4 is unknown. It is possible that TSP2 interferes with the ability of Jagged-1 to block delta-like-4 mediated notch activation and causes an increase notch signaling when both ligands are expressed but decreases notch signaling when only Jagged-1 is expressed. Future studies should address whether differences in ligand and/or receptor expression account for the different effects TSP2 has on MSC versus the cell types used in the previous report. By extension, the effects of different notch ligands on notch activation and MSC proliferation and differentiation should also be investigated.

Whether the effects of TSP2 on MSC proliferation and/or differentiation are mediated through notch signaling will require demonstration of direct functional interactions. This will require better characterization of the molecular interaction between TSP2 and notch. Our experiments that show GSI treatment increases adipogenesis in both TSP2-null and wild-type cells suggests that TSP2 exerts its effect on notch activation upstream of the γ-secretase cleavage step, perhaps by interfering with notch ectodomain shedding. Examining the effects of TSP2 on notch signaling when different notch receptor constructs (full-length, lacking ectodomain, and NICD) are over-expressed should allow elucidation of notch domains responsible for interaction with TSP2. We show here that the type I repeat domains are required for TSP2s' effect on inhibiting notch signaling. Determining if the type I repeats are required for TSP2 effects on MSC function

should also provide some evidence for whether TSP2 acts through notch to exert its influence on MSC.

We also examined the effects of expressing a dominant negative form of mastermind like-1(dnMAML) in bone development in vivo. We found that Col2.3Cre driven expression of dnMAML causes vertebral malformations similar to that seen in Alagille Syndrome patients. Alagille Syndrome is caused by mutations in Jagged-1 and the vertebral malformations in this disease are thought to arise from disruption of cyclic expression of notch target genes during somitogenesis. In addition to vertebral malformations, Alagille Syndrome patients develop osteoporosis at a young age. Whether the decrease in bone mass seen in these patients is due to mutations in Jagged-1 having an effect on skeletal tissue or whether it arises secondary to other features of the syndrome is however not well understood. The observation that Col2.3Cre/dnMAML$^{fl/-}$ mice develop similar vertebral malformations to Alagille syndrome patients suggests that the Col2.3 promoter drives dnMAML expression in somites. Col2.3Cre/dnMAML$^{fl/-}$ mice may therefore be a useful model to elucidate the mechanism for vertebral malformation and decrease in bone mass seen in Alagille Syndrome patients.

We also show that driving dnMAML expression in early limb-bud mesenchymal progenitors using Prx-1Cre mice results in a decrease in trabecular bone volume fraction at 8 weeks of age without causing any significant change in any trabecular bone parameter at 6 or 14.5 months of age. Our results are in contrast to previous reports by Hilton et al that showed massive

accumulation of trabecular bone at 8 weeks and a severe decrease in bone mass at 6 months of age when notch signaling was inactivated using the same Prx-1Cre mice to delete Notch 1 and Notch 2 (5). One possible explanation for the contradictory observations is that the effects of reducing notch activation using a dominant negative approach results in a different phenotypic outcome than inactivating the pathway using deletion models such those used in the Hilton et al study. Another possible explanation is that inactivating only CSL mediated, canonical notch signaling using dnMAML gives a different outcome than disrupting Notch signaling upstream of CSL. Hilton et al's study has shown that Hey-1 concentration is the limiting factor in the interaction between Hey-1 and Runx-2 therefore it possible that reducing Hey-1 levels may not be sufficient to relieve its effect on inhibiting Runx-2's activity. To determine that the effects of blocking canonical notch signaling specifically results in a different outcome than interfering with notch signaling upstream of CSL (non-canonical signaling) will therefore require testing in other mouse models, such as floxed RPBJ-κ mice (gene coding for CSL protein) in which the CSL gene can be conditionally disrupted in mice using Cre recombinase.

We found that inducing dnMAML expression globally starting at 8 weeks in Mx1Cre/dnMAML$^{fl/fl}$ mice results in a decrease in trabecular bone mass at 6 month of age. The observation that 6 month old Prx-1Cre/dnMAML mice do not display any change in trabecular bone, in conjunction with the observation that CFU-F numbers are not significantly altered in Mx1Cre/dnMAML mice, suggests that the decrease in bone mass in Mx1Cre/dnMAML mice may be due to an

increase in bone resorption rather than due to a change in bone formation. Histomorphometric analysis of Mx1Cre/dnMAML bones should be preformed to determine whether the decrease in bone mass arises from a decrease in bone formation or an increase in bone resorption. The decrease in bone mass when dnMAML is globally activated should raise caution to treatment strategies that aim to pharmacologically block notch signaling to increase bone formation. As well, γ-secretase inhibitors are in clinical trials for treatment of Alzheimer's Disease. Our results suggest that a decrease in bone mass may arise as a side-effect from such treatments. Our observation that immobilized Jagged-1 increases MSC numbers and that the cells retain the potential to differentiate into adipocytes as demonstrated by an increase in lipid accumulation indicates that transiently activating notch signaling using immobilized ligands may be useful to expand MSC in vitro and in vivo.

An intriguing question that has emerged from our work (and which has been conceptually explored in other studies) is whether notch signaling maintains "stemness" in MSC. "Stemness" can be defined as the ability to undergo self renewal, but cell surface markers that identify murine MSC with self-renewal potential are not currently available. An alternative approach to assess self-renewal is to perform in vitro assays in which individual CFU-F's are passaged and re-plated at low density then determining the number of secondary colonies that are derived from the initial colony. Such experiments are difficult because mouse MSC require non-adherent cells and the non-adherent cells often contain cells that are also able to form colonies when they are re-plated. A study by

Sacchetti et al recently showed that a self-renewing population of osteoprogenitor cells in humans can be prospectively isolated using the cell surface marker CD146. CD146 expression was also shown to decreases with osteogenic differentiation and with passage (6). Whether activating notch signaling maintains "stemness" should be investigated in human cells by plating MSC on Jagged-1 coated plates and determining whether the number of cells that express CD146 increases.

Elucidation of the molecular mechanism by which notch may maintain "stemness" should also be pursued further. Previous studies have shown that both Hey-1 and NICD physically interact with Runx-2 and inhibits its transcriptional activity at the osteocalcin promoter. In addition to its role in activating transcription of genes required for osteogenesis, intriguing studies by Dr. Gary Stein's group have shown that Runx-2 remains associated with chromosomes during mitosis and causes epigenetic changes in daughter cells that program them to maintain a differentiated phenotype (7). It will be interesting to determine whether notch signaling interferes with this function of Runx-2 to maintain MSC "stemness" by activating the notch signaling pathway and determining whether Runx-2 is associated with mitotic chromosomes. It will also be interesting if activating notch signaling in osteoblasts could cause de-differentiation. As an example, fate tracking experiments in which permanently labeled osteoblasts (such as by osteocalcin-cre mediated recombination and expression of a floxed GFP protein) are plated on Jagged-1 then induced to

differentiate into other lineages can be performed to assess whether notch signaling induces de-differentiation of committed osteoblasts.

Figure 5.1

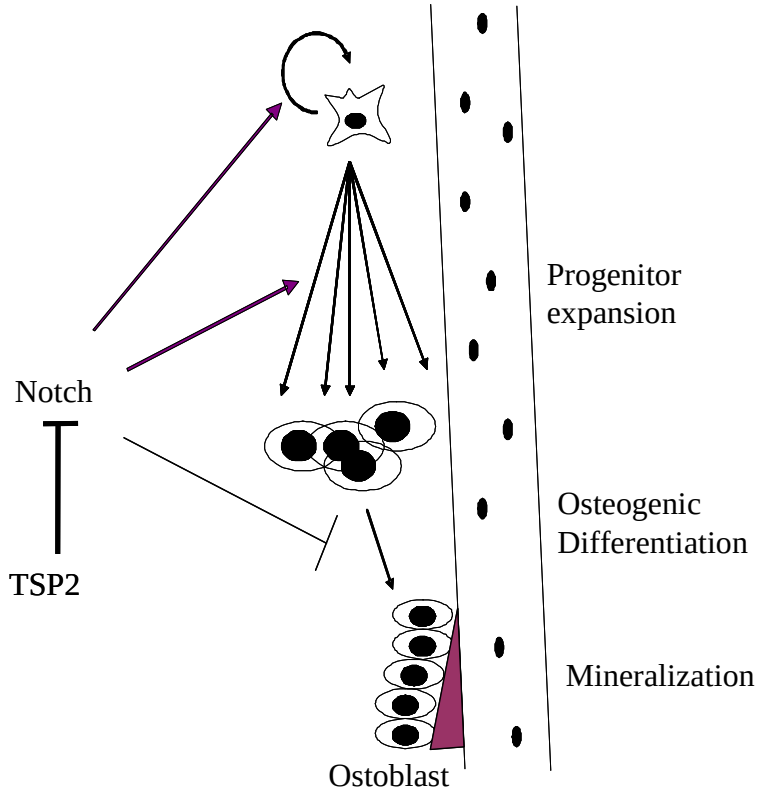

Figure 5.1 Model for TSP2-Notch interaction in MSC fate determination. In this model TSP2 negatively regulates notch signaling which in turn decreases MSC proliferation and increases osteogenic differentiation. In the absence of TSP2, notch signaling increases and results in a decrease in osteogenic differentiation and an expansion of the osteoprogenitor pool.

REFERENCES

1. Sims, N. A., and Gooi, J. H. (2008) Bone remodeling: Multiple cellular interactions required for coupling of bone formation and resorption. *Seminars in cell & developmental biology* **19**, 444-451

2. Martin, T., Gooi, J. H., and Sims, N. A. (2009) Molecular mechanisms in coupling of bone formation to resorption. *Critical reviews in eukaryotic gene expression* **19**, 73-88

3. Mauck, K. F., and Clarke, B. L. (2006) Diagnosis, screening, prevention, and treatment of osteoporosis. *Mayo Clinic proceedings* **81**, 662-672

4. Cooper, C. (1999) Epidemiology of osteoporosis. *Osteoporosis International* **9 Suppl 2**, S2-8

5. Holroyd, C., Cooper, C., and Dennison, E. (2008) Epidemiology of osteoporosis. *Best Practice & Research Clinical Endocrinology & Metabolism* **22**, 671-685

6. Baldock, P. A., Need, A. G., Moore, R. J., Durbridge, T. C., and Morris, H. A. (1999) Discordance between bone turnover and bone loss: effects of aging and ovariectomy in the rat. *J Bone Miner Res* **14**, 1442-1448

7. Wronski, T. J., Lowry, P. L., Walsh, C. C., and Ignaszewski, L. A. (1985) Skeletal alterations in ovariectomized rats. *Calcified tissue international* **37**, 324-328

8. Ferguson, V. L., Ayers, R. A., Bateman, T. A., and Simske, S. J. (2003) Bone development and age-related bone loss in male C57BL/6J mice. *Bone* **33**, 387-398

9. Parfitt, A. M., Villanueva, A. R., Foldes, J., and Rao, D. S. (1995) Relations between histologic indices of bone formation: implications for the pathogenesis of spinal osteoporosis. *J Bone Miner Res* **10**, 466-473

10. Parfitt, A. M., Han, Z. H., Palnitkar, S., Rao, D. S., Shih, M. S., and Nelson, D. (1997) Effects of ethnicity and age or menopause on osteoblast function, bone mineralization, and osteoid accumulation in iliac bone. *J Bone Miner Res* **12**, 1864-1873

11. Burkhardt, R., Kettner, G., Bohm, W., Schmidmeier, M., Schlag, R., Frisch, B., Mallmann, B., Eisenmenger, W., and Gilg, T. (1987) Changes in trabecular bone, hematopoiesis and bone marrow vessels in aplastic anemia, primary osteoporosis, and old age: a comparative histomorphometric study. *Bone* **8**, 157-164

12. Friedenstein, A. J., Piatetzky, S., II, and Petrakova, K. V. (1966) Osteogenesis in transplants of bone marrow cells. *Journal of embryology and experimental morphology* **16**, 381-390

13. Friedenstein, A. J., Chailakhjan, R. K., and Lalykina, K. S. (1970) The development of fibroblast colonies in monolayer cultures of guinea-pig bone marrow and spleen cells. *Cell and tissue kinetics* **3**, 393-403

14. Friedenstein, A. J., Chailakhyan, R. K., Latsinik, N. V., Panasyuk, A. F., and Keiliss-Borok, I. V. (1974) Stromal cells responsible for transferring the microenvironment of the hemopoietic tissues. Cloning in vitro and retransplantation in vivo. *Transplantation* **17**, 331-340

15. Friedenstein, A. J., Deriglasova, U. F., Kulagina, N. N., Panasuk, A. F., Rudakowa, S. F., Luria, E. A., and Ruadkow, I. A. (1974) Precursors for fibroblasts in different populations of hematopoietic cells as detected by the in vitro colony assay method. *Experimental hematology* **2**, 83-92

16. Pittenger, M. F., Mackay, A. M., Beck, S. C., Jaiswal, R. K., Douglas, R., Mosca, J. D., Moorman, M. A., Simonetti, D. W., Craig, S., and Marshak, D. R. (1999) Multilineage potential of adult human mesenchymal stem cells. *Science (New York, N.Y* **284**, 143-147

17. Friedenstein, A. J., Chailakhyan, R. K., and Gerasimov, U. V. (1987) Bone marrow osteogenic stem cells: in vitro cultivation and transplantation in diffusion chambers. *Cell and tissue kinetics* **20**, 263-272

18. Caplan, A. I. (1991) Mesenchymal stem cells. *J Orthop Res* **9**, 641-650

19. Bianco, P., Robey, P. G., and Simmons, P. J. (2008) Mesenchymal stem cells: revisiting history, concepts, and assays. *Cell stem cell* **2**, 313-319

20. Fu, L., Zhu, L., Huang, Y., Lee, T. D., Forman, S. J., and Shih, C. C. (2008) Derivation of neural stem cells from mesenchymal stemcells: evidence for a bipotential stem cell population. *Stem cells and development* **17**, 1109-1121

21. Porada, C. D., Zanjani, E. D., and Almeida-Porad, G. (2006) Adult mesenchymal stem cells: a pluripotent population with multiple applications. *Current stem cell research & therapy* **1**, 365-369

22. Deng, J., Petersen, B. E., Steindler, D. A., Jorgensen, M. L., and Laywell, E. D. (2006) Mesenchymal stem cells spontaneously express neural proteins in culture and are neurogenic after transplantation. *Stem cells (Dayton, Ohio)* **24**, 1054-1064

23. Long, M. W. (2001) Osteogenesis and bone-marrow-derived cells. *Blood cells, molecules & diseases* **27**, 677-690

24. Ducy, P., and Karsenty, G. (1995) Two distinct osteoblast-specific cis-acting elements control expression of a mouse osteocalcin gene. *Molecular & Cellular Biology* **15**, 1858-1869

25. Geoffroy, V., Ducy, P., and Karsenty, G. (1995) A PEBP2 alpha/AML-1-related factor increases osteocalcin promoter activity through its binding to an

osteoblast-specific cis-acting element. *Journal of Biological Chemistry* **270**, 30973-30979

26. Lee, B., Thirunavukkarasu, K., Zhou, L., Pastore, L., Baldini, A., Hecht, J., Geoffroy, V., Ducy, P., and Karsenty, G. (1997) Missense mutations abolishing DNA binding of the osteoblast-specific transcription factor OSF2/CBFA1 in cleidocranial dysplasia. *Nature genetics* **16**, 307-310

27. Mundlos, S., Otto, F., Mundlos, C., Mulliken, J. B., Aylsworth, A. S., Albright, S., Lindhout, D., Cole, W. G., Henn, W., Knoll, J. H., Owen, M. J., Mertelsmann, R., Zabel, B. U., and Olsen, B. R. (1997) Mutations involving the transcription factor CBFA1 cause cleidocranial dysplasia. *Cell* **89**, 773-779

28. Komori, T., Yagi, H., Nomura, S., Yamaguchi, A., Sasaki, K., Deguchi, K., Shimizu, Y., Bronson, R. T., Gao, Y. H., Inada, M., Sato, M., Okamoto, R., Kitamura, Y., Yoshiki, S., and Kishimoto, T. (1997) Targeted disruption of Cbfa1 results in a complete lack of bone formation owing to maturational arrest of osteoblasts. *Cell* **89**, 755-764

29. Otto, F., Thornell, A. P., Crompton, T., Denzel, A., Gilmour, K. C., Rosewell, I. R., Stamp, G. W., Beddington, R. S., Mundlos, S., Olsen, B. R., Selby, P. B., and Owen, M. J. (1997) Cbfa1, a candidate gene for cleidocranial dysplasia syndrome, is essential for osteoblast differentiation and bone development. *Cell* **89**, 765-771

30. Ducy, P., Zhang, R., Geoffroy, V., Ridall, A. L., and Karsenty, G. (1997) Osf2/Cbfa1: a transcriptional activator of osteoblast differentiation. *Cell* **89**, 747-754

31. Nakashima, K., Zhou, X., Kunkel, G., Zhang, Z., Deng, J. M., Behringer, R. R., and de Crombrugghe, B. (2002) The novel zinc finger-containing transcription factor osterix is required for osteoblast differentiation and bone formation. *Cell* **108**, 17-29

32. Baek, W. Y., Lee, M. A., Jung, J. W., Kim, S. Y., Akiyama, H., de Crombrugghe, B., and Kim, J. E. (2009) Positive regulation of adult bone formation by osteoblast-specific transcription factor osterix. *J Bone Miner Res* **24**, 1055-1065

33. Yang, X., Matsuda, K., Bialek, P., Jacquot, S., Masuoka, H. C., Schinke, T., Li, L., Brancorsini, S., Sassone-Corsi, P., Townes, T. M., Hanauer, A., and Karsenty, G. (2004) ATF4 is a substrate of RSK2 and an essential regulator of osteoblast biology; implication for Coffin-Lowry Syndrome. *Cell* **117**, 387-398

34. Yu, V. W., Akhouayri, O., and St-Arnaud, R. (2009) FIAT is co-expressed with its dimerization target ATF4 in early osteoblasts, but not in osteocytes. *Gene Expr Patterns* **9**, 335-340

35. Yu, V. W., El-Hoss, J., and St-Arnaud, R. (2009) FIAT inhibition increases osteoblast activity by modulating Atf4-dependent functions. *Journal of cellular biochemistry* **106**, 186-192

36. Yu, S., Franceschi, R. T., Luo, M., Zhang, X., Jiang, D., Lai, Y., Jiang, Y., Zhang, J., and Xiao, G. (2008) Parathyroid hormone increases activating transcription factor 4 expression and activity in osteoblasts: requirement for osteocalcin gene expression. *Endocrinology* **149**, 1960-1968

37. Yu, V. W., Gauthier, C., and St-Arnaud, R. (2006) Inhibition of ATF4 transcriptional activity by FIAT/gamma-taxilin modulates bone mass accrual. *Annals of the New York Academy of Sciences* **1068**, 131-142

38. Xiao, G., Jiang, D., Ge, C., Zhao, Z., Lai, Y., Boules, H., Phimphilai, M., Yang, X., Karsenty, G., and Franceschi, R. T. (2005) Cooperative interactions between activating transcription factor 4 and Runx2/Cbfa1 stimulate osteoblast-specific osteocalcin gene expression. *The Journal of biological chemistry* **280**, 30689-30696

39. Yu, V. W., Ambartsoumian, G., Verlinden, L., Moir, J. M., Prud'homme, J., Gauthier, C., Roughley, P. J., and St-Arnaud, R. (2005) FIAT represses ATF4-mediated transcription to regulate bone mass in transgenic mice. *The Journal of cell biology* **169**, 591-601

40. Li, H., Marijanovic, I., Kronenberg, M. S., Erceg, I., Stover, M. L., Velonis, D., Mina, M., Heinrich, J. G., Harris, S. E., Upholt, W. B., Kalajzic, I., and Lichtler, A. C. (2008) Expression and function of Dlx genes in the osteoblast lineage. *Developmental biology* **316**, 458-470

41. Samee, N., de Vernejoul, M. C., and Levi, G. (2007) Role of DLX regulatory proteins in osteogenesis and chondrogenesis. *Critical reviews in eukaryotic gene expression* **17**, 173-186

42. Holleville, N., Mateos, S., Bontoux, M., Bollerot, K., and Monsoro-Burq, A. H. (2007) Dlx5 drives Runx2 expression and osteogenic differentiation in developing cranial suture mesenchyme. *Developmental biology* **304**, 860-874

43. Ryoo, H. M., Hoffmann, H. M., Beumer, T., Frenkel, B., Towler, D. A., Stein, G. S., Stein, J. L., van Wijnen, A. J., and Lian, J. B. (1997) Stage-specific expression of Dlx-5 during osteoblast differentiation: involvement in regulation of osteocalcin gene expression. *Molecular endocrinology (Baltimore, Md* **11**, 1681-1694

44. Sabatakos, G., Rowe, G. C., Kveiborg, M., Wu, M., Neff, L., Chiusaroli, R., Philbrick, W. M., and Baron, R. (2008) Doubly truncated FosB isoform (Delta2DeltaFosB) induces osteosclerosis in transgenic mice and modulates expression and phosphorylation of Smads in osteoblasts independent of intrinsic AP-1 activity. *J Bone Miner Res* **23**, 584-595

45. Kveiborg, M., Sabatakos, G., Chiusaroli, R., Wu, M., Philbrick, W. M., Horne, W. C., and Baron, R. (2004) DeltaFosB induces osteosclerosis and decreases adipogenesis by two independent cell-autonomous mechanisms. *Molecular and cellular biology* **24**, 2820-2830

46. Sabatakos, G., Sims, N. A., Chen, J., Aoki, K., Kelz, M. B., Amling, M., Bouali, Y., Mukhopadhyay, K., Ford, K., Nestler, E. J., and Baron, R. (2000) Overexpression of DeltaFosB transcription factor(s) increases bone formation and inhibits adipogenesis. *Nature medicine* **6**, 985-990

47. Eferl, R., Hoebertz, A., Schilling, A. F., Rath, M., Karreth, F., Kenner, L., Amling, M., and Wagner, E. F. (2004) The Fos-related antigen Fra-1 is an activator of bone matrix formation. *The EMBO journal* **23**, 2789-2799

48. Roschger, P., Matsuo, K., Misof, B. M., Tesch, W., Jochum, W., Wagner, E. F., Fratzl, P., and Klaushofer, K. (2004) Normal mineralization and nanostructure of sclerotic bone in mice overexpressing Fra-1. *Bone* **34**, 776-782

49. McCauley, L. K., Koh-Paige, A. J., Chen, H., Chen, C., Ontiveros, C., Irwin, R., and McCabe, L. R. (2001) Parathyroid hormone stimulates fra-2 expression in osteoblastic cells in vitro and in vivo. *Endocrinology* **142**, 1975-1981

50. Jochum, W., David, J. P., Elliott, C., Wutz, A., Plenk, H., Jr., Matsuo, K., and Wagner, E. F. (2000) Increased bone formation and osteosclerosis in mice overexpressing the transcription factor Fra-1. *Nature medicine* **6**, 980-984

51. Tontonoz, P., Hu, E., and Spiegelman, B. M. (1995) Regulation of adipocyte gene expression and differentiation by peroxisome proliferator activated receptor gamma. *Current opinion in genetics & development* **5**, 571-576

52. Tontonoz, P., Hu, E., and Spiegelman, B. M. (1994) Stimulation of adipogenesis in fibroblasts by PPAR gamma 2, a lipid-activated transcription factor. *Cell* **79**, 1147-1156

53. MacDougald, O. A., and Lane, M. D. (1995) Transcriptional regulation of gene expression during adipocyte differentiation. *Annual review of biochemistry* **64**, 345-373

54. Muruganandan, S., Roman, A. A., and Sinal, C. J. (2009) Adipocyte differentiation of bone marrow-derived mesenchymal stem cells: cross talk with the osteoblastogenic program. *Cell Mol Life Sci* **66**, 236-253

55. Rozman, C., Feliu, E., Berga, L., Reverter, J. C., Climent, C., and Ferran, M. J. (1989) Age-related variations of fat tissue fraction in normal human bone marrow depend both on size and number of adipocytes: a stereological study. *Experimental hematology* **17**, 34-37

56. Meunier, P., Aaron, J., Edouard, C., and Vignon, G. (1971) Osteoporosis and the replacement of cell populations of the marrow by adipose tissue. A quantitative study of 84 iliac bone biopsies. *Clinical orthopaedics and related research* **80**, 147-154

57. Moerman, E. J., Teng, K., Lipschitz, D. A., and Lecka-Czernik, B. (2004) Aging activates adipogenic and suppresses osteogenic programs in mesenchymal marrow stroma/stem cells: the role of PPAR-gamma2 transcription factor and TGF-beta/BMP signaling pathways. *Aging cell* **3**, 379-389

58. Verma, S., Rajaratnam, J. H., Denton, J., Hoyland, J. A., and Byers, R. J. (2002) Adipocytic proportion of bone marrow is inversely related to bone formation in osteoporosis. *Journal of clinical pathology* **55**, 693-698

59. Bennett, C. N., Ouyang, H., Ma, Y. L., Zeng, Q., Gerin, I., Sousa, K. M., Lane, T. F., Krishnan, V., Hankenson, K. D., and MacDougald, O. A. (2007) Wnt10b increases postnatal bone formation by enhancing osteoblast differentiation. *J Bone Miner Res* **22**, 1924-1932

60. Bennett, C. N., Longo, K. A., Wright, W. S., Suva, L. J., Lane, T. F., Hankenson, K. D., and MacDougald, O. A. (2005) Regulation of osteoblastogenesis and bone mass by Wnt10b. *Proceedings of the National Academy of Sciences of the United States of America* **102**, 3324-3329

61. Ross, S. E., Hemati, N., Longo, K. A., Bennett, C. N., Lucas, P. C., Erickson, R. L., and MacDougald, O. A. (2000) Inhibition of adipogenesis by Wnt signaling. *Science (New York, N.Y* **289**, 950-953

62. Lazarenko, O. P., Rzonca, S. O., Suva, L. J., and Lecka-Czernik, B. (2006) Netoglitazone is a PPAR-gamma ligand with selective effects on bone and fat. *Bone* **38**, 74-84

63. Lecka-Czernik, B., Moerman, E. J., Grant, D. F., Lehmann, J. M., Manolagas, S. C., and Jilka, R. L. (2002) Divergent effects of selective peroxisome proliferator-activated receptor-gamma 2 ligands on adipocyte versus osteoblast differentiation. *Endocrinology* **143**, 2376-2384

64. Grey, A. (2009) Thiazolidinedione-induced skeletal fragility--mechanisms and implications. *Diabetes, obesity & metabolism* **11**, 275-284

65. Grey, A., Bolland, M., Gamble, G., Wattie, D., Horne, A., Davidson, J., and Reid, I. R. (2007) The peroxisome proliferator-activated receptor-gamma agonist rosiglitazone decreases bone formation and bone mineral density in healthy postmenopausal women: a randomized, controlled trial. *The Journal of clinical endocrinology and metabolism* **92**, 1305-1310

66. Hong, J. H., Hwang, E. S., McManus, M. T., Amsterdam, A., Tian, Y., Kalmukova, R., Mueller, E., Benjamin, T., Spiegelman, B. M., Sharp, P. A., Hopkins, N., and Yaffe, M. B. (2005) TAZ, a transcriptional modulator of mesenchymal stem cell differentiation. *Science (New York, N.Y* **309**, 1074-1078

67. Kousteni, S., and Bilezikian, J. P. (2008) The cell biology of parathyroid hormone in osteoblasts. *Current osteoporosis reports* **6**, 72-76

68. Pettway, G. J., Schneider, A., Koh, A. J., Widjaja, E., Morris, M. D., Meganck, J. A., Goldstein, S. A., and McCauley, L. K. (2005) Anabolic actions of PTH (1-34): use of a novel tissue engineering model to investigate temporal effects on bone. *Bone* **36**, 959-970

69. Chen, H. L., Demiralp, B., Schneider, A., Koh, A. J., Silve, C., Wang, C. Y., and McCauley, L. K. (2002) Parathyroid hormone and parathyroid hormone-related

protein exert both pro- and anti-apoptotic effects in mesenchymal cells. *The Journal of biological chemistry* **277**, 19374-19381

70. Imai, Y., Nakamura, T., Matsumoto, T., Takaoka, K., and Kato, S. (2009) Molecular mechanisms underlying the effects of sex steroids on bone and mineral metabolism. *Journal of bone and mineral metabolism* **27**, 127-130

71. Imai, Y., Kondoh, S., Kouzmenko, A., and Kato, S. (2008) Regulation of bone metabolism by nuclear receptors. *Molecular and cellular endocrinology*

72. Canalis, E. (2003) Mechanisms of glucocorticoid-induced osteoporosis. *Current opinion in rheumatology* **15**, 454-457

73. Delany, A. M., Dong, Y., and Canalis, E. (1994) Mechanisms of glucocorticoid action in bone cells. *Journal of cellular biochemistry* **56**, 295-302

74. Friedman, M. S., Long, M. W., and Hankenson, K. D. (2006) Osteogenic differentiation of human mesenchymal stem cells is regulated by bone morphogenetic protein-6. *Journal of cellular biochemistry* **98**, 538-554

75. Kaplan, F. S., Fiori, J., LS, D. L. P., Ahn, J., Billings, P. C., and Shore, E. M. (2006) Dysregulation of the BMP-4 signaling pathway in fibrodysplasia ossificans progressiva. *Annals of the New York Academy of Sciences* **1068**, 54-65

76. Fiori, J. L., Billings, P. C., de la Pena, L. S., Kaplan, F. S., and Shore, E. M. (2006) Dysregulation of the BMP-p38 MAPK signaling pathway in cells from patients with fibrodysplasia ossificans progressiva (FOP). *J Bone Miner Res* **21**, 902-909

77. Shore, E. M., Xu, M., Feldman, G. J., Fenstermacher, D. A., Cho, T. J., Choi, I. H., Connor, J. M., Delai, P., Glaser, D. L., LeMerrer, M., Morhart, R., Rogers, J. G., Smith, R., Triffitt, J. T., Urtizberea, J. A., Zasloff, M., Brown, M. A., and Kaplan, F. S. (2006) A recurrent mutation in the BMP type I receptor ACVR1 causes inherited and sporadic fibrodysplasia ossificans progressiva. *Nature genetics* **38**, 525-527

78. Xiao, Y. T., Xiang, L. X., and Shao, J. Z. (2007) Bone morphogenetic protein. *Biochemical and biophysical research communications* **362**, 550-553

79. Gong, Y., Slee, R. B., Fukai, N., Rawadi, G., Roman-Roman, S., Reginato, A. M., Wang, H., Cundy, T., Glorieux, F. H., Lev, D., Zacharin, M., Oexle, K., Marcelino, J., Suwairi, W., Heeger, S., Sabatakos, G., Apte, S., Adkins, W. N., Allgrove, J., Arslan-Kirchner, M., Batch, J. A., Beighton, P., Black, G. C., Boles, R. G., Boon, L. M., Borrone, C., Brunner, H. G., Carle, G. F., Dallapiccola, B., De Paepe, A., Floege, B., Halfhide, M. L., Hall, B., Hennekam, R. C., Hirose, T., Jans, A., Juppner, H., Kim, C. A., Keppler-Noreuil, K., Kohlschuetter, A., LaCombe, D., Lambert, M., Lemyre, E., Letteboer, T., Peltonen, L., Ramesar, R. S., Romanengo, M., Somer, H., Steichen-Gersdorf, E., Steinmann, B., Sullivan, B., Superti-Furga, A., Swoboda, W., van den Boogaard, M. J., Van Hul, W., Vikkula, M., Votruba, M., Zabel, B., Garcia, T., Baron, R., Olsen, B. R., and Warman, M. L.

(2001) LDL receptor-related protein 5 (LRP5) affects bone accrual and eye development. *Cell* **107**, 513-523

80. Kang, S., Bennett, C. N., Gerin, I., Rapp, L. A., Hankenson, K. D., and Macdougald, O. A. (2007) Wnt signaling stimulates osteoblastogenesis of mesenchymal precursors by suppressing CCAAT/enhancer-binding protein alpha and peroxisome proliferator-activated receptor gamma. *The Journal of biological chemistry* **282**, 14515-14524

81. Ge, C., Xiao, G., Jiang, D., and Franceschi, R. T. (2007) Critical role of the extracellular signal-regulated kinase-MAPK pathway in osteoblast differentiation and skeletal development. *The Journal of cell biology* **176**, 709-718

82. Franceschi, R. T., Xiao, G., Jiang, D., Gopalakrishnan, R., Yang, S., and Reith, E. (2003) Multiple signaling pathways converge on the Cbfa1/Runx2 transcription factor to regulate osteoblast differentiation. *Connective tissue research* **44 Suppl 1**, 109-116

83. Xiao, G., Jiang, D., Thomas, P., Benson, M. D., Guan, K., Karsenty, G., and Franceschi, R. T. (2000) MAPK pathways activate and phosphorylate the osteoblast-specific transcription factor, Cbfa1. *The Journal of biological chemistry* **275**, 4453-4459

84. Luo, W., Shitaye, H., Friedman, M., Bennett, C. N., Miller, J., Macdougald, O. A., and Hankenson, K. D. (2008) Disruption of cell-matrix interactions by heparin enhances mesenchymal progenitor adipocyte differentiation. *Experimental cell research* **314**, 3382-3391

85. McBeath, R., Pirone, D. M., Nelson, C. M., Bhadriraju, K., and Chen, C. S. (2004) Cell shape, cytoskeletal tension, and RhoA regulate stem cell lineage commitment. *Developmental cell* **6**, 483-495

86. Alford, A. I., and Hankenson, K. D. (2006) Matricellular proteins: Extracellular modulators of bone development, remodeling, and regeneration. *Bone* **38**, 749-757

87. Bornstein, P. (2000) Matricellular proteins: an overview. *Matrix Biol* **19**, 555-556

88. Delany, A. M., Kalajzic, I., Bradshaw, A. D., Sage, E. H., and Canalis, E. (2003) Osteonectin-null mutation compromises osteoblast formation, maturation, and survival. *Endocrinology* **144**, 2588-2596

89. Lawler, J. (2000) The functions of thrombospondin-1 and-2. *Current opinion in cell biology* **12**, 634-640

90. Bornstein, P., Devarayalu, S., Li, P., Disteche, C. M., and Framson, P. (1991) A second thrombospondin gene in the mouse is similar in organization to thrombospondin 1 but does not respond to serum. *Proc.Natl.Acad.Sci.U.S A* **88**, 8636-8640

91. Bornstein, P., O'Rourke, K., Wikstrom, K., Wolf, F. W., Katz, R., Li, P., and Dixit, V. M. (1991) A second, expressed thrombospondin gene (Thbs2) exists in the mouse genome. *J.Biol.Chem.* **266**, 12821-12824

92. Shingu, T., and Bornstein, P. (1993) Characterization of the mouse thrombospondin 2 gene. *Genomics* **16**, 78-84

93. Bornstein, P. (1992) Thrombospondins: structure and regulation of expression. *Faseb J* **6**, 3290-3299

94. Kyriakides, T. R., Zhu, Y. H., Yang, Z., and Bornstein, P. (1998) The distribution of the matricellular protein thrombospondin 2 in tissues of embryonic and adult mice. *J Histochem Cytochem* **46**, 1007-1015

95. Taylor, D. K., Meganck, J. A., Terkhorn, S., Rajani, R., Naik, A., O'Keefe, R. J., Goldstein, S. A., and Hankenson, K. D. (2009) Thrombospondin-2 influences the proportion of cartilage and bone during fracture healing. *J Bone Miner Res* **24**, 1043-1054

96. Armstrong, L. C., Bjorkblom, B., Hankenson, K. D., Siadak, A. W., Stiles, C. E., and Bornstein, P. (2002) Thrombospondin 2 inhibits microvascular endothelial cell proliferation by a caspase-independent mechanism. *Molecular biology of the cell* **13**, 1893-1905

97. Kyriakides, T. R., Zhu, Y. H., Yang, Z., Huynh, G., and Bornstein, P. (2001) Altered extracellular matrix remodeling and angiogenesis in sponge granulomas of thrombospondin 2-null mice. *The American journal of pathology* **159**, 1255-1262

98. Hankenson, K. D., Bain, S. D., Kyriakides, T. R., Smith, E. A., Goldstein, S. A., and Bornstein, P. (2000) Increased marrow-derived osteoprogenitor cells and endosteal bone formation in mice lacking thrombospondin 2. *J Bone Miner.Res.* **15**, 851-862

99. Bornstein, P., Armstrong, L. C., Hankenson, K. D., Kyriakides, T. R., and Yang, Z. (2000) Thrombospondin 2, a matricellular protein with diverse functions. *Matrix Biol* **19**, 557-568

100. Kyriakides, T. R., Leach, K. J., Hoffman, A. S., Ratner, B. D., and Bornstein, P. (1999) Mice that lack the angiogenesis inhibitor, thrombospondin 2, mount an altered foreign body reaction characterized by increased vascularity. *Proceedings of the National Academy of Sciences of the United States of America* **96**, 4449-4454

101. Kyriakides, T. R., Zhu, Y. H., Smith, L. T., Bain, S. D., Yang, Z., Lin, M. T., Danielson, K. G., Iozzo, R. V., LaMarca, M., McKinney, C. E., Ginns, E. I., and Bornstein, P. (1998) Mice that lack thrombospondin 2 display connective tissue abnormalities that are associated with disordered collagen fibrillogenesis, an increased vascular density, and a bleeding diathesis. *The Journal of cell biology* **140**, 419-430

102. Hankenson, K. D., Bain, S. D., Kyriakides, T. R., Smith, E. A., Goldstein, S. A., and Bornstein, P. (2000) Increased marrow-derived osteoprogenitor cells and endosteal bone formation in mice lacking thrombospondin 2. *J Bone Miner Res* **15**, 851-862

103. Hankenson, K. D., and Bornstein, P. (2002) The secreted protein thrombospondin 2 is an autocrine inhibitor of marrow stromal cell proliferation. *J Bone Miner Res* **17**, 415-425

104. de Fraipont, F., Nicholson, A. C., Feige, J. J., and Van Meir, E. G. (2001) Thrombospondins and tumor angiogenesis. *Trends in molecular medicine* **7**, 401-407

105. Meng, H., Zhang, X., Hankenson, K. D., and Wang, M. M. (2008) Thrombospondin2 binds and potentiates Notch signaling proteins. *PNAS* **submitted**

106. Fiuza, U. M., and Arias, A. M. (2007) Cell and molecular biology of Notch. *The Journal of endocrinology* **194**, 459-474

107. Mumm, J. S., and Kopan, R. (2000) Notch signaling: from the outside in. *Dev Biol* **228**, 151-165

108. Rebay, I., Fleming, R. J., Fehon, R. G., Cherbas, L., Cherbas, P., and Artavanis-Tsakonas, S. (1991) Specific EGF repeats of Notch mediate interactions with Delta and Serrate: implications for Notch as a multifunctional receptor. *Cell* **67**, 687-699

109. Artavanis-Tsakonas, S., Rand, M. D., and Lake, R. J. (1999) Notch signaling: cell fate control and signal integration in development. *Science* **284**, 770-776

110. Brou, C., Logeat, F., Gupta, N., Bessia, C., LeBail, O., Doedens, J. R., Cumano, A., Roux, P., Black, R. A., and Israel, A. (2000) A novel proteolytic cleavage involved in Notch signaling: the role of the disintegrin-metalloprotease TACE. *Mol Cell* **5**, 207-216

111. Okochi, M., Steiner, H., Fukumori, A., Tanii, H., Tomita, T., Tanaka, T., Iwatsubo, T., Kudo, T., Takeda, M., and Haass, C. (2002) Presenilins mediate a dual intramembranous gamma-secretase cleavage of Notch-1. *Embo J* **21**, 5408-5416

112. Wang, W., and Struhl, G. (2004) Drosophila Epsin mediates a select endocytic pathway that DSL ligands must enter to activate Notch. *Development* **131**, 5367-5380

113. Iso T, K. L., Hamamori Y (2003) HES and HERP families: multiple effectors of the Notch signaling pathway. *J Cell Physiol* **194**, 237-255.

114. Dumortier, A., Wilson, A., MacDonald, H. R., and Radtke, F. (2005) Paradigms of notch signaling in mammals. *International journal of hematology* **82**, 277-284

115. Van De Bor, V., and Giangrande, A. (2001) Notch signaling represses the glial fate in fly PNS. *Development (Cambridge, England)* **128**, 1381-1390

116. Ye, Y., Lukinova, N., and Fortini, M. E. (1999) Neurogenic phenotypes and altered Notch processing in Drosophila Presenilin mutants. *Nature* **398**, 525-529

117. Vervoort, M., Merritt, D. J., Ghysen, A., and Dambly-Chaudiere, C. (1997) Genetic basis of the formation and identity of type I and type II neurons in Drosophila embryos. *Development (Cambridge, England)* **124**, 2819-2828

118. Morrison, S. J., Perez, S. E., Qiao, Z., Verdi, J. M., Hicks, C., Weinmaster, G., and Anderson, D. J. (2000) Transient Notch activation initiates an irreversible switch from neurogenesis to gliogenesis by neural crest stem cells. *Cell* **101**, 499-510

119. Chiba, S. (2006) Notch signaling in stem cell systems. *Stem Cells* **24**, 2437-2447

120. Fre, S., Huyghe, M., Mourikis, P., Robine, S., Louvard, D., and Artavanis-Tsakonas, S. (2005) Notch signals control the fate of immature progenitor cells in the intestine. *Nature* **435**, 964-968

121. Maillard, I., Tu, L., Sambandam, A., Yashiro-Ohtani, Y., Millholland, J., Keeshan, K., Shestova, O., Xu, L., Bhandoola, A., and Pear, W. S. (2006) The requirement for Notch signaling at the beta-selection checkpoint in vivo is absolute and independent of the pre-T cell receptor. *The Journal of experimental medicine* **203**, 2239-2245

122. Tanigaki, K., and Honjo, T. (2007) Regulation of lymphocyte development by Notch signaling. *Nat Immunol* **8**, 451-456

123. Molofsky, A. V., Pardal, R., and Morrison, S. J. (2004) Diverse mechanisms regulate stem cell self-renewal. *Curr Opin Cell Biol* **16**, 700-707

124. Wilson, A., and Radtke, F. (2006) Multiple functions of Notch signaling in self-renewing organs and cancer. *FEBS letters* **580**, 2860-2868

125. Stanger, B. Z., Datar, R., Murtaugh, L. C., and Melton, D. A. (2005) Direct regulation of intestinal fate by Notch. *Proceedings of the National Academy of Sciences of the United States of America* **102**, 12443-12448

126. van Es, J. H., van Gijn, M. E., Riccio, O., van den Born, M., Vooijs, M., Begthel, H., Cozijnsen, M., Robine, S., Winton, D. J., Radtke, F., and Clevers, H. (2005) Notch/gamma-secretase inhibition turns proliferative cells in intestinal crypts and adenomas into goblet cells. *Nature* **435**, 959-963

127. Maillard, I., Koch, U., Dumortier, A., Shestova, O., Xu, L., Sai, H., Pross, S. E., Aster, J. C., Bhandoola, A., Radtke, F., and Pear, W. S. (2008) Canonical notch signaling is dispensable for the maintenance of adult hematopoietic stem cells. *Cell stem cell* **2**, 356-366

128. Weber, J. M., Forsythe, S. R., Christianson, C. A., Frisch, B. J., Gigliotti, B. J., Jordan, C. T., Milner, L. A., Guzman, M. L., and Calvi, L. M. (2006) Parathyroid hormone stimulates expression of the Notch ligand Jagged1 in osteoblastic cells. *Bone* **39**, 485-493

129. Burns, C. E., Traver, D., Mayhall, E., Shepard, J. L., and Zon, L. I. (2005) Hematopoietic stem cell fate is established by the Notch-Runx pathway. *Genes & development* **19**, 2331-2342

130. Duncan, A. W., Rattis, F. M., DiMascio, L. N., Congdon, K. L., Pazianos, G., Zhao, C., Yoon, K., Cook, J. M., Willert, K., Gaiano, N., and Reya, T. (2005) Integration of Notch and Wnt signaling in hematopoietic stem cell maintenance. *Nature immunology* **6**, 314-322

131. Spinner, N. B. (1999) Alagille syndrome and the notch signaling pathway: new insights into human development. *Gastroenterology* **116**, 1257-1260

132. Colombo, C., Okolicsanyi, L., and Strazzabosco, M. (2000) Advances in familial and congenital cholestatic diseases. Clinical and diagnostic implications. *Dig Liver Dis* **32**, 152-159

133. Krantz, I. D., Piccoli, D. A., and Spinner, N. B. (1999) Clinical and molecular genetics of Alagille syndrome. *Current opinion in pediatrics* **11**, 558-564

134. Shifley, E. T., and Cole, S. E. (2007) The vertebrate segmentation clock and its role in skeletal birth defects. *Birth Defects Res C Embryo Today* **81**, 121-133

135. Olsen, I. E., Ittenbach, R. F., Rovner, A. J., Leonard, M. B., Mulberg, A. E., Stallings, V. A., Piccoli, D. A., and Zemel, B. S. (2005) Deficits in size-adjusted bone mass in children with Alagille syndrome. *Journal of pediatric gastroenterology and nutrition* **40**, 76-82

136. Quiros-Tejeira, R. E., Ament, M. E., Heyman, M. B., Martin, M. G., Rosenthal, P., Gornbein, J. A., McDiarmid, S. V., and Vargas, J. H. (2000) Does liver transplantation affect growth pattern in Alagille syndrome? *Liver Transpl* **6**, 582-587

137. Engin, F., Yao, Z., Yang, T., Zhou, G., Bertin, T., Jiang, M. M., Chen, Y., Wang, L., Zheng, H., Sutton, R. E., Boyce, B. F., and Lee, B. (2008) Dimorphic effects of Notch signaling in bone homeostasis. *Nat Med* **14**, 299-305

138. Zanotti, S., Smerdel-Ramoya, A., Stadmeyer, L., Durant, D., Radtke, F., and Canalis, E. (2008) Notch inhibits osteoblast differentiation and causes osteopenia. *ENDOCRINOLOGY* **149**, 3890-3899

139. Hilton, M. J., Tu, X., Wu, X., Bai, S., Zhao, H., Kobayashi, T., Kronenberg, H. M., Teitelbaum, S. L., Ross, F. P., Kopan, R., and Long, F. (2008) Notch signaling maintains bone marrow mesenchymal progenitors by suppressing osteoblast differentiation. *Nat Med* **14**, 306-314

140. Logan, M., Martin, J. F., Nagy, A., Lobe, C., Olson, E. N., and Tabin, C. J. (2002) Expression of Cre Recombinase in the developing mouse limb bud driven by a Prxl enhancer. *Genesis* **33**, 77-80

141. Deregowski, V., Gazzerro, E., Priest, L., Rydziel, S., and Canalis, E. (2006) Role of the RAM domain and ankyrin repeats on notch signaling and activity in cells of osteoblastic lineage. *J Bone Miner Res* **21**, 1317-1326

142. Deregowski, V., Gazzerro, E., Priest, L., Rydziel, S., and Canalis, E. (2006) Notch 1 overexpression inhibits osteoblastogenesis by suppressing Wnt/beta-catenin but not bone morphogenetic protein signaling. *The Journal of biological chemistry* **281**, 6203-6210

143. Sciaudone, M., Gazzerro, E., Priest, L., Delany, A. M., and Canalis, E. (2003) Notch 1 impairs osteoblastic cell differentiation. *Endocrinology* **144**, 5631-5639

144. Tezuka, K., Yasuda, M., Watanabe, N., Morimura, N., Kuroda, K., Miyatani, S., and Hozumi, N. (2002) Stimulation of osteoblastic cell differentiation by Notch. *J Bone Miner Res* **17**, 231-239

145. Shindo, K., Kawashima, N., Sakamoto, K., Yamaguchi, A., Umezawa, A., Takagi, M., Katsube, K., and Suda, H. (2003) Osteogenic differentiation of the mesenchymal progenitor cells, Kusa is suppressed by Notch signaling. *Exp Cell Res* **290**, 370-380

146. Nobta, M., Tsukazaki, T., Shibata, Y., Xin, C., Moriishi, T., Sakano, S., Shindo, H., and Yamaguchi, A. (2005) Critical regulation of bone morphogenetic protein-induced osteoblastic differentiation by Delta1/Jagged1-activated Notch1 signaling. *The Journal of biological chemistry* **280**, 15842-15848

147. Guentchev, M., and McKay, R. D. (2006) Notch controls proliferation and differentiation of stem cells in a dose-dependent manner. *Eur J Neurosci* **23**, 2289-2296

148. Delaney, C., Varnum-Finney, B., Aoyama, K., Brashem-Stein, C., and Bernstein, I. D. (2005) Dose-dependent effects of the Notch ligand Delta1 on ex vivo differentiation and in vivo marrow repopulating ability of cord blood cells. *Blood* **106**, 2693-2699

149. Fujimaki, R., Toyama, Y., Hozumi, N., and Tezuka, K. (2006) Involvement of Notch signaling in initiation of prechondrogenic condensation and nodule formation in limb bud micromass cultures. *J Bone Miner Metab* **24**, 191-198

150. Watanabe, N., Tezuka, Y., Matsuno, K., Miyatani, S., Morimura, N., Yasuda, M., Fujimaki, R., Kuroda, K., Hiraki, Y., Hozumi, N., and Tezuka, K. (2003) Suppression of differentiation and proliferation of early chondrogenic cells by Notch. *J Bone Miner Metab* **21**, 344-352

151. Ross, D. A., Hannenhalli, S., Tobias, J. W., Cooch, N., Shiekhattar, R., and Kadesch, T. (2006) Functional analysis of Hes-1 in preadipocytes. *Mol Endocrinol* **20**, 698-705

152. Baron, M., Aslam, H., Flasza, M., Fostier, M., Higgs, J. E., Mazaleyrat, S. L., and Wilkin, M. B. (2002) Multiple levels of Notch signal regulation (review). *Mol Membr Biol* **19**, 27-38

153. Kessler, C. B., and Delany, A. M. (2007) Increased Notch 1 expression and attenuated stimulatory G protein coupling to adenylyl cyclase in osteonectin-null osteoblasts. *Endocrinology* **148**, 1666-1674

154. Minamizato, T., Sakamoto, K., Liu, T., Kokubo, H., Katsube, K., Perbal, B., Nakamura, S., and Yamaguchi, A. (2007) CCN3/NOV inhibits BMP-2-induced osteoblast differentiation by interacting with BMP and Notch signaling pathways. *Biochemical and biophysical research communications* **354**, 567-573

155. Sakamoto, K., Yamaguchi, S., Ando, R., Miyawaki, A., Kabasawa, Y., Takagi, M., Li, C. L., Perbal, B., and Katsube, K. (2002) The nephroblastoma overexpressed gene (NOV/ccn3) protein associates with Notch1 extracellular domain and inhibits myoblast differentiation via Notch signaling pathway. *The Journal of biological chemistry* **277**, 29399-29405

156. Meng, H., Zhang, X., Hankenson, K. D., and Wang, M. M. (2009) Thrombospondin 2 potentiates notch3/jagged1 signaling. *The Journal of biological chemistry* **284**, 7866-7874

157. Meng, H., Zhang, X., Hankenson, K. D., and Wang, M. M. (2009) Thrombospondin2 potentiates notch3/Jagged1 signaling. *J Biol Chem*

158. Engler, A. J., Sen, S., Sweeney, H. L., and Discher, D. E. (2006) Matrix elasticity directs stem cell lineage specification. *Cell* **126**, 677-689

159. Bradshaw, A. D., Graves, D. C., Motamed, K., and Sage, E. H. (2003) SPARC-null mice exhibit increased adiposity without significant differences in overall body weight. *Proceedings of the National Academy of Sciences of the United States of America* **100**, 6045-6050

160. Nie, J., and Sage, E. H. (2009) SPARC inhibits adipogenesis by its enhancement of beta-catenin signaling. *The Journal of biological chemistry* **284**, 1279-1290

161. Ferron, M., Hinoi, E., Karsenty, G., and Ducy, P. (2008) Osteocalcin differentially regulates beta cell and adipocyte gene expression and affects the development of metabolic diseases in wild-type mice. *Proceedings of the National Academy of Sciences of the United States of America* **105**, 5266-5270

162. Lee, N. K., Sowa, H., Hinoi, E., Ferron, M., Ahn, J. D., Confavreux, C., Dacquin, R., Mee, P. J., McKee, M. D., Jung, D. Y., Zhang, Z., Kim, J. K., Mauvais-Jarvis, F., Ducy, P., and Karsenty, G. (2007) Endocrine regulation of energy metabolism by the skeleton. *Cell* **130**, 456-469

163. Voros, G., Maquoi, E., Demeulemeester, D., Clerx, N., Collen, D., and Lijnen, H. R. (2005) Modulation of angiogenesis during adipose tissue development in murine models of obesity. *Endocrinology* **146**, 4545-4554

164. Darlington, G. J., Ross, S. E., and MacDougald, O. A. (1998) The Role of C/EBP Genes in Adipocyte Differentiation. *JOURNAL OF BIOLOGICAL CHEMISTRY* **273**, 30057-30060

165. Sfeir, Z., Ibrahimi, A., Amri, E., Grimaldi, P., and Abumrad, N. (1997) Regulation of FAT/CD36 gene expression: further evidence in support of a role of the protein in fatty acid binding/transport. *Prostaglandins, leukotrienes, and essential fatty acids* **57**, 17-21

166. Qiu, Z., Wei, Y., Chen, N., Jiang, M., Wu, J., and Liao, K. (2001) DNA synthesis and mitotic clonal expansion is not a required step for 3T3-L1 preadipocyte differentiation into adipocytes. *The Journal of biological chemistry* **276**, 11988-11995

167. Ross, D. A., Rao, P. K., and Kadesch, T. (2004) Dual roles for the Notch target gene Hes-1 in the differentiation of 3T3-L1 preadipocytes. *Molecular and cellular biology* **24**, 3505-3513

168. Hankenson, K. D., James, I. E., Apone, S., Stroup, G. B., Blake, S. M., Liang, X., Lark, M. W., and Bornstein, P. (2005) Increased osteoblastogenesis and decreased bone resorption protect against ovariectomy-induced bone loss in thrombospondin-2-null mice. *Matrix Biol* **24**, 362-370

169. Cooke, P. S., and Naaz, A. (2004) Role of estrogens in adipocyte development and function. *Experimental biology and medicine (Maywood, N.J* **229**, 1127-1135

170. Nishida, S., Endo, N., Yamagiwa, H., Tanizawa, T., and Takahashi, H. E. (1999) Number of osteoprogenitor cells in human bone marrow markedly decreases after skeletal maturation. *Journal of bone and mineral metabolism* **17**, 171-177

171. Muschler, G. F., Nitto, H., Boehm, C. A., and Easley, K. A. (2001) Age- and gender-related changes in the cellularity of human bone marrow and the prevalence of osteoblastic progenitors. *J Orthop Res* **19**, 117-125

172. Maillard, I., Fang, T., and Pear, W. S. (2005) Regulation of lymphoid development, differentiation, and function by the Notch pathway. *Annual review of immunology* **23**, 945-974

173. Piccoli, D. A., and Spinner, N. B. (2001) Alagille syndrome and the Jagged1 gene. *Semin Liver Dis* **21**, 525-534

174. Shinkai, Y., Tsuji, T., Kawamoto, Y., and Kunieda, T. (2004) New mutant mouse with skeletal deformities caused by mutation in delta like 3 (Dll3) gene. *Exp Anim* **53**, 129-136

175. Hilton, M. J., Tu, X., Wu, X., Bai, S., Zhao, H., Kobayashi, T., Kronenberg, H. M., Teitelbaum, S. L., Ross, F. P., Kopan, R., and Long, F. (2008) Notch signaling maintains bone marrow mesenchymal progenitors by suppressing osteoblast differentiation. *Nature medicine* **14**, 306-314

176. Maillard, I., Weng, A. P., Carpenter, A. C., Rodriguez, C. G., Sai, H., Xu, L., Allman, D., Aster, J. C., and Pear, W. S. (2004) Mastermind critically regulates Notch-mediated lymphoid cell fate decisions. *Blood* **104**, 1696-1702

177. Liu, F., Woitge, H. W., Braut, A., Kronenberg, M. S., Lichtler, A. C., Mina, M., and Kream, B. E. (2004) Expression and activity of osteoblast-targeted Cre recombinase transgenes in murine skeletal tissues. *The International journal of developmental biology* **48**, 645-653

178. Tu, L., Fang, T. C., Artis, D., Shestova, O., Pross, S. E., Maillard, I., and Pear, W. S. (2005) Notch signaling is an important regulator of type 2 immunity. *The Journal of experimental medicine* **202**, 1037-1042

179. Vujovic, S., Henderson, S. R., Flanagan, A. M., and Clements, M. O. (2007) Inhibition of gamma-secretases alters both proliferation and differentiation of mesenchymal stem cells. *Cell proliferation* **40**, 185-195

180. Garces, C., Ruiz-Hidalgo, M. J., Font de Mora, J., Park, C., Miele, L., Goldstein, J., Bonvini, E., Porras, A., and Laborda, J. (1997) Notch-1 controls the expression of fatty acid-activated transcription factors and is required for adipogenesis. *The Journal of biological chemistry* **272**, 29729-29734

181. Bai, S., Kopan, R., Zou, W., Hilton, M. J., Ong, C. T., Long, F., Ross, F. P., and Teitelbaum, S. L. (2008) NOTCH1 regulates osteoclastogenesis directly in osteoclast precursors and indirectly via osteoblast lineage cells. *The Journal of biological chemistry* **283**, 6509-6518

182. Engin, F., and Lee, B. (2009) NOTCHing the bone: Insights into multi-functionality. *Bone*

183. Engin, F., Bertin, T., Ma, O., Jiang, M. M., Wang, L., Sutton, R. E., Donehower, L. A., and Lee, B. (2009) Notch signaling contributes to the pathogenesis of human osteosarcomas. *Human molecular genetics* **18**, 1464-1470